MOLECULAR AND BIOCHEMICAL STUDIES OF PROBIOTIC PROPERTIES OF *LACTOBACILLUS FERMENTUM* NKN51

Ph.D. THESIS

by

REKHA SHARMA

DEPARTMENT OF BIOTECHNOLOGY
INDIAN INSTITUTE OF TECHNOLOGY ROORKEE
ROORKEE-247 667 (INDIA)
JUNE, 2015

MOLECULAR AND BIOCHEMICAL STUDIES OF PROBIOTIC PROPERTIES OF *LACTOBACILLUS FERMENTUM* NKN51

A THESIS

Submitted in partial fulfilment of the
Requirements for the award of the degree
of

DOCTOR OF PHILOSOPHY
in

BIOTECHNOLOGY

by

REKHA SHARMA

DEPARTMENT OF BIOTECHNOLOGY
INDIAN INSTITUTE OF TECHNOLOGY ROORKEE
ROORKEE-247 667 (INDIA)
JUNE, 2015

INDIAN INSTITUTE OF TECHNOLOGY ROORKEE
ROORKEE

CANDIDATE'S DECLARATION

I hereby certify that the work which is being presented in the thesis entitled **"MOLECULAR AND BIOCHEMICAL STUDIES OF PROBIOTIC PROPERTIES OF *LACTOBACILLUS FERMENTUM* NKN51"** is in partial fulfilment of the requirements for the award of the Degree of Doctor of Philosophy and submitted in the Department of Biotechnology of the Indian Institute of Technology Roorkee, Roorkee is an authentic record of my own work carried out during a period from January, 2009 to June, 2015 under the supervision of Dr. Naveen Kumar Navani, Associate Professor, Department of Biotechnology, Indian Institute of Technology Roorkee, Roorkee.

The matter presented in this thesis has not been submitted by me for the award of any other degree of this or any other Institute.

Signature of Candidate

This is to certify that the above statement made by the candidate is correct to the best of my knowledge.

Signature of Supervisor

The Ph.D. Viva-Voce Examination of **Mrs**. **Rekha Sharma**, Research Scholar, has been held on..... .

Chairman, SRC **Signature of External Examiner**

This is to certify that the student has made all the corrections in the thesis.

Signature of Supervisor **Head of the Department**

Dated:

ABSTRACT

Probiotics are health beneficial microbes which constitutes normal gut flora and live in a mutualistic relationship with the host. Owing to their health benefic nature probiotics are commercially available as food supplements. Most widely used Probiotic genera are *Lactobacillus* and *Bifidobacterium*. However genetic basis of the health beneficiary properties of probiotic microbes are poorly understood which leads to inconsistent results and limits attribution of measurable effect to the microbes. Understanding the molecular insights of probiotic properties will support their scientific use contributing towards more judicious applications in health and food industry.

The present study involves screening of fermented dairy product and infant gut flora for isolation of lactic acid bacteria. 15 isolates obtained after screening were identified as lactic acid bacteria by biochemical analysis and 16S rRNA sequencing. Probiotic potential of all the isolates was analyzed by screening of four important attributes; phytase production, *in-vitro* cholesterol removal, asparaginase production and bile salt hydrolase production. Out of all isolates NKN51 have shown good phytase activity and *in-vitro* cholesterol removal ability. NKN52 and NKN55 were good asparaginase and bile salt hydrolase producers. Besides this NKN53 and NKN59 have also shown good asparaginase activity. NKN52 and NKN55 were identified as *L. bevis* and NKN53 was *Weisella paramesenteroides*. There are no reports of asparaginase production from any of these microbes in literature, hence the study reports novel finding of asparaginase production by *L. bevis* and *Weisella paramesenteroides*. Asparaginase is an antineoplastic enzyme and may contribute significantly to the anticancer property of these microbes. NKN51 was identified as *Lactobacillus fermentum* it has shown good cholesterol reducing effect *in vitro* from synthetic medium. Cholesterol reducing effect is a much desirable character in *Lactobacilli* as hypercholesterolemia is one of the biggest health threats worldwide. Along with that, high phytase activity of NKN51 made us to choose the isolate for furthes studies.

Inositol hexakisphosphate (IP6 or phytate) degradation by commensal gut flora has drawn much attention in last few years because of its antinutritive properties and role in inter-kingdom signalling. Still genetic information of IP6 degradation is lacking from most of the gut flora. In present study we have cloned and characterized a novel protein tyrosine phosphatase like phytase (PTPLP) from probiotic bacterium *Lactobacillus fermentumNKN51* (phyLf). phyLf shown high substrate specificity towards IP6 with Maximum enzyme activity at pH 5, temperature 60^{o}C and 100mM ionic strength. IP6 degradation was further confirmed by

Zymography and HPLC analysis. Among various reported PTPs, phyLf exhibited exceptionally high resistance against oxidative inactivation by H_2O_2. Enzyme activity was not much affected by disulphide bond denaturants and chelating agent. Specific activity, Michaelis-Menten's constant (Km) and Catalytic turnover number (K_{cat}) for IP6 were 174.5U mg^{-1}, 0.7735mM and 84.31 sec^{-1} respectively. Bioinformatic and Phylogenetic analysis have shown that except for active site, it does not share much homology with previously reported PTPLPs and lies at interphase of PTPLP and MptpB like proteins, hence constitutes a new subclass of PTPLPs. Thus far phyLf represents the first phytase gene characterized from genera *Lactobacillus*. Widely accepted probiotic properties of this genus enable its phytase to be more acceptable for human consumption

Further *in-vitro* cholesterol reducing effect of *Lactobacillus fermentumNKN51* was analysed. An increase in growth of NKN51 was reported in presence of cholesterol in comparatively nutritionally scarce medium, M17-thioglycollate, which clearly indicates cholesterol assimilation or metabolization by bacteria. To further confirm the cholesterol consumption by *Lactobacillus fermentumNKN51* the isolate was allowed to grow in M17 medium supplemented with fluorescent cholesterol analog, NBD-cholesterol and a distinct shift was observed in fluorescence spectrum of cells grown in presence of fluorescent cholesterol in comparison to control cells in flow cytometric analysis. The result suggests and confirms the assimilation of cholesterol by *Lactobacillus fermentum* NKN51. The study provides experimental proof to the concept of cholesterol assimilation by Lactobacilli for imparting hypocholesterolemic effect. For mechanistic insight of cholesterol consumption, putative 3beta hydroxy steroid dehyrogenase gene was cloned and characterized from the genome of *Lactobacillus fermentum* NKN51. Cholesterol dehydrogenase activity of the protein product was confirmed by zymography and biochemical analysis. These findings give a way to explore the complete mechanism of cholesterol consumption in *Lactobacilli*. And provide scientific basis to the concept of hypocholesterolemic effect of *Lactobacilli*.

In fourth part of the study a facile single step green method of synthesizing silver nanoparticles functionalized with an antibacterial peptide from a food-grade lactic acid bacterium has been reported. The synthesized enterocin coated silver nanoparticles show broad spectrum inhibition against a battery of food borne pathogenic bacteria without any detectable toxicity to red blood cells. The present results evince that a new category of biocide based on silver nanoparticles coated with food-grade antibacterials can be developed using simple methods.

ACKNOWLEDGEMENT

This thesis is an outcome of the past five years, wherein I grew stronger, accepted failures and strived harder for success. I have been accompanied and supported by many people during this journey. I feel honoured that I have now the opportunity to express my gratitude to all those people who contributed directly or indirectly to this endeavour.

I would start with thanking GOD, for bestowing his choicest blessings on me and always providing a guiding light for me to walk on the right path of life. Without his grace, this would not have been possible.

My sincere gratitude and heartfelt thanks to my guide and mentor Dr. Naveen Kumar Navani, Assistant Professor, Department of Biotechnology, IIT Roorkee. I am fortunate to be given an opportunity to work under his supervision. His mentorship was paramount in providing a well rounded experience consistent my long-term career goals. His constant focus on precision, enlightening ideas, constructive criticism and scientific freedom helped me pave my way towards becoming an independent researcher. I am deeply indebted to him for believing that a hypothesis which was put forth as being implausible could actually be validated. His unfaltering encouragement to pursue challenges throughout this program helped me immensely. I owe him more than words express.

I am grateful to Dr. Ranjana Pathania for her invaluable suggestions and inputs in shaping my work. Her ideas and encouragement towards my work proved very helpful.

I feel overwhelmed in thanking Dr. Partha Roy, Professor and Head Department of Biotechnology for providing necessary facilities, support and cooperation in the Department for research.

I extend my heartfelt thanks to my student research committee (SRC) Dr. A.K. Sharma, Chairman SRC and Professor Shishir Sinha, Professor Department of Chemical Engineering for their encouragement and suggestions.

I extend a note of thanks to the staff members of my lab and department Mr. Jain , Mr. V.P Saini, Shashi madam, Mohan, Akshay and Anil ji and for providing technical assistance and care .

I seize the opportunity to express my special thanks to, Dr. Piyush,, Dr. Paramesh, Tamoghna, Tapas, Pardeep, Dr. Santosh, Manasi and Abhijeet, for their kind support for the completion of the thesis.

The members of my lab contributed immensely to my personal and professional time at IIT Roorkee. The group has been a source of friendships as well as good advice, collaboration and providing a stimulating and fun filled environment. I want to thank all the members of my lab CBDD Dr. Rajnikant, Dr. Supriya, Dr. Tarun, Dr. Jitendra, Atin, Amit, Anjul, Timsy, Rajat, Vandana, Shahnawaz, Vineet, Jawed, Arshad and Dr.Ila for providing a helping hand during my research work. I am grateful to my friends Pooja kesari and Jyoti tomar for all their support and suggestions during this period. I am also indebted to the students I have had the pleasure to work with.

I thank with love my husband Nagesh Kumar for his patience and unconditional trust. He has been my best friend and a great companion who loved, supported, encouraged and helped me to get through this period in the most positive way.

Last but not the least I owe it to my family for believing in me and supporting me throughout my life. I fall short of words when I come to think of my family's contribution. Their endless patience and priceless words of advice have helped me make it so far.

Besides this, several people have knowingly and unknowingly helped me in the successful completion of this project. I thank all of them.

Financial assistance provided by CSIR is gratefully acknowledged.

Roorkee ***(Rekha Sharma)***

CONTENTS

LIST OF FIGURES

LIST OF TABLES

ABBREVIATIONS

AFM	Atomic microscopy
ATP	Adenosine Triphosphate
BME	*β-Mercaptoethanol*
BCP	Bromocresol purple
BSH	Bile salt hydrolase
CD	Circular dichroism
CFU	Colony forming unit
CSNPs	Citrate capped nanoparticles
CV	Crystal violet
DLS	Dynamic light scattering
DNA	Deoxyribonucleic acid
EDTA	Ethylene diamine tetra acetic acid
ECMP	*E. coli.* ATCC 25922 membrane protein
En-SNP	Enterocin capped silver nanoparticles
FTIR	Fourier transform infrared
g	Grams
3βHSD	3β Hydroxysteroid dehydrogenase
Kan	Kanamycin
kDa	Kilodalton
L	Liter
LAB	Lactic acid bacteria
LB	Luria Bertani
LBMP	*P. acidilactici* LB42 membrane protein
MRS medium	deMan Rogosa Sharpe medium
MIC	Minimum inhibitory concentration

mA	milli Ampere
mg	milligram
min	minutes
ml	milliliter
mM	millimolar
Ni-NTA	Nickle Nitrilotriacetic acid
nm	nanometer
nM	nanomolar
O.D	Optical density
En SNPs	Enterocin capped silver nanoparticles
PCR	Polymerase chain reaction
PTPLP	Protein tyrosine phosohatase like phytase
pH	power of hydrogen
RNA	Ribonucleic acid
ROS	Reactive oxygen species
RLS	Resonance Light Scattering
rpm	rotation per minute
RT	Room temperature
s	seconds
SDS	Sodium dodecyl sulphate
SEM	Scanning electron microscopy
SPR	Surface plasmon resonance
TAE	Tris Acetate EDTA buffer
TBE	Tris Borate EDTA buffer
TE	Tris EDTA
TEM	Transmission electron microscopy
TEMED	N ,N,N,N – Tetra methyl ethyl diamine

UV	ultraviolet
µg	microgram
µl	microliter
µM	micromolar
°C	Degree Celsius
A_{620}/A_{520}	Absorbance ratio of 620 and 520 nm

CHAPTER 1
INTRODUCTION

Probiotics are micro-organisms, which confer health benefits to the host when consumed in adequate amount. These microbes usually constitute normal gut flora. Human gut is colonized by trillions of microbial cells, which directly interact with human body through intestinal epithelium. After skin, gut epithelium is second most exposed surface of body to the external environment. Skin is comparatively thicker and non penetrable surface while intestinal epithelium presents comparatively weak barrier or more interactive surface for food and microbes ingested, hence microbial colonization of intestinal lumen directly affects the host health. Being an absorptive surface it can readily absorb toxic or health beneficiary by products of colonizing bacteria and its outcome affects the health status of the host. Probiotic microbes live in a symbiotic relationship imparting various health benefits to the host. Since probiotics are normal gut flora they can present safe and effective solution to various health problems and can provide faster approach to show beneficial effect as they remain in constant contact with body. Health benefits of probiotic microbes are well accepted but mechanism of action of most of the probiotic properties is poorly understood. Lack of precise knowledge of mechanism of action is a major setback in their acceptability in medicinal and commercial usage. Most of the probiotic microbes belong to the group of lactic acid bacteria. *Lactobacillus* and *Bifidobacterium* genera are most widely used. This research was initiated with an aim to bridge the gap between health benefits believed to be associated with probiotic bacteria and scientific investigation of the same. Overall the work is centered on *Lactobacilli*.

With the aim of selection of potential probiotic microbes first part of the study involves isolation of lactic acid bacteria from diverse niches and identification by biochemical characterization and 16S rRNA gene sequencing. Further screening of their important probiotic properties like phytase production, cholesterol consumption, asparaginase production and bile salt hydrolase activity was done. Screening of probiotic properties enabled the selection of isolates showing multiple probiotic effects with good magnitude. Out of all isolates NKN51 was selected for further studies because of its promising probiotic properties. It has been identified as *Lactobacillus fermentum* on the basis of biolog and molecular sequencing.

In second part of the study molecular and biochemical characterization of phytase activity of *Lactobacillus fermentum*NKN51 was done. Phytase is an enzyme which hydrolyzes phytic acid. Phytic acid or inositol hexa phosphate (IP6) is a major form of phosphate storage in food of plant origin [1]. It acts as a strong chelating agent and binds phosphorus, minerals and proteins in food and makes them unavailable for absorption in gut. Antinurtitive properties of phytate generate the need of phytate degradation in food. Phytase enzyme degrades phytates and releases bound minerals and proteins and makes them bioavailable in gut. Addition of phytases in food increases nutrient value of food[2]. Various commercial phytases are used as poultry and other livestock feed additive which improves their health significantly [2]. Nonetheless there is need of safer sources of phytases for being acceptable as human food additive. Phytase activity of gut colonizing probiotic bacteria can increase the nutritional value of food by degrading phytate in food articles by fermentation. Upon gut colonization the bacteria can enhance bioavailability of nutrients by degrading phytate in ingested food. Also phytase from probiotic bacteria may prove more acceptable for human consumption [3]. In a recent study, *Stentz et al.* (2014) have reported that phytase produced by *Bacteroides thetaiotaomicron* can promote intracellular calcium signaling in intestinal epithelial cells and hence involved in cross-kingdom dialogue [4]. Inositol phosphates are involved in host cell signaling but bacteria do not use inositol signaling cascade hence metabolism of IP6 by gut flora establishes an inter kingdom signaling system. Gut inhabiting *Bacteroids* and *Bifidobacteria* are reported to produce phytases of class histidine acid phosphatase but no phytase of this class is found in firmicutes including *Lactobacillus* [4]. Phytase activity of *Lactobacillus* is reported in various studies but no genetic or molecular proof is available till date, besides there are the reports of non specific acid hydrolysis of phytate and no information of enzyme responsible for this effect is available. In present study after preliminary screening for phytase activity of NKN51 bioinformatic analysis of genome sequence of *Lactobacillus fermentum* was done to select putative phytase encoding genes. Bioinformatic analysis and phylogenetic placement enabled *in-vivo* function prediction and elucidation of unique features of the protein encoded by selected gene. Further, cloning, expression and purification were done to characterize biochemical and biophysical properties of the protein product. Enzyme tolerance against reactive oxygen species was determined as tyrosine phosphates are very sensitive for oxidative inactivation by H_2O_2. And Lactobacilli are reported to induce *in-vivo* H_2O_2 generation by host cells. [5]. Further secondary structure analysis and comparative molecular modeling was done to analyze the structural specifications of the novel phytase.

In the third part of this study cholesterol assimilation property of NKN51 was examined. Cholesterol is one of the biggest health threats of present times, and a major factor involved in development of cardiovascular diseases. Hypercholesterolemia increases the risk of heart attacks three times in cardiovascular diseases [6]. Along with it, hypercholesterolemia generates other health complications like insulin resistance and increased blood pressure due to impaired vasodilation or formation of plaques on the walls of arteries [7]. Since cholesterol is a normal component of body tissues, regulation of disturbed cholesterol homeostasis is complicated. No safe and effective treatment for hypercholesterolemia is available till date. Present therapies used to reduce blood cholesterol level are expensive and have severe side effects. Therefore there is an urgent need of safe and effective solution to this problem. Cholesterol lowering probiotic bacteria can provide safe solution to the hypercholesterolemia but efficacy of cholesterol reducing effect of probiotic bacteria is still to be examined. Concept of cholesterol lowering effect of gut flora has been well established. As it has been observed that germ free mice excretes out unmodified cholesterol while cholesterol is converted into coprostanol in traditionally raised mice [8]. Still there is no information available for mechanism of cholesterol reduction and enzymes involved in this process in gut. As unculturable microbes constitutes majority of the gut flora, role of culturable symbionts in cholesterol conversion is still imprecise. Very few studies reported coprostanol formation by culturable *Lactobacilli* and there is a lack of solid experimental proofs on assimilation, conversion or degradation of cholesterol by *Lactobacilli* [9]. Various modes of action have been proposed for this property e.g. bile salt hydrolysis, incorporation of cholesterol into bacterial cell wall, binding of cholesterol to bacterial cell surface, direct cholesterol assimilation by bacteria and conversion of cholesterol into coprostanol by intracellular or extracellular enzyme activity. Bile salt deconjugation has been suggested as a mode of cholesterol reduction in body but bile hydrolyzing bacteria can not reduce cholesterol in *in vitro* from synthetic culture media. While few studies reported efficient cholesterol lowering effect of *Lactobacilli* which can reduce cholesterol *in-vitro* from culture media [10]. Hence direct cholesterol assimilation by *Lactobacilli* has been proposed as a mechanism of cholesterol reducing effect. Still mechanism of cholesterol assimilation by lactobacilli is not known. Few studies suggest cholesterol conversion into coprostanol by intermediate formation of cholestenone and coprostanone [11] while in a report *Lye et al* (2010) suggested direct cholesterol conversion into coprostanol by cholesterol reductase activity, but no protein or gene involved in this process has been reported [9].

In third part of the study, *in vitro* cholesterol assimilation ability of NKN51 was monitored by examining the growth profile in M17-thioglycollate media supplemented with cholesterol, M17 is comparatively nutrient scarce medium than MRS, and hence effect of cholesterol on growth of *Lactobacillus* in slightly nutrient deficient condition is reported. For visualization of Cholesterol assimilation by NKN51, the isolate was grown in presence of fluorescent cholesterol analog, NBD-cholesterol and analysis of cells was done by fluorescence active cell sorting with the aid of flow cytometer. Mechanistic evaluation of cholesterol assimilation was done by bioinformatics analysis of genome of *Lactobacillus fermentum* for encoding proteins involved in cholesterol consumption. Selection of gene was done on the basis of prior knowledge of enzymes involved in cholesterol consumption in non-symbiotic bacteria. Since analysis of proposed pathways revealed similar primary reaction for cholesterol conversion in both symbiotic and non symbiotic bacteria. Selected gene sequence was cloned and expressed in a heterologous host *E. coli* BL21AI. Functional analysis of the expressed protein was done by zymography. Phylogenetic analysis was done to determine the distribution of orthologs of selected protein in other firmicutes and its phylogenetic distance from previously reported cholesterol dehydrogenases.

Spoilage and contamination of food is a huge problem in tropical countries like India, where high ambient temperature, lack of proper refrigeration conditions and unorganized sector contribute to several instances of food poisoning cases. Milk, being an excellent source of nutrition allows growth of all bacterial species including pathogens. There is a need to develop strategies for containment of the undesirable bacteria from milk products. Nanobiotics; use of nanoparticles for bacterial control has been chosen as a strategy for investigation into control of food spoilage bacteria in this part of study. For this purpose, green synthesis of silver nanoparticles was done by using bacteriocin, produced by food grade lactic acid bacterium *Enterococcus faecium*FH99, as a capping agent. Bacteriocins produced by lactic acid bacteria (LAB) have been employed in food industry because of their safety and bio-preservative properties. An attempt was made to potentiate the antibacterial spectrum of SNPs and enterocin to exploit the nanotechnological principles to synthesize enterocin-capped silver nanoparticles (En-SNPs). The generalized scheme for the preparation of En-SNPs is depicted in Figure 1. The antibacterial potential of the as-prepared nanoparticles was evaluated against a number of food-borne pathogens. In order to understand the mechanism of action of En-SNPs, interaction studies with the outer membrane protein of representative gram negative and gram-positive bacterial strains were carried out. In this study we

report the green synthesis, antibacterial potential, and interaction of bacteriocin-capped SNPs with bacterial membrane proteins.

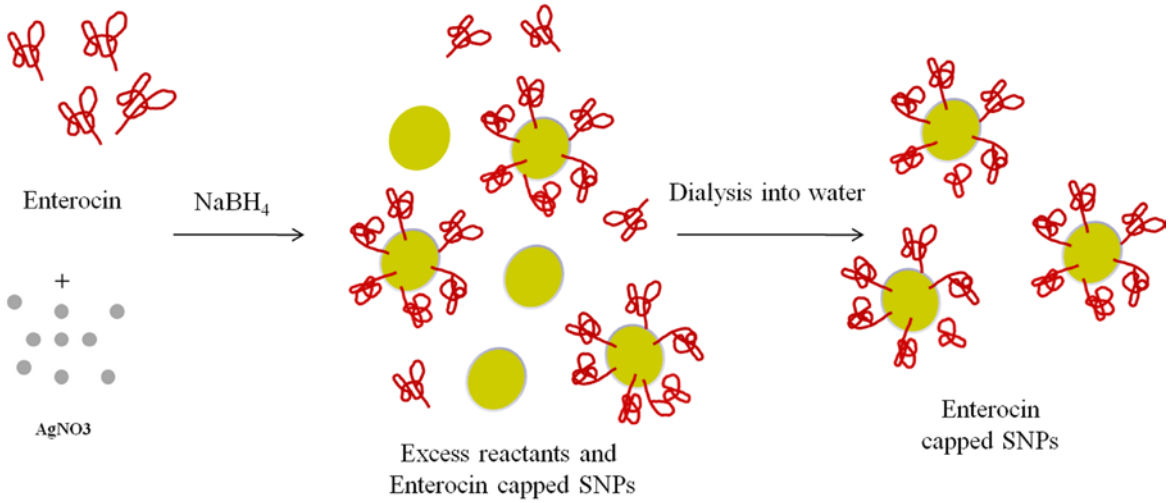

Figure 1.1: Schematic representation of En-SNPs synthesis.

CHAPTER 2
REVIEW OF LITERATURE

Probiotics are health beneficial microbes which are known to confer health benefits to the host when administered in adequate amounts. Concept of probiotics was basically given by nobel Laurent Élie Metchnikoff, who suggested that "all old age related disabilities are due to toxins derived from putrefying bacteria in gut, which convert phagocytes from defender against pathogens to destroyers of body tissues". Intestine is one of the largest interphase between external environment and body as intestinal mucosa is in permanent contact with trillions of the microbial cells which constitutes the gut flora. Colonizing microbial cells outnumbers the complete human body cells and combined genome of micro-flora represents much greater genetic diversity than the human genome. Hence, gut flora constitutes a virtual organ in intestine and its metabolome plays crucial role in human health [12]. Studies show that animals, born and raised under germ-free sterile conditions, show impaired development; and are more prone to infections than traditionally raised mice [13]. Various metagenomic studies show that the majority of gut flora is unculturable while culturable flora mainly comprises low GC content (*Lactobacilli*) to high GC content (*Bifidobacteria*) gram positive bacteria. These microbes exist in symbiotic and nutritional relationship with gut epithelium and compete with pathogens for colonization surface and nutrition [14]. Eukaryotes have developed dedicated pattern recognition receptors and signaling pathways which recognize microbial molecular patterns to determine host- microbe interaction as pathogenic conflict or symbiotic dialogue [15]. Furthermore, these microbes have to cope with host immune response, certain bacterial molecules helps in acclimatization of gut flora. Proteins and metabolites of symbiotic flora impart additional health benefits to the host and exhibit immunomodulatory effects. Together, these health beneficiary effects are called as probiotic effects and the conferring microbes are called as probiotics [16]. Major bacterial genera considered as probiotics include *Lactobacilli, Pediococci, Bifidobacterium, Leuconostoc* and few species of *Enterococci* and *Streptococci,* collectively these bacteria are termed as Lactic acid bacteria (LAB) due to the formation of lactic acid as end product of homolactic or heterolactic sugar fermentation.

Probiotic health benefits results due to the collective attribute of different probiotic properties. Although few probiotic properties are very well documented but mechanistic insight of most of the probiotic effects is unexplored. Major probiotic health benefits are as follows-

2.1. Prevention of irritable bowel syndrome

Two major inflammatory bowel diseases (IBD) are ulcerative colitis and crohn's disease. Both of these conditions arise by the overproduction of inflammatory cytokines due to environmental, immune and bacterial factors. Although the reason of IBD is complex, certain probiotic bacteria are reported to ameliorate the symptoms of IBD by inhibiting the growth of pathogenic bacteria and hence, reducing the toxic microbial metabolites. Certain probiotic microbes or combinations show anti-inflammatory effect and modulate the abnormal immune response towards homeostasis.

2.2 Immunomodulatory effects

Since symbionts are microbes, they would evoke some immune response which could be immunostimulatory or immunosuppressing. These immunomodulatory effects help in the development and maintenance of the normal basal immune response in host [17]. Immunostimulatory probiotics helps in eradication of pathogens by stimulating an enhanced immune response against them while immunosuppressing probiotics reduce the anaphylactic or inflammatory response evoked by the pathogens and their toxins (septic shocks).

2.3 Antibacterial properties

Probiotic microbes inhibit the growth of pathogens by various means. They pose competitive inhibition for colonization by occupying the intestinal surface and acid production by lactic acid bacteria inhibits growth of pathogens. Certain probiotic microbes produce bacteriocins like enterocin, pediocin etc. which inhibits the growth of the pathogens. Clinical studies have shown that the incidence of infections decrease in dental caries and respiratory tract infections due to probiotics [18, 19]. Immune system's function ability is improved by probiotics by increasing the numbers of plasma cells, natural killer cells and T lymphocytes and eventually enhanced phagocytosis [20].

2.4 Antiallergic effect

Some LAB modulates allergic responses, an observation suggested at least in part, due to the cytokine function regulation.[21] Clinical studies have shown that administration of probiotic bacteria can prevent reoccurrences of inflammatory bowel disease in adults [21], as well as improve milk intolerance [22]. The mechanism used to influence immune system by probiotics remains unclear, but response of T-lymphocytes towards inflammatory stimuli is a potential

mechanism under concern [23]. In 2003, studies have reported that combination of *L. reuteri* DSM 122460 and *L. rhamnosus* 19070-2 can treat atopic dermatitis or eczema. In the later studies, researchers have reported upto 20% decrease in cases of atopic dermatitis [24].

2.5 Nutrition availability

Probiotics increases the nutrition availability to the host. Bacterial enzymes like cellulase, xylanase, phytase and various other hydrolases helps in the digestion of indigestible food components efficiently and makes them bioavailable for gut absorption. Along with it, certain probiotics are known to produce vitamin K, folic acid and vitamin B12 [25, 26].

2.6 Anticancer effect

Gastric ulcers caused by gut pathogens increases the risk of cancer development. Probiotic microbes are known to inhibit growth of pathogenic microbes like *Helicobacter pylori, Clostridia* and *E. coli* in gut and alter their pro-carcinogenic enzymes activity like beta-glucuronidase [27, 28]. Along with it, production of short chain fatty acids like sodium butyrate and anticancer enzymes like asparaginase by probiotic microbes may prove helpful in cancer prevention.

2.7 Cholesterol reduction

High blood cholesterol is one of the biggest problems of the date; still no safe and effective treatment is available. In various studies, some probiotic bacteria are reported to reduce the blood cholesterol level in hypercholesterolemic mice [29]. Although, no clinical efficacy has been proved yet, still preliminary reports are available on cholesterol reducing effect. Two modes are proposed for cholesterol reduction by probiotic bacteria, one is bile salt hydrolase production which inturn leads to increased bile salt degradation in intestine which eventually increases cholesterol consumption for bile formation in liver and hence reduces blood cholesterol level. Another mode is direct cholesterol consumption by bacteria which is converted into byproducts like coprostanol which is incorporated in bacterial cell wall or excreted out of body [9].

2.8 Blood pressure

Some reports show production of ACE-inhibitor like compounds by LAB during milk fermentation, consumption of which may cause mild reduction in hypertension [30].

Although extensive research is in progress to explore the in-depth knowledge of therapeutic effects of probiotics. Still molecular details of precise mechanism of most of the probiotic

properties are unknown. *In-vitro* health effects do not reproduce *in-vivo* in most of the human trials even with the significantly promising laboratory strains. This questions efficacy of probiotic food supplement and holds back their therapeutic and commercial usage. 260 claims have been rejected by European Food Safety Authority due to insufficient scientific proofs of probiotic health effects (https://en.wikipedia.org/wiki/Probiotic#cite_note-110). Detailed study of the bacterial functional genomics, effector molecules, pathways involved in probiotic effects and host response towards them is needed to establish well defined strain specific properties [31]. This would enable therapeutic usage of scientifically supported probiotic supplements with well defined health claims.

Probiotics such as *Lactobacilli* can help animal's growth by degrading non-degradable food constituents like Inositol phosphates. Inositol phosphates are widely distributed in eukaryotic system. One of the most abundant form is inositol hexakis phosphate (IP6) or phytic acid [32]. Inositol phosphates are involved in host cell signaling and regulates cell division, proliferation and apoptosis, while human gastrointestinal tract lacks any enzyme which can degrade major form of inositol poly phosphates i.e. IP6 in food and largely dependent on their gut flora for digestion of IP6 [32]. Ionic form of it is called phytate, which forms salts with cationic metal ions. Phytate is the major form of phosphorus storage in plants, it constitutes ~80% of phosphorus content in grains and seeds. Being highly negatively charged phytate binds with metal ions, proteins and sugars. Plants utilize phytate during germination and development to obtain these essential nutrients. Initially, only phosphate storage was thought to be the function of phytate but recently it has been reported that biological role of phytate is much more diverse than storage molecule. It has been reported to be involved in various cellular processes like DNA repair, RNA processing, RNA transport, apoptosis and pathogenicity [32, 33]. Importance of phytate on animal is clearly exemplified by the observation that deletion of IP6 synthesizing enzyme in mouse embryos resulted in a lethal phenotype. Except for IP6, various other forms of inositol phosphates are involved in animal cell signalling system like PIP2, IP3 in calcium signalling system [34].

Prokaryotes lack IP6 or any other form of inositol phosphates but still several inositol phosphates hydrolyzing enzymes are found in bacteria and archea, playing role in diverse processes like phosphorus scavenging and pathogenicity [4, 32].

2.9 Chemistry of IP6

Inositol hexa phosphate have 12 protonation sites on six phosphate heads (Figure 2.1), 6 out of these sites have pKa values around 1.1 to 1.2, three protons have pKa values around 6 to 7.7 while last three have pKa values around 9.2 to 9.6 [32]. Although, pKa value of the sites depends on counter ions in the solution, at normal physiological pH IP6 have -6 to -9 charge. Being highly charged molecule, it acts as strong chelator for cationin proteins, sugars and metal ions.

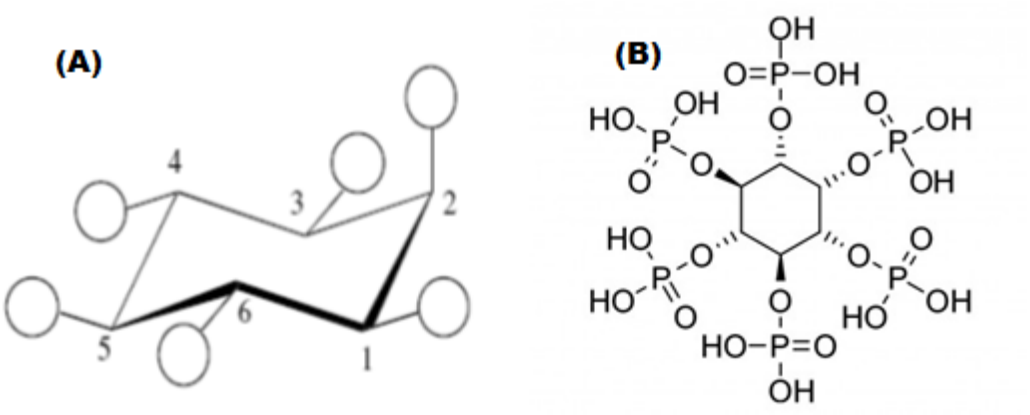

Figure 2.1: (A)Inositol hexakisphosphate in energetically favoured form with five equatorial phosphate and one axial phosphate. Chair confirmation of the molecule resembles a turtle (Arganof's Turtle) (B) 2D Chemical structure of phytate.

2.10 Phytases

Phytase is a generic term of phytate degrading enzymes which can differ in their structural and biochemical properties and mode of action, based on which they have been classified. Bacterial and fungal phytases are the most studied phytases because of their commercial usage as livestock feed supplement [35]. Phytase usually degrades phytate at a specific site and remove phosphates in highly ordered manner. Product of the first reaction releases the site and becomes substrate for the subsequent reaction [32]. Except for the phytase of *Bacillus subtilis* which sequentially removes two phosphates from 6^{th} and 4^{th} position and then releases the product IP4 [32]. Based on the site of hydrolysis phytases are classified as 3-phytases (E.C.3.1.3.8), 4-phytases (E.C.3.1.3.26) and 5-phytases (E.C.3.1.3.72). While on the basis of mechanism of action and structural differences phytases are classified into four major classes: histidine acid phosphatases (HAP), beta propeller phytases (BPP), purple acid phosphatases (PAP) and protein tyrosine phosphatase like phytases (PTPLP).

2.10.1 Histidine acid phosphatases

Phytases of class histidine acid phosphatase are the most widely distributed [32]. They have highly conserved active site pattern RHGXRXP and a C-terminal HD domain. Mechanism of their catalytic action is extensively studied [36]. They follow two step reaction: in the first part of the reaction, conserved site histidine forms bond with sessile phosphate, resulting in the formation of phospho- histidine intermediate while in second step of the reaction, conserved active site aspartic

acid abstracts a proton from water molecule and hydrolyzes the phospho- histidine intermediate [32]. According to the recent findings, all HAPs are not phytases and substrate specificity depends largely on substrate specificity site of the protein [37].

Recently two new members of the class histidine acid phosphatase are reported by *Juan Antonio et al* (2012) from *Bifidobacteri*um with slight modification in active site pattern i.e. RHGSRXX in place of RHGXRXP [3].

2.10.2 Beta propeller phytases

As the name of the enzyme indicates, structure of these enzymes is like propeller made up of 6 beta strands [37]. Initially, these enzymes were identified in *Bacillus* sp. [38] and it was considered that they are not widely distributed in nature [38], but in 2007 reports showed that a vast majority of BPPs are found distributed in the marine environment. Beta propeller phytases are strictly dependent on Ca+ ions for their mechanism of action, although various divalent cations can substitute Ca+ but none is as effective as calcium [32]. BPPs have two binding sites: affinity site and cleavage site and they only act on the substrates which bind in both binding sites simultaneously. For this reason the major degradation product of BPPs is IP3 [32].

2.10.3 Purple acid phosphatases

Phytases of this class have active site pattern of purple acid phosphatases. These are metallo proteins and have binuclear metal centre [37]. Phytases of this class show low enzyme activity for IP6, only reported PAP from soyabean show significant phytase activity [32, 37]. Structural features and mechanism of these phytases are extensively studied. These metalloenzymes form homodimer and each monomer has N-terminal antiparallel beta strands and large C-terminal α+β domain. 2-α helix of each monomer interacts to form the dimer [32].

2.10.4 Protein tyrosine phosphatase like phytase

This class of phytases is recently described; these are also called as cysteine phytases because of conserved active site cysteine residue. Conserved active site pattern of this class is HCXXGXXRT or C X_5R(S/T) [32]. Active site signature sequence forms a P-loop or phosphate binding loop and a mobile general acid loop (GA-loop) having a conserved aspartic acid residue which works as a proton donor during enzyme reaction [32]. PTPLPs were first reported in a rumen microbes and reports suggest that PTPLPs are the predominant phytases in rumen [1, 39]. Whereas various pathogens are also reported to have PTPLPs like *Clostridium* sp., *Pseudomonas*

syringae, *Xanthomonas campestris* and the predatory bacterium *Bdellovibrio bacteriovorus* [40]. The exact function of PTPLPs is not known but they are involved in pathogenesis in *Pseudomonas syringae* [41].

2.11 Phytases in food

Phytate is the major form of phosphate storage in cereals and legumes and other food of plant origin. Table 2.1 summarises the content of phytate in different food articles.

Table 2.1: Phytate content in different food articles.

Food types	Phytate (mg/g)
Cereals	
Rice (polished, cooked)	1.2–3.7
Rice (unpolished, cooked)	12.7–21.6
Maize bread	4.3–8.2
Unleavened maize bread	12.2–19.3
Wheat bread	3.2–7.3
Unleavened wheat bread	3.2–10.6
Rye bread	1.9–4.3
Sourdough rye bread	0.1–0.3
French bread	0.2–0.4
Flour bread (70% wheat, 30% rye)	0.4–1.1
Flour bread (30% wheat, 70% rye)	0–0.4
Cornflakes	0.4–1.5
Oat flakes	8.4–12.1
Pasta	0.7–9.1
Sorghum	5.9–11.8
Oat porridge	6.9–10.2
Legume-based food	
Green peas (cooked)	1.8–11.5
Soybeans	9.2–16.7
Tofu	8.9–17.8
Lentils (cooked)	2.1–10.1
Peanuts	9.2–19.7
Chickpea (cooked)	2.9–11.7
Cowpea (cooked)	3.9–13.2
Black beans (cooked)	8.5–17.3
White beans (cooked)	9.6–13.9
Kidney beans (cooked	8.3–13.4
Miscellaneous	
Sesame seeds (toasted)	39.3–57.2
Soy protein isolate	2.4–13.1
Soy protein concentrate	11.2–23.4
Buckwheat	9.2–16.2
Amaranth grain	10.6–15.1

High content of phytate in the seeds and grains forms highly concentrated feed for poultry and other livestocks. This excess of phytate binds minerals and proteins and form unabsorbable complexes, whereas monogastric animals lacks any phytate degrading enzyme in their gut [32].

Anti-nutritive properties of phytate lower the nutrition value of the food. Undigested phytate complexes excrete out and run off in soil and water bodies, where degradation by algal or fungal enzymatic activity leads to eutrophication (i.e. algal bloom) and phosphorus pollution problem [42] [43]. Addition of phytate degrading enzymes has been successfully used in the livestocks. Supplementation of phytase in food reduces the phytate excretion upto 90% [44].

Iron deficiency has been a widespread nutrition problem. Amount of iron absorbed in the body depends on iron uptake and its absorption in gut. To solve the deficiency problem, iron supplementation is given in food or as a pharmaceutical preparation [35]. But these strategies are not very successful in reduction of iron deficiency [35]. The Major cause of iron deficiency is high phytate content in cereals and legumes based diets. One sustainable solution to this problem is high phytase production in transgenic plants [45].

In aquaculture industry, fishmeal is very expensive and there is a need of alternative feed options of plant origin, but high phytate content of plant origin diet limits there usage as fishmeal. Addition of phytase by any means, to plant based feed can reduce this problem successfully. Also, it would reduce phosphorus pollution by reducing excretion of phytate in the fish waste.

2.12 Strategies used to overcome the anti-nutritive effect of phytate in food

2.12.1 Transgenic plants

One strategy to overcome the phytic acid problem in animal feed is cloning and expression of bacterial phytases in plants and utlilization of transgenic crops as animal feed. Various transgenic crops has been developed as bioreactor of bacterial phytase e.g. appA protein of *E.coli* was cloned in transgenic algae *Chlamydomonas reinharditi* [46]. Similarly, *Aspergillus niger* phytase was cloned in *Arabidopsis* [47]. *phyA* gene of *Aspergillus fumigates* was successfully cloned and expressed in rice endosperm for better availability of iron from the rice. Feeding transgenic crop based food to animals has shown as effective results as supplementation of microbial phytases to animal food [35].

2.12.2 Addition of phytases as a food supplement

Addition of phytase as a food supplement is widely used method to overcome nutrient deficiency due to phytic acid. Various microbial phytases are commercially available as animal feed supplement. Table 2.2 shows commercially available phytases in market.

Table 2.2: Commercial phytases available in market as a feed supplement.

Commercial product®	Company	Phytase type	Phytase source
Finase®	ABVista	3-phytase	*Trichoderma reesei*
Finase® EC	ABVista	6-phytase	*E. coli* gene expressed in *Trichoderma reesei*
Natuphos®	BASF	3-phytase	*Aspergillus Niger*
Natuzyme	Bioproton	phytase (type not specified)	*Trichoderma longibrachiatum /Trichoderma reesei*
OPTIPHOS®	Huvepharma AD	6-phytase	*E. coli* gene expressed in *Pichia pastoris*
Phytase sp1002	DSM	3-phytase	A Consensus gene expressed in *Hansenula polymorpha*
Quantum®2500D, 5000L	ABVista	6-phytase	*E. coli* gene expressed in *Pichia pastoris* or *Trichoderma reesei*
Ronozyme® Hi-Phos (M/L)	DSM/Novozymes	6-phytase	*Citrobacter braakii* gene expressed in *Aspergillus oryzae*
Rovabio® PHY	Adisseo	3-phytase	*Penicillium funiculosum*

(Image source: http://www.google.com/patents/WO2013102430A1?cl=en)

As dscribed before addition of phytase in animal feed can reduce phytate excretion upto 90% [48] , hence addition of microbial phytases in food provides solution to the antinutritive effect of phytate. But most of the commercially available microbial phytases are unacceptable as human food supplement. And there is still need of safer sources for human food supplementation.

2.12.3 Phytase producing probiotics

Probiotics are the health beneficial microbes and generally regarded as safe for human consumption. Phytase producing probiotic microbes can present a safe and effective solution for the need of human consumable phytase supplement.[49, 50] Knowledge of indigenous phytase in probiotic genera is very limited hence various studies have shown cloning of heterologous phytase genes in *Lactobacilli* and there use as food additive. *Zuo et al* have done cloned *Aspergillus ficcum* phytase in *Lactobacillus casei* [51]. *Askelson et al* have shown cloning of *Bacillus subtilis* phytase in various *Lactobacilli* and their supplementation as food additives that have improved the health of the chickens [2].

Few recent studies have reported phytases from probiotic microbes. *Ramos et al* (2012) [3] have reported novel phytases of class histidine acid phosphatase from *Bifidobacterium longum* and *Bifidobacterium pseudocatenulatum*. *Stentz et al* (2014) [4] have reported mammalian inositol poly phosphate phosphatase like phytase from gut inhabiting *Bacteroides thetaiotaomicron.* High

safety profile of probiotic microbes make them acceptable for human consumption. Also phytase producing probiotic microbes can be directly supplemented as food additive and there is no need of enzyme purification and downstream processing. As *Lactobacilli* are aerotolerant and easy culturable probiotic microbes and most widely used probiotic genera, phytase producing *Lactobacilli* can prove safe and effective supplement for human food. Various studies have reported phytase production from *Lactobacilli* but still there is a lack of genetic and molecular knowledge and strong experimental proofs for the property as some reports suggested non specific acid hydrolysis and lack of true phytase activity [52].

According to WHO global status report on non communicable diseases 2014, cardiovascular diseases (CVDs) are leading cause of deaths worldwide and are one of the four major non-communicable diseases (NCDs) [6]. CVDs are predicted to remain the leading cause of deaths by 2030, affecting 23.6 million lives around the world [6]. Out of various other factors, hypercholesterolemia is the major causes of CVDs. Hypercholesterolemia increases the risk of heart attack three times more than the normal cholesterol level [6]. Hence, blood cholesterol level management is indispensable to reduce the global mortality rate due to CVDs. The major factors affecting the blood cholesterol level are due to improper food habits, ingestion of high fat diets, stagnant life style, family history and increasing age. Since cholesterol is an essential component of body tissues and required in normal body functioning, its level management is complicated as excess cholesterol reducing drugs may affect the normal body function. Various pharmacological and non-pharmacological methods are available to control hypercholesterolemia but still there is need of more safer and effective methods as cholesterol lowering drugs are expensive and show adverse side effects [7]. Cholesterol consuming probiotic bacteria may provide safe and cost effective solution to the problem. But efficacy and mechanistic insight of this method is yet to be proven/worked out. Major drawback in application of probiotics is inconsistencies in the results [53]. Certain strains show hypocholesterolemic effect in animal models but they fail to reproduce the same effect in human models, also few strains are proved to be effective in one human trial, fail to repeat the effect in other study e.g. administration of *Lactobacillus acidophilus* GG to various populations in different studies have proved effective for some populations but not for all [53]. Further, lack of the knowledge of exact mechanism of action restrains/limits the assessment of strain specific hypocholesterolemic effect and its efficacy and dosage needed in different physiological conditions.

Human intestine takes up ~1g cholesterol per day, including dietary cholesterol intake and cholesterol synthesized in liver, near about half of that is reabsorbed in intestine (there is huge variation in reabsorption value per individual) [53]. Cholesterol is consumed in the formation of different cell membranes; it is precursor of bile, steroid hormone and vitamins. Bile and cholesterol are ported into intestine from where either they are reabsorbed or excreted out. Hence, balance of blood cholesterol level is maintained by daily input and output. Normal blood cholesterol level is 0.3g/dL, which is regulated by the liver. Two major pathways of cholesterol excretion proposed in animal body are:

1) Biliary excretion of excess cholesterol, in which cholesterol is converted into bile salts and part of it is reabsorbed in intestine and unabsorbed bile is excreted out of body [7].

2) Direct excretion of unabsorbed dietary and biliary cholesterol from intestine. Besides,, according to some recent studies, a pathway called transintestinal cholesterol efflux (TICE) in animal models like mice was to account for 70% of total neutral faecal sterol excretion. But contribution of TICE in cholesterol excretion in human is still to be verified [7].

The biliary mode of cholesterol excretion is quantitatively more important in normal physiological condition than TICE [7]. It is well established that intestinal microbiota metabolizes cholesterol, as germ free mice excrete out unmodified cholesterol while in conventionally raised mice cholesterol is converted into coprostanol by microbial activity in the gut [8]. Hence, microflora metabolizes cholesterol and limits its availability to host but extent of this effect is directly proportional to the ratio and population size of cholesterol assimilating microbes in gut microflora. Although exact mechanism of cholesterol lowering effect of symbiotic flora is not known but several hypothesis has been proposed including bile salts hydrolysis by probiotic bacterium, co-precipitation of cholesterol with bile, cholesterol uptake by gut flora and conversion into coprostanol or incorporation in bacterial cell membrane [53].

2.13 Bile salt hydrolysis

Bile salt hydrolysis by probiotic bacteria is mediated by bacterial bile salt hydrolase (BSH) enzyme [54]. Several bile salt hydrolases are reported from lactic acid bacteria including *Lactobacilli*. Hydrolysis of bile salts forms bile acids; bile acids are less water soluble and less likely to get absorbed than the bile salts hence excreted out of intestine [53]. Also, bile is required for the micelle formation for lipid digestion; degradation of the bile inhibits micelle formation and reduces fat absorption from gut. Degradation and excretion of bile out of intestine instigates cholesterol consumption in *de novo* bile synthesis in liver. This eventually reduces blood cholesterol [53]. Various studies have reported reduction in blood cholesterol level by BSH producing microbes, but inconsistent results and inefficacy in human trial are also reported [53]. Various strains of lactic acid bacteria are reported to assimilate the cholesterol from laboratory medium, in few species cholesterol assimilation is noticed to occur in the presence of bile only, e.g. *Lactobacillus acidophilus* was reported to assimilate cholesterol in anaerobic condition and presence of bile. (Gilliland et al, 1985) suggested that these conditions mimic physiological

condition of intestine. Hence, this property would enable the bacteria to assimilate cholesterol in the intestine [55]. Exact mode of cholesterol assimilation by LAB is not known till date. Some researchers have suggested co-precipitation of cholesterol in the presence of deconjugated bile at low pH, could be the reason of cholesterol removal from media (Tahri et al. 1995). As in a study Klaver and Van der meer (1993) showed that even in the absence of bacterial cells, cholesterol co-precipitation occurs in culture medium in presence of deconjugate bile acid at pH 5.5. Although precipitated cholesterol redissolves after adjusting the pH of the solution 7, but since small intestine pH is higher than 6, this mechanism does not seem to be involved *in vivo*[55]. Further investigation of *in vitro* cholesterol consumption by six *Lactobacillus acidophilus* strains was done by Meei-YN Lin, 2000. They reported upto 57% cholesterol uptake by *Lactobacillus acidophilus* ATCC4356, when grown anaerobically in a medium supplemented with bile. Authors concluded that *in vivo* cholesterol reduction by *Lactobacillus acidophilus* occurs due to direct assimilation of cholesterol and not due to co-precipitation with bile acid as pH of intestine is neutral to alkaline. In an another study, Walker and Gilliland examined *in vitro* bile tolerance, bile deconjugation and cholesterol removal capacity of 19 *Lactobacillus acidophilus* strains and they found no significant correlation in bile deconjugation, bile tolerance and cholesterol assimilation by *Lactobacillus acidophilus* [56]. Hence, there could be other mode of direct cholesterol assimilation and cholesterol lowering effect of LAB.

2.14 Cholesterol assimilation

Although cholesterol conversion into coprostanol by the gut microbial activity has been known from 1930s [57] but very few information is available about mechanism of action and microbes involved in this conversion. Coprostanol is a lesser absorbable form of cholesterol, which excretes out in faeces [58, 59]. Some amount of cholesterol assimilated by gut flora is incorporated in bacterial cell membrane. Hence, cholesterol assimilation by gut flora helps in the reduction in cholesterol absorption in intestine. Two pathways are proposed for the microbial conversion of cholesterol into coprostanol.

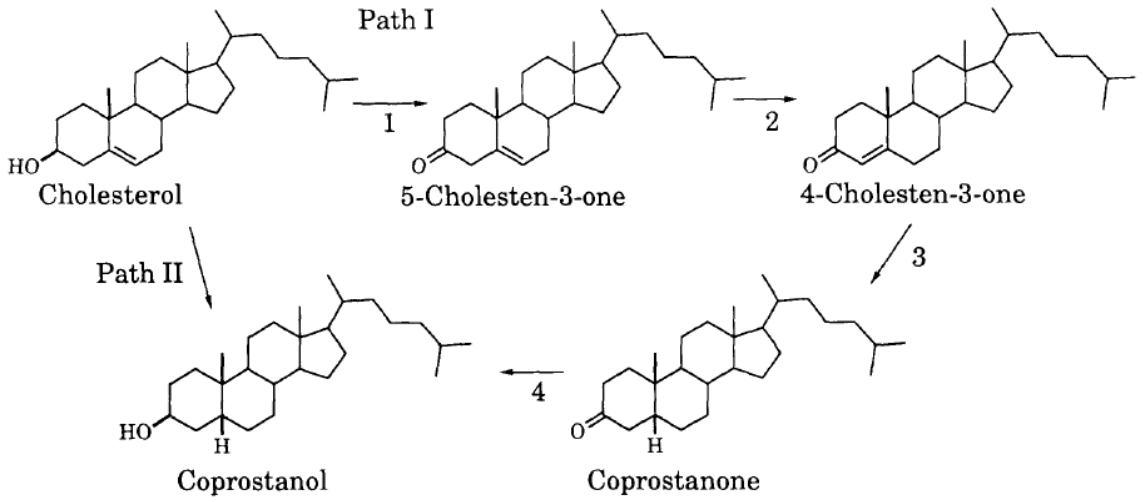

Figure 2.2: Proposed pathway for conversion of cholesterol into coprostanol.

As described in Fig.2.2 Path one shows cholesterol conversion by intermediate formation of cholestenone and coprostanone while Path two shows direct cholesterol conversion into cholesterol by reduction of Δ^5 double bond. *Björkhem et al.* (1971) studied anaerobic conversion of radiolabelled cholesterol into coprostanol by incubation with rat ceacal content and the study reported various significant findings [58]. They reported path 1 is the main mode of coprostanol formation because of the presence of intermediates cholestenone and coprostanone in incubation mixture [58]. Also, incubation of radiolabelled cholestenone with caecal content resulted in the formation of coprostanol. The study further reported that the first reaction i.e. oxidation of 3β-hydroxyl group as a crucial rate limiting step of total conversion of cholesterol into coprostanol. Hence, this study reported in the presence of enzymes involved in coprostanol formation, in rat ceacal flora metabolome in Path 1.

Dewei et al (1996) reported cholesterol conversion into coprostanol by *Eubacterium coprostanoligens* ATCC51222 under anaerobic conditions via path 1 i.e. by intermediate formation of cholestenone, and in absence of cholesterol reductase activity [11]. In 2007, *Gerard et al* reported conversion of cholesterol into coprostanol anaerobically by *Bacteroides* sp. strain 8, a member of common gut inhabiting genera *Bacteroides* [57]. This study also reported conversion pathway involved is path1. Also, no cholesterol reductase activity was detected. In 2010, *Lye et al* reported extracellular and intracellular cholesterol reductase activity from various *Lactobacilli* [9]. But no polypeptide sequence or genetic information was given for the enzymes. Conclusively, very few reports are available for microbes involved in cholesterol conversion into coprostanol, while

no genetic or molecular information is known till date. Most of the studies reported cholesterol conversion by intermediate cholestenone formation. First step of this pathway is similar to the oxidative catabolization of cholesterol, i.e. dehydrogenation of 3β hydroxyl group. Enzyme involved in this reaction should be rate determining for anaerobic cholesterol conversion [58]. Two possible enzymes are reported to be involved in this reaction; FAD dependent cholesterol oxidase or NAD or NADP dependent 3β hydroxysteroid dehydrogenase (3β HSD) [60]. Presence of cholesterol active enzyme either of these class in genome and proteome of gut inhabiting microbe may suggest mode of cholesterol consumption by the microbe. Also it would provide prospects for elucidation of proteomic and genetic insight of the pathway.

Agriculture is known to be the backbone of most of the developing countries providing food for the humans in a direct or indirect manner. Farming is an art of producing food, feed, fiber and many other edible products by means of cultivating particular plants and raising livestocks. The world population is on a steady rise and is expected to reach 9 billion by 2050, which certainly demands the global agricultural productivity to keep pace with the rising demand of the population. With rapid urbanization across developed countries food handling system has changed to meet the food demand of the population. This magnitude of demand for food has increased the steps in handling the food; extending its storage, processing and distribution further in the food chain, thus creating new ecological niches to which the microorganism from different geographic location may adapt and raise problem for the food industries to solve. The chances of food contamination increase with time. Therefore, it is of interest to extend the shelf life of the food product to avoid economic losses, to ameliorate the incidences of food borne illness and to meet the demand of the growing world population by the use of preservatives.

2.15. Chemical and Biological preservation method

Although chemical preservatives are being extensively used, but there is an increased concern over the consumptions of these foods, thus, creating a demand for unprocessed or minimally processed food. Therefore, there has been great interest in antimicrobial agents produced by biological means i.e microorganism. Biopreservation is a method by means of which food products shelf life is extended along with the enhanced food safety by using natural or controlled microflora or their antimicrobial products [61]. Among the broad range of antibacterial products released by the microorganisms, bacteriocins especially produced by lactic acid bacteria (LAB), including the genera *Lactobacillus, Lactococcus, Enterococcus, Streptococcus, Pediococcus, Leuconostoc* and *Bifidobacterium,* have attracted the much of the attentions as a tool for food preservation.

2.16 Bateriocin as biological antimicrobial agent

Bacteriocins are ribosomally synthesized antimicrobial peptides or proteins [62]. Bacteriocins are nontoxic to eukaryotic cells and are generally recognized as safe substances. LAB are well known for their capacity to produce bacteriocins [63, 64]. Given the high prevalence and pivotal roles that this group of bacteria plays in food and health, structure, biosynthesis, genetics, and food application of LAB bacteriocins have been studied extensively [65-67]. *Enterococci*

belonging to a category of LAB that are gaining popularity. They produce bacteriocins that belong to the class II bacteriocins and are small, hydrophobic, thermo-stable, wide pH range stable and active against many Gram-positive bacteria such as *Clostridium spp*., *Staphylococcus spp*., *Listeria spp*., *Bacillus spp*. and a few Gram-negative ones [68]. Enterocin, produced by *Enterococcus faecium* FH99 is a 6.5kDa bacteriocin which has antibacterial activity against a myriad of Gram-positive bacteria, including the major food borne pathogen, *Listeria monocytogenes* and other lactic acid spoilage bacteria [44]. The mode of action of bacteriocin ranges from the pore formation in the cytoplasmic membrane, inhibition of cell wall synthesis and inactivation of enzymes. Different strategies have been adopted for the application of bacteriocin in food: addition of the bacteriocin or the addition of bacteriocin producing strains.

2.17 Antibacterial drug resistance

Extensive and injudicious uses of antibiotics have lead to the emergence of antibiotic resistance and public health crisis[69, 70]. Also development of antibiotic resistance is compounded by factors like slow drug development pipeline and limited investment in drug discovery. Bacterial resistances to bacteriocin (Nisin) has been reported in literature for *Staphylococcus aureus*, *Streptococcus bovis* and *Listeria monocytogenes* [71]. The knowledge of mechanism of resistance towards bacteriocin is limited compared to the antibiotics. Although some reports have shown the resistance mechanism targeted to the manosephsophotransferase (Man-PTS) system which act as the receptor for most of the bacteriocins. Downregulation of Man-PTS gene expression have been shown to be responsible for bacteriocin resistance in *Listeira monocytogenes* [72]. As the conventional antimicrobial drugs have failed to control the diseases caused by the MDR strains, therefore there is direct need of novel antimicrobial agent to confront the challenges imposed by these superbugs. Therefore, utilization of modern technologies such as nanotechnology and nanobiotechnolgy may be necessary to the field of agriculture and food science [73-75].

2.18 Nanotechnology in food preservation

Nanotechnology involves the characterization, fabrication and or manipulation of structures, devices or materials that have at least one dimension [76-78](or contain components with at least one dimension) that is approximately 1–100 nm in length [79]. When particle size is reduced below this threshold, the resulting material exhibits physical and chemical properties that

are significantly different from the properties of macroscale materials composed of the same substance. Since its emergence, nanotechnology has revolutionized the scientific world [79]. There are hardly any branches of science and technology where it does not put its impression. The magical touch of nanotechnology not only enriches the field of modern medicine and cosmetics but also establishes its presence in food, environmental remediation, conserving renewable energies, protecting medical devices from the pathogenic microorganisms [80, 81]. In 2008, investment on nanotechnology was over $15 billion worldwide in research and development (public and private) and over 400,000 researchers were employed across the globe [82]. Nanotechnologies are projected to impact at least $3 trillion across the global economy by 2020, and nanotechnology industries worldwide may require at least 6 million workers to support them by the end of the decade [82]. Despite the excitement surrounding nanotechnology and the abundance of funding dollars being poured into it, however, one industry which has been slow to catch on is the food industry. Although public opinion about nanotechnology stands between neutrality to slightly positive [83]., consumer are still sceptical about application of nanotechnology in food [84]. Nevertheless, application of nanotechnology has been appreciated by scientists and industrialists in virtually every sector of food industry (Fig 2.3) from agriculture (pesticides detection; and targeted genetic engineering) to food processing (e.g., encapsulation of flavor or odor enhancers; food textural or quality improvement; new gelation or viscosifying agents) to food packaging (e.g., pathogen, gas or abuse sensors; anticounterfeiting devices, UV-protection, and stronger, more impermeable polymer films) to nutrient supplements (e.g., nutraceuticals with higher stability and bioavailability) [85-87]

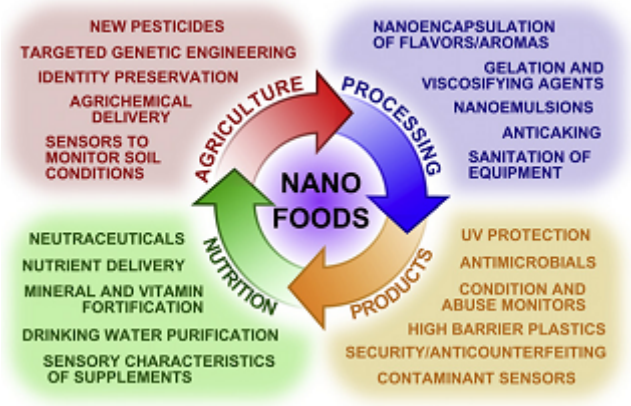

Figure 2.3: Multiple aspects of nanobiotics

Undeniably, the most active area of food nanoscience research and development is packaging: the global nano-enabled food and beverage packaging market was 4.13 billion US dollars in 2008 and has been projected to grow to 7.3 billion by 2014, representing an annual growth rate of 11.65% (http://www.innoresearch.net/report_summary). This is likely connected to the fact that the public has been shown in some studies to be more willing to embrace nanotechnology in ‘‘out of food’’ applications than those where nanoparticles are directly added to foods [88]. Despite an explosion of growth in this area, food nanotechnology is still a lesser-known subfield of the greater nanotechnology spectrum, even among professional nanotechnologists.

Nanomaterials in the form of nanorods, nanospheres, nanoscaffolds and a variety of nanoparticles (NPs) are eligible candidates contributing to applications such as solar energy conversion, medicine, catalysis, electronics, optics, environmental, water treatment [89] and biomedicine [90]. Metal NPs are of special interest due to their property of surface plasmon resonance in the UV-visible region [91]. Modifications in NPs via functionalization with biocompatible materials have made NPs potential candidates for cancer diagnosis and treatment. They have also proven to be promising bio-imaging agents when conjugated to fluorescent molecules. [92] The unique physical properties of nanoparticles have been utilized for diverse applications which are important to improve the quality of human life.

2.19 Silver nanoparticles

Silver is known for its antibacterial activity since time immemorial. Silver is still used clinically, though the formulation of silver has changed from bulk silver in coins through ionic silver to currently being used in the form of nanosilver. Silver, whether in ionic or nanoparticle form, is toxic to microorganisms [93]. The toxicity of silver is highest amongst the metals and follows the order: Ag > Hg > Cu > Cd > Cr >Pb > Co > Au > Zn > Fe > Mn > Mo > Sn [94]

Silver based nanoparticles (AgNPs) have gained an increasing attention now because of its extraordinary physicochemical and biological properties. In addition to its excellent electrical and thermal conductivity, it has good chemical stability and catalytic potential. In terms of biological effect, silver based nanoparticles have broad spectrum antimicrobial potency. Because of this quality, AgNPs are extensively used in various consumer products of daily use, including plastics, soaps, pastes, food and textiles. Apart from this, the silver nanoparticles have been adopted by the healthcare industries as an anti-inflammatory agent [95], wound healer [96] and also for treatment

of burns [97]. In addition, silver in nano form evinces low toxicity to mammalian cells [94]. Various databases indicate that the research interest on AgNPs is escalating rapidly since last 10 years.

Ag-NPs have some big role to play in these circumstances because of its broad spectrum antimicrobial activity as and low toxicity. Various research articles show that Ag-NPs are effective against a wide variety of microorganisms. The efficiency of the nanoparticle depends on its quality, in particular its size and physicochemical properties [98, 99]. Therefore, an efficient and economically feasible method of synthesis is the key to success of silver based nano-biotechnology research. There are multiple approaches that have been developed and followed by various research groups across the globe. The most frequently used methodology of synthesizing Ag-NPs includes chemical synthesis, physical synthesis, photochemical synthesis and biological synthesis [100-107].

Studies have concluded that silver nanoparticles offer better antibacterial activity as they allow more effective contact with bacteria due to their large surface area property. The possible ways silver nanoparticles exert their antimicrobial activity after interacting with bacterial cells is by (a) release of silver ions and generation of reactive oxygen species (ROS); (b) interaction with membrane protein and disrupting its function; (c) disturbing the cell membrane permeability by accumulation; (d) entering into the cells, releasing the silver ions and generating ROS thus causing DNA damage [108, 109]. Because of these distinct antibacterial properties, several rapid and efficient methods for silver nanoparticle synthesis have emerged as a research area of interest for biomedical applications. [99, 110, 111]. Several reports of biological synthesis using bacterial cells, fungi and plant extracts have shown to mediate the silver nanoparticle formation [112]. On the basis of these biosynthetic mechanism, different biological molecules such as proteins [113],peptides [114, 115], antimicrobial peptides [116] [117], carbohydrates and antibiotics [117, 118] [119] have been explored to direct the molecular control of silver nanoparticles. Additionally, a combination of biomolecules with inorganic compounds have led to the development of novel particles with merged functional properties of both the compounds.

Developments in nanotechnology have provided means to modify nanomaterials and in turn their properties thus, giving an opportunity to modulate the antibacterial spectrum [120-122]. Silver NPs by themselves have great antibacterial potential yet it will be desirable if enhancement of their antibacterial activity can be accomplished. Amongst the many, one of the suitable

contenders for this augmentation is their conjugation with bacteriocins. Bacteriocins (antibacterial peptides) capped SNPs could be used against a number of Gram-negative and Gram-positive food-borne bacterial pathogens.

In the present study, an attempt has been made to potentiate the antibacterial spectrum of silver NPs and enterocin exploiting the nanotechnological principles to synthesize enterocin capped silver nanoparticles (En-SNPs). The generalized scheme for the preparation of En-SNPs is depicted in Figure 1. The antibacterial potential of nanoparticles has been evaluated against a number of food borne pathogens. In order to understand the mechanism of action of En-SNPs, interaction studies with the outer membrane protein of representative Gram-negative and Gram-positive bacterial strains have been carried out. In this study, we report green synthesis, antibacterial potential and interaction of bacteriocin capped silver NPs with bacterial membrane proteins.

CHAPTER 3
MATERIAL AND METHODS

3.1. Materials

3.1.1. Media

3.1.1.1. MRS broth

52.2 g MRS broth powder (Merck, Germany) was dissolved in 500 ml of distilled water and final volume was adjusted to 1000 ml with distilled water. The liquid media was autoclaved at 121 °C for 15 min.

3.1.1.2. MRS-thiolglycolate agar

55 g MRS broth powder (Merck, Germany) was dissolved in a litre of distilled water and supplement it with 0.05% sodium thiolglycolate (Himedia, India).1.5% agar-agar powder (Himedia, India) was added to the suspension and autoclaved at 121°C for 15 min and plates were prepared.

3.1.1.3. TOS-propionate-Li-Mupirocin agar

6.93 g of TOS-priopionate agar base (Merck, Germany) was dissolved in 95 ml of distilled water with constant heating and stirring until the agar base dissolves completely and autoclave it at 121°C (15 lb/in^2) for 15 min. The base medium was allowed to cool in a waterbath kept at 48°C. Lithium-mupirocin supplement was added aseptically to the cooled base medium with final concentration of 50 µg/ml and agar plates were prepared.

3.1.1.4. Reinforced Clostridial medium (RCM)

50 g of reinforced clostridial agar powder (Himedia, India) was dissolved in to a 500 ml of distilled water. Final volume was adjusted to 1000 ml with distilled water. The liquid media was autoclaved at 121°C (15 lb/in^2) for 15 min.

3.1.1.5. MRS-bromocresol purple (MRS-BCP) agar

55 g MRS broth powder (Merck, India) was dissolved in 1000 ml of distilled water and supplemented with 0.4 µg/ml final concentration of bromocresol purple (Himedia, India). 1.5% agar-agar powder (Himedia, India) was added to the suspension and autoclaved at 121°C (15 lb/in^2) for 15 min and plates were prepared.

3.1.1.6. MRS-phyate agar

55 g of MRS broth powder (Merck, India) and 15 g of bacteriological agar were dissolved into 500 ml of distilled water and final volume was adjusted to 1000 ml with distilled water. The media was autoclaved at 121°C (15 lb/in^2) for 15 min. After autoclaving, MRS agar was cooled down to 50°C and supplemented with filter sterilized sodium phytate (4 g/l) and calcium chloride (2 g/l) before preparing the plates.

3.1.2. Reagents and buffers

3.1.2.1. Grams staining kit (Merck, Germany)

Primary stain; crsytal violet solution, mordant; gram's iodine solution, decolourizer; 95% ethanol, counter stain; safranin solution.

3.1.2.2. Plasmid isolation buffers

*S1: 50 mM glucose, 10 mM EDTA, 25 mM Tris-HCl of pH8.

S2:1% SDS, 0.2N NaOH.

S3: 3M Sodium acetate

3.1.2.3. Protein purification buffers

3.1.2.3.1. Lysis buffer

Reagents	Concentration
Tris-HCl buffer (pH 8)	20 mM
Glycerol	10%
NaCl	300 mM

Imidazole	5 mM
Lysozyme	200 µg/ml
RNase	5 µg/ml
DNase	10 µg/ml

3.1.2.3.2. Equilibration buffer (pH 8)

Reagents	**Concentration**
Tris-HCl buffer (pH 8)	20 mM
Glycerol	10%
NaCl	300 mM
Imidazole	10 mM

3.1.2.4. Wash Buffer 1 (pH 8)

Reagents	**Concentration**
Tris-HCl buffer (pH 8)	20 mM
Glycerol	10%
NaCl	300 mM
Imidazole	20 mM

3.1.2.5. Wash Buffer 2 (pH 8)

Reagents	**Concentration**
Tris-HCl buffer (pH 8)	20 mM
Glycerol	10%
NaCl	300 mM
Imidazole	50 mM

3.1.2.6. Elution Buffer (pH 8)

Reagents	**Concentration**
Tris-HCl buffer (pH 8)	20 mM
Glycerol	10%
NaCl	300 mM
Imidazole	300 mM

3.1.2.7. Polyacrylamide gel electrophoresis (PAGE)

Solution A: A stock solution of 29 % (w/v) acrylamide and 1 % (w/v) bisacrylamide premix was used from Himedia.

Solution B: Resolving gel buffer, 1.5 M Tris-HCl pH 8.8

Solution C: Stacking gel buffer, 1.0 M Tris-HCl pH 6.8

Solution D: 10 % (w/v) SDS in distilled water

Solution E: 10 % ammonium per sulphate (APS freshly prepared) in distilled water

Solution F: N, N, N,'' N''- tetramethylenediamine TEMED

3.1.2.8. Table 3.1: Composition and preparation of 12% SDS-PAGE gel

Reagents	Resolving gel 12 % (ml)	Stacking gel-5 % (ml)
Solution A	4	0.5
Solution B	2.5	--
Solution C	--	0.38
Solution D	0.1	0.02
Solution E	0.1	0.02
Solution F	0.004	0.003
Distilled water	3.3	2.5
Total volume (ml)	**10**	**3**

3.1.2.9. Table 3.2: Composition of preparation of SDS-PAGE sample buffer

Reagents	Volume (ml)/Weight (mg)
Distilled water	4 ml
0.5 M Tris HCL	1.25 ml
50 % glycerol	2 ml
10 % SDS	2 ml
Bromophenol blue	1.5 mg
β- mercaptoethanol	0.5 ml

3.1.2.10. Sodium borohydrate (100 mM)

37.8 mg of sodium borohydrate salt (Merck, India) was dissolved in 10 ml of milliQ water. This solution was prepared freshly.

3.1.2.11. Bacterial strain used in this study

Enterococcus faecium FH99, *Pediococcus acidilactici* LB42, *Escherichia coli* ATCC 25922, *Bacillus cereus*, *Klebsiella pneumoniae*, *Listeria monocytogenes*, *Micrococcus luteus*, *Shigella flexneri* and *Staphylococcus aureus.*

3.1.3. Oligonucleotides

Table 3.1 List of oligonucleotides used in this study

Name	Sequences (5' to 3')
phyF	AAT CCATG G TGACCACCGTGTCTTTAAATCGC
phyR	CATAAGCTTTTAATGATGATGATGATGATGAATGAGGTAGAGTTGTTTGAG
hsdF	TTACATATGTTGATTACCGTCACCGGGGC
hsdR	CAT AAGCTTTTAATAGAAGGAAGGCTTATCGCC

3.2. Methods

3.2.1. Isolation of lactic acid bacteria (LAB)

Dairy samples were collected from diverse sites/locations and extreme ecological conditions. Selective isolation of lactic acid bacteria was done in deMan, Rogosa and Sharpe (MRS) medium (Merck, Germany) supplemented with 0.05% sodium thiolglycolate. In brief, the samples were serially diluted in sterile 1X phosphate buffer saline (PBS) and spread on MRS-thiolglycolate plates. Further the plates were incubated at 37^{o}C for 24 to 48 h. Colonies with different morphologies were picked and sub-cultured on fresh MRS plates.

For isolation of obligate anaerobes from dairy and infant faeces, samples were diluted in 1X PBS and spread on MRS-thiolglycolate agar and Bifido selective TOS-propionate agar

supplemented with 50 µg/ml Mupirocin (Merck, Germany). The plates were further incubated at 37^{o}C in anaerobic chamber/jar with gas-pack (Merck, Germany) for 48 to 64 h. After incubation, colonies with different morphologies were picked and subcultured on Reinforced Clostridial agar (Merck, Germany).

3.2.2. Identification of isolated lactic acid bacteria (LAB)

3.2.2.1. Morphological characterization by Gram staining

A thin smear of the test bacterium was made on to a glass slide by suspending a single colony of test bacteria in a drop of 1X PBS. The prepared smear was allowed to air dry and the bacterial cells were heat fixed onto the slide. After fixing, the smear on the slide was covered with crystal violet solution for 1 min. The excess stain was washed off by placing the slide under the stream of slow flowing water. Later, the smear was covered with gram's iodine (mordant) for 1 min. After a min, mordant was drained under running water and the slide was decolorized by dripping 95% ethanol on smear until the alcohol runs almost clear. After decolorization, slide was washed with water and finally stained with safranin solution for 1 min and then washed with distilled water. Slide was left for air drying and then observed under 100X oil immersion objective of Nikon TX-eclipse inverted microscope.

3.2.2.2. Biochemical characterization

Preliminary biochemical characterization of the isolates was done for general characters of lactic acid bacteria.

3.2.2.2.1. Catalase test

Catalase activity of the isolates was examined by making smear of the isolates on a clean glass slide in a drop of 1X PBS. Fresh culture of the isolates was used to prepare smear. A drop of 3% H_2O_2 was placed on the smear and observed for bubble production. Bubble production indicates positive catalase activity in test isolate.

3.2.2.2.2. Acid production

MRS-BCP plates containing 0.4 µg/ml bromocresol purple (BCP) as pH indicator in MRS agar, were prepared for analysis of acid production by isolates. Test organisms were streaked on

MRS-BCP plates and incubated at 37^{o}C for 24 h. Acid production was analyzed by change in the color of indicator from red to yellow.

3.2.2.2.3. Microbial identification based on carbon assimilation by Biolog

Biochemical characterization of different isolates based on utilization of diverse carbon source was determined by Biolog phenotype GEN III and Biolog anaerobic AN-plates (MicroStation™ System/MicroLog Hayward, USA). Each well of the 96 well microtitre plate contained single carbon source, with appropriate positive and negative controls. Positive and negative substrate utilization activity was determined by taking OD of the developed color, at 590-750 nm. In brief, all isolates were resuspended in universal inoculating fluid IF-A (for GEN III plates) and IF-C (for AN-plates). Each well was inoculated with 100 µl of resuspended culture and incubated at 37°C for 24 to 48 h [123].

3.2.2.2.4. 16S rRNA gene amplification and sequencing

Genomic DNA isolation for different isolates was done by genomic DNA extraction kit (Himedia, India). Gene coding for 16S rRNA was amplified by a set of universal eubacterial 16SrRNA gene primers; 5'-AGAGTTTGATCMTGGCTCAG-3' (27F, forward) and 5'-CGGTTACCTTGTTACGACTT-3' (1942R, reverse). Composition of PCR reaction mixture used was as follows-

PCR mixture:

Reagents	**Volume (µl)**
10X reaction buffer	5 µl
2 mM dNTPs	5 µl
10 µM forward primer	1.5 µl
10 µM reverse primer	1.5 µl
Hotstar Taq-DNA polymerase (1 U/ µl)	0.5 µl
Nuclease free water	35 µl
Template (Genomic DNA)	1µl (50ng)
Total	50 µl

PCR amplification of 16S rRNA gene was done using following program.

PCR program

Steps	Temperature (°C)	Time (min)
1	95	5
2	95	1
3	55	0.45
4	72	1
	Repeat step 2-4 for 30 times	
6	72	10
7	4	Hold

Amplified 16S rRNA gene was purified by Qiaquick gel extraction kit (Qiagen, Netherlands) and sent for sequencing to Eurofins Genomics India Pvt Ltd. Sequencing results were analysed by aligning the amplified sequences with non redundant nucleotide sequence database, and 16S-rRNA gene sequences database of the GenBank using the Basic Local Alignment Search Tool (BLAST) algorithm available at NCBI.

3.2.3. Screening of isolates for phytase production

Phytase activity of each strain was investigated by point inoculation of each isolate on MRS-phytate plates. Precipitate of calcium phytate formed by chelation of calcium by phytate turns the plate turbid. All isolates were point inoculated on MRS-phytate plates and incubated at 37°C for 24 to 48 h for formation of zone of clearance around the test microbe, due to hydrolysis of calcium phytate precipitates. Sometimes lactic acid bacteria produces zone of clearance around the colony due to acid production. To remove false acid zone plates were flooded with 2% aqueous cobalt chloride solution (w/v) and kept for 30 min at room temperature. After 30 min of incubation, $CoCl_2$ solution was replaced with freshly prepared solution containing equal volumes of 6.25% aqueous ammonium molybdate (w/v), 0.42% aqeous ammonium vanadate (w/v) and incubated for 5 mins at room temperature. Re-precipitation occurs in false acid zones on phytate plates while no re-precipitation occurs in zones formed due to phytate hydrolysis by phytase.

3.2.4. Screening of isolates for cholesterol lowering effect

For screening of cholesterol lowering effect 2% fresh overnight cultures of all isolates were inoculated in MRS broth containing 0.2% sodium thiolglycolate, 0.2% oxgall (Himedia, India) and 100 µg/ml cholesterol (Merck, Germany). Cholesterol is insoluble in water hence cholesterol stock solution (10 mg/ml) was prepared by adding 10 mg cholesterol in 950 µl isopropanol and 50 µl Tween-20 solutions. Further this mixture is added to the sterile medium just before the inoculation of test microbe. After inoculation, all cultures were incubated at 37^{o}C for 24 to 48 h and samples were drawn after every 12 h to estimate the amount of cholesterol reduced in MRS broth.

3.2.5. Cholesterol estimation

Cholesterol estimation was done by modified Rudel and Morris (1973) [124]. In this method, 500 µl of culture supernatant was taken in clean glass test tube and sequential addition of 3 ml of 95% ethanol and 2 ml of 50% KOH was done and mixed thoroughly for saponification of saponifiable lipids. All contents were incubated at 60^{o}C for 15 min and then cooled down. 5 ml hexane was added to each tube and mixed thoroughly followed by the addition of 3 ml distilled water to each tube. The tubes were allowed to stand for 60 min at room temperature (RT) for phase separation. After phase separation, 2.5 ml of upper hexane layer was drawn and placed in a fresh clean test tube. Hexane was evaporated at 60^{o}C under the flow of N_2 gas. The residual material was dissolved in 4 ml of o-phthalaldehyde reagent (50 mg o-phthalaldehyde / 100ml glacial acetic acid) and allowed to stand at room temperature for 10 mins. Thereafter, 2ml concentrated sulfuric acid was slowly added to each glass tube and kept at room temperature for 10 mins. Color developed after 10 mins was read at 550 nm. Percentage cholesterol removal was estimated by following formula:

$$\% \text{ Cholestrol removal} = \{Chl_{uninoculated} - Chl_{inoculated}\} \times 100$$

$Chl_{uninoculated}$ was OD of uninoculated medium and
$Chl_{inoculated}$ was OD of inoculated medium.

3.2.6. Screening for bile salt hydrolase production

Bile salt hydrolase (BSH) production by lactic acid bacteria was analyzed by streaking isolates on MRS-thiolglycolate and RCM agar plates supplemented with 0.5% oxgall for aerobic

and anaerobic cultures respectively. Plates were incubated at 37^{o}C for 48 h. Anaerobic cultures were incubated in Anaerocult® A mini gas pack (Merck, Germany) at 37^{o}C for 48 h. After incubation, the plates were analyzed for formation of zone of precipitation around bacterial growth. Hydrolysis of bile salts causes formation of insoluble precipitates around the colony of strains exhibiting bile salt hydrolase activity.

3.2.7. Standard curve for ammonia estimation by Nesseler's reagent

1.179 g ammonium sulfate was dissolved in 100 ml distilled water to prepare the stock solution. Working solution of 1 µmole NH_3 ml^{-1} was prepared by diluting 1.4 ml of stock solution to 100 ml with distilled water. Different volumes of this solution were mixed with reaction mixture in place of crude enzyme to make standard solutions of varying ammonia concentration and 200 µl of Nessler's Reagent was added to the mixture and incubated for 10 min at room temperature for color development and absorbance at 480 nm was recorded [125]. Basic reaction of ammonium ion with nessler's reagent is as follows:

$$NH_4^+ + 2[HgI_4]^{-2} + 4OH^- \longrightarrow HgO.Hg(NH_2)I\ (BROWN) + 7I^- + 3H_2O$$

3.2.8. Screening for asparaginase production

For screening of asparaginase production, aerotolerant cultures were grown in MRS broth containing 0.5% asparagine and anaerobic cultures were grown in RCM broth containing 0.5% asparagines and incubated at 37°C for 48 h. After incubation, 1.5 ml of culture was centrifuged at 10000 rpm for 5 mins and the culture supernatant obtained from each strain was transferred into fresh 1.5 ml microtube. Cell pellet of 5 ml culture was washed with PBS buffer and re-suspended in 300 µl Bug Buster (Novagen, Germany). Resuspended bacterial cells were lyzed by freeze-thaw or sonication method. Freezing was done at -80˚C for 15 min and thawing at 37°C for 3-4 min. Freeze and thaw was performed for 10-12 cycles before complete lysis of cells by sonication. Cell lysis was done by sonicating the freeze-thawed cells for 10 cycles with intermittent pulse-on and pulse-off for 30 seconds for each cycle. Cell debris was removed by centrifugation at 13000 rpm for 15 min. Supernatant was used as cell-free extract for examining the asparginase activity by Nessler's reagent [125].

3.2.9. Estimation of L-asparaginase activity

L-asparaginase activity was measured by a standard method using Nessler's reagent [125]. Rate of L-asparagine hydrolysis being determined by measuring the ammonia released. 100 µl of cell extract and supernatant were taken as crude enzyme in separate microfuge tubes for testing. Subsequently 200 µl of 0.1M asparagine solution in 100 mM Tris-HCl buffer (pH 8.0) was added. The microfuge tubes were incubated at 37°C for 10 min and latter stopped by adding 50 µl of 1.5 M Tri-chloroacetic acid. The resulting mixture was centrifuged at 11000 rpm for 1-2 min followed by addition of 100 µl of Nessler's reagent. The reaction color was allowed to develop for 10 min. Absorbance at 480 nm was taken in 96 µl well-plate for each sample, which gave an estimate of enzyme activity when compared with the standard curve values. The activity unit (**U)** is defined as nmoles of ammonia liberated per min per mg of protein.

3.2.10. Growth profile of *Lactobacillus fermentum* NKN51 in presence of cholesterol

Effect of cholesterol on growth profile of *Lactobacillus fermentum* NKN51 was determined in M17 minimal medium. 10% of fresh overnight culture of *Lactobacillus fermentum* NKN51 was inoculated in M17 medium supplemented with 0.1% sodium thiolglycolate and 100 µg/ml cholesterol, M17- thiolglycolate. Medium without cholesterol was taken as control culture medium. Cell density was observed by taking OD at 600 nm after intervals of 6 h.

3.2.11. Analysis of fluorescent cholesterol consumption by *Lactobacillus fermentum* NKN51 by flow cytometer

In-vitro cholesterol assimilating property of *Lactobacillus fermentum* NKN51 was further analyzed by growing the bacteria in M17 medium containing 22-NBD cholesterol (22-(N-(7-Nitrobenz-2-Oxa-1,3-Diazol-4-yl)Amino)-23,24-Bisnor-5-Cholen-3β-Ol) which is a fluorescent cholesterol analog (Molecular probes^{TM}, Life technologies, USA). Stock solution (~1 mg/ml) of NBD-cholesterol was prepared in ethanol. M17-thiolglycolate medium was supplemented with 15µg/ml NBD cholesterol and 1.5 µl/ml tween-20 was inoculated with 10% fresh overnight culture (in M17 medium) of *Lactobacillus fermentum* NKN51 and incubated at 37°C for 36 h. Control cells were grown in M17-thiolglycolate medium (without NBD-cholesterol) at 37°C for 36 h. After 36 h of incubation, 1.5 ml of bacterial culture was taken in microcentrifuge tubes and centrifuged at 8000 rpm for 5 min, washed twice with 1X PBS and finally resuspended in 750 µl of 1X PBS.

Cholesterol uptake by bacterial cells was analyzed by flow cytometer (BD FACS Verse™ BD Biosciences, USA).

3.2.12. Screening and analysis of putative phytase and 3β-hydroxysteriod dehydrogenase (3β –HSD) from *Lactobacillus fermentum* NKN51 genome using bioinformatics tools

Different classes of phyatses and putative 3βHSD were searched in genome of *Lactobacillus fermentum NKN51* using Prosite patterns by EMBOSS FUZZPRO (http://emboss.bioinformatics.nl/cgi-bin/emboss/fuzzpro). Selected sequences were compared with prokaryotic and eukaryotic cluster of orthologous gene databases (COG and KOG) for function prediction. Further, protein motifs were analyzed by comparing the sequence with KEGG SSDB (Sequence Similarity DataBase). Sequence alignments and phylogenetic analysis were performed using Constraint-Based Alignment Tool (COBALT) (http://www.st-va.ncbi.nlm.nih.gov/tools/cobalt) and Molecular Evolutionary Genetics Analysis tool MEGA 6, respectively [126]. Secondary structure prediction was done by PSIpred and DSSP.

3.2.13. Cloning of putative phytase (LAF_1794; *phyLf*) and 3β HSD (LC40_0723; *hsdLf*) encoding genes of *Lactobacillus fermentum* NKN51

3.2.13.1. PCR amplification

PCR amplification of selected gene sequences i:e putative phytase and putative 3βHSD from genome of *Lactobacillus fermentum* NKN51 was done by Hot star Taq DNA polymerase (Qiagen, Netherlands) using forward primer (phyF and hsdF) and reverse (phyR and hsdR) primer. Sequences of the oligos are listed in Table 3.1.

Reagents	Stock concentrations	Final concentrations	Volume (µl)
Qiagen PCR Buffer	10X	1X	10 µl
dNTPs	2 mM	0.2 mM	10 µl
Forward primer	10 µM	0.4 µM	4 µl
Reagents	**Stock concentrations**	**Final concentrations**	**Volume (µl)**
Reverse primer	10 µM	0.4 µM	4 µl
Hot star Taq DNA polymerase	2 U/µl	2 U	1 µl
Template	100 ng/µl	200 ng	2 µl
Nuclease free water	--	--	69 µl
Final volume	--	--	100 µl

Following PCR program was used for gene amplification:

Steps	Temperature (°C)	Time (min)
1	95	15
2	94	1
3	52	0.30
4	72	1
Repeat step 2-4 for 5 times		
Steps	**Temperature (°C)**	**Time (min)**
5	94	1
6	55	0.30
7	72	1
Repeat step 5-7 for 25 times		
8	72	10
9	4	Hold

3.2.13.2. Digestion

Cloning of putative phytase (LAF_1794; ***phyLf***) and 3β HSD (LC40_0723; ***hsdLf***) gene encoding for phytase phyLf and 3βHSDLf respectively was done in pET28a (Novagen) vector with arabinose inducible T7 promoter and kanamycin resistance marker. phyLf gene was cloned into *NcoI* and *HindIII* restriction sites while *hsdLf* gene was cloned into *NdeI* and *HindIII* sites of pET28a. PCR amplified genes and vector were double digested with respective restriction enzymes. Composition of double digestion reaction for vectors and PCR products was as follows

Reagents	Volume (µl)
NEBuffer 2.1	5
NcoI/NdeI	1
HindIII	1
Vector/ PCR product	39 (~1.5µg)
Nuclease free water	4
Final volume	50

Digestion reactions were incubated at 37°C for 3 h. After incubation, 1 µl calf intestinal phosphatase (CIP) (New England Biolabs, USA) was added to the digestion mixture of vectors and incubated for 25 min at 37°C. Heat inactivation of restriction enzymes was done at 65°C for 20 min after completion of digestion.

3.2.13.3. PCR purification of digested vectors and PCR products

Double digested pET28a and amplified genes were run on 1% agarose gel at 75 V for proper separation. After separation of DNA bands, appropriate size DNA bands were excised from gel with clean, sharp blades. Gel purification was done by QIAquick Gel Extraction Kit (Qiagen) according to manufacturer's instruction. Three volumes of binding buffer (QG) was mixed with 1 gel volume and incubated at 50°C for 5 to 10 min or until the gel fragment was dissolved in QG, with intermittent vortexing. After complete solubilization of gel in QG buffer, 1 gel volume isopropanol was added and mixed properly. The whole mixture was applied on QIAquick spin column (Qiagen) for DNA binding with silica column and centrifuged at 12000 rpm for 1 min. Flow through was discarded and 750 µl wash buffer PE was added to the column and centrifuged at 12000 rpm for 1 min. Flow through was discarded and column was given an additional free spin of 1 min at 12000 rpm for removal of residual wash buffer. For elution of bound DNA, column was placed in a fresh micro-centrifuge tube and 30 µl pre-warmed elution buffer (EB) was added to the centre of the column and centrifuged at 12000 rpm for 1 min.

3.2.13.4. Ligation

Digested vectors were ligated with their respective amplified genes (digested with similar restriction enzymes) by using T4 DNA ligase enzyme (Fermentas, USA). In ligation reaction, molar ratio of vector and insert was kept 1:3. Composition of ligation reaction mixture is as follows:

Reagents	**Volume (µl)**
T4 DNA ligase buffer (Fermentas)	1
T4 DNA ligase 10U/ µl	0.5
ATP(10mM)	0.5
pET28a (100 ng)	2
Amplicon (300 ng)	6
Final volume	10 µl

The reaction mixture was incubated at 16^{o}C for 15 h.

3.2.13.5. Transformation isolation of recombinant plasmid

Ligated product of 1 µl was transformed in 50 µl electro-competent cells of *E. coli* DH5α. This mixture was transferred to a pre-chilled electroporation cuvette and subjected to electric pulse of 2.3 kV for 5 seconds. After electroporation, 1 ml of SOC medium was quickly added to relieve the cells from electric shock and the transformed cells were transferred in a sterile microcentrifuge tube and further incubated at 37°C, at 250 rpm for 1 h. After incubation, cells were harvested by centrifugation at 3000 rpm for 5 min at RT and the pellet was resuspended in 150 µl SOC medium. Transformed cells were spread on LB-kan agar plates (supplemented with 50 µg/ml kanamycin) and incubated at 37°C for 12 to 14 h.

3.2.13.6. Screening of clones for insert

Recombinant plasmids were isolated from transformants and analyzed for confirmation of cloning of desired gene by double digestion with respective enzymes, i.e. *Nco*I and *Hind*III for *phyLf* (encoding for putative phytase phylL) gene and *Nde*I and *Hind*III for *hsdLf* (encoding for putative hsdLf) gene. Digested products were checked on 1 % agarose gel.

3.2.13.7. Isolation of recombinant plasmid

For isolation of recombinant plasmid, 1.5 ml of freshly grown overnight culture of transformants was centrifuged at 8000 rpm for 5 min. Pellet was resuspended in 150 µl pre-cooled re-suspension buffer S1*. 200 µl lysis buffer S2* was added to cells and mixed properly by inverting the micro-centrifuge tubes. 300 µl neutralization buffer was added and mixed properly with the mixture. Tube was kept in ice for 5 min and centrifuged at 12000 rpm for 10 min. The clear supernatant was transferred to fresh microcentrifuge tube and mixed with equal volume of phenol: chloroform: isoamyl alcohol mixture. Mixture was centrifuged at 12000 rpm for 10 min for phase separation. Upper aqueous layer was carefully aspired by micropipette and transferred to a fresh microcentrifuge tube. Equal amount of isopropanol was mixed properly with aqueous layer and kept at 4^{o}C for 1 h followed by centrifugation at 12000 rpm for 10 min, supernatant was discarded and pellet was washed with ice cold 70% ethanol at 12000 rpm for 5 min. The pellet was allowed to dry at RT for removal of any trace of alcohol. Dry pellet was dissolved in 30 µl nuclease free water.

Recombinant plasmids isolated from *E. coli* DH5α were double digested with respective restriction enzymes (as described in *3.4.13.2*) and run on 1.0% agarose gel for confirmation of insert in plasmid. Plasmid containing clones were sent to Eurofins Scientific, India to analyze the sequence and orientation of the cloned fragment.

3.2.14. Overexpression and purification of proteins and SDS-PAGE

For overexpression studies, arabinose inducible T7 promoter of pET28a expression vector was induced in *E. coli* BL21-AI (Life Technologies) host cells. To check the expression of phyLf and 3βhsdLF, respective recombinant vectors pET28a-phyLf and pET28a-hsdlf were transformed into electro-competent *E. coli* BL21-AI cells.

3.2.14.1. Induction and overexpression of proteins

For induction, *E. coli* BL21-AI cells harboring recombinant vectors were grown to ~0.5 OD_{600} and induced with 0.75 % filter sterilized aqueous arabinose (Himedia, India) solution. Further, cells were incubated at 250 rpm shaking condition for 4 h at 37°C (Kuhner incubator, Switzerland). In order to confirm the expression of proteins, 1 ml cell culture was withdrawn from the induced and uninduced samples (without arabinose induction) in 1.5 ml microcentrifuge tubes (Tarson, India) and centrifuged at 12,000 rpm for 10 min to pellet down the cells. Samples were prepared by boil-prep method, wherein respective cell pellets were resuspended in 1 X SDS gel loading buffer and heated at 92°C for 5 min (Dry bath; GeneI, Bangalore). The expression of recombinant Histidine tagged phyLf and 3βhsdLF was analyzed on 12% SDS-PAGE (Bio-RAD mini gel assembly).

3.2.14.2. Protein purification by metal affinity chromatography (Ni-NTA) and quantification of protein

E. coli BL21-AI cells harbouring recombinant plasmids pET28a-*phyLf* and pET28a-*hsdLf* were induced under optimized conditions for large scale purification of his tagged PhyLf and hsdLf respectively. Further, the induced culture was centrifuged at 10000 rpm for10 min. at 4°C to pellet down the cells. The cells were resuspended in 10 ml of lysis buffer (*section 3.1.2.3.1*) and lysed using French press at 20000 psi. The cellular debris was settled down by centrifugation at 20000 rpm for 20 min at 4°C. The supernatant (crude extract) was carefully transferred in an autoclaved 15 ml centrifuge tube. Briefly, Ni-NTA column was prepared by loading 4 ml of Ni-

NTA resin (Qiagen, USA) on to a bed of glass wool in 10 ml of syringe column. The column was equilibrated with 40 ml (10 bead volume of Ni-NTA beads) of equilibration buffer (*section 3.1.2.3.2*) prior to loading the supernatant. The protein lysate was loaded to the equilibrated Ni-NTA column and incubated for 30 min at 4 °C. After incubation, the flow through was collected and the column was washed with 40 ml of wash buffer 1 (*section 3.1.2.4*) and subsequently with 40 ml of wash buffer 2 (*section 3.2.1.5*). Elution of protein was done with 15 ml of elution buffer in aliquots of 1.5 ml (*section 3.2.1.6*). Eluted fractions were analyzed on 15% SDS-PAGE to check the purity of protein. After analysis, the eluted fractions containing the recombinant proteins were pooled and imidazole was removed by passing it through the 10 kDa centrifugal devices (hydrosart, Sartorious, Germany) according to the manufactures protocol. Buffer exchange was performed twice with 50 ml of 20 mM tris-HCl buffer pH 8.0 and the protein sample was concentrated to 1 ml. The concentration of the dialyzed protein samples were estimated using Micro BCA™ Protein Assay Kit (Thermo Scientific, Pierce, USA), as per manufacturers instruction.

3.2.14.3. Sodium Dodecyl Sulphate- Polyacrylamide Gel Electrophoresis (SDS-PAGE)

3.2.14.3.1. Casting of gel

Gel electrophoresis was done using Bio-Rad mini format 1 D electrophoresis system (tetra cell). A sandwich of glass plates were assembled and were held by using clamps. Resolving gel was prepared by mixing all the components followed by the addition of APS and TEMED solutions. The mixture was gently mixed and poured between the plates using 1 ml micro-pipette and leaving the adequate space at the top for pouring the stacking gel after polymerization. After completion of polymerization, overlay was poured-off and top of gel was washed several times with de-ionized water to remove any un-polymerized acrylamide. Stacking gel was poured similarly as the resolving gel and comb immediately inserted into the mixture to form wells. After polymerization of stacking gel, comb was carefully removed and formed wells were rinsed with de-ionized water and polymerized gel was used for electrophoresis.

3.2.14.3.2. Sample preparation

Protein samples were diluted with sample buffer at 2:1. for SDS PAGE, samples were first denatured at 95°C for 5 min and then, centrifuged 12,000 X *g* for 5 min to attain soluble fraction of

protein in the supernatant; separating the cellular debris. The supernatant was loaded onto the gel for further analysis.

3.2.14.3.3. Electrophoresis

Gel was placed in electrophoresis system and chamber was filled with tris-glycine buffer. Total 30 µl of sample was loaded on the gel using micropipette. Electrophoresis was carried out at a constant voltage of 100 volt for 2 h until dye reached to the bottom. Gel after electrophoresis was removed and stained for 4 h with gentle shaking in 0.25 % Coomassie Brilliant blue R-250 (w/v) in methanol:glacial acetic acid:water (50:10:40) at RT. The stained gel was destained for 6 h using destaining solution methanol:glacial acetic acid:water (50:10:40) with gentle shaking on gel rocker. This destaining procedure was repeated many times to get protein bands over a clear background.

3.2.15. Zymography

3.2.15.1. Zymography of hsdLf

Zymography of hsdLf for cholesterol dehydrogenase activity was performed by *In-gel* activity analysis in 4% staking and 6% resolving native polyacrylamide gel. β-mercaptoethanol was omitted from gel loading dye for zymographic analysis. Native gel was run in Bio-Rad PAGE assembly at 80 V for 2 to 3 h in 4°C chamber. After electrophoresis, gel was washed properly with milliQ water and immediately soaked in reaction mixture containing buffered substrate along with color developing compounds [127], at 37°C in dark for 3 to 4 h or until the color develops. Composition of reaction mixture is as follows:

Reagents	**Concentration**
Cholesterol	25 µM
NAD	0.5 mM
Nitrotetrazolium blue	0.2 mg/ml
Phenazine methosulphate	0.1 mg/ml
Tris-HCl buffer (pH-8)	100 mM

3.2.15.2. Phytase zymographic analysis

For zymographic analysis of phytase phyLf, *In-gel* phytase assay was performed in 4% staking and 6% resolving native polyacrylamide gel [128]. After electrophoresis, gel was socked in 4% sodium phytate solution in 100 mM acetate buffer (pH 5.0) of 100 mM NaCl ionic strength, for 10 to 12 h at 37°C. Thereafter, gel was rinsed with milliQ water and transferred to malachite green staining solution **(**1.8% ammonium molybdate, 0.3% (w/v) malachite green in 7.5% HCl) and incubated at 37°C for extended time till green color band appeared to confirm the presence of phyLf activity.[128]

3.2.16. Biochemical characterization of hsd*Lf*

To analyze the 3β HSD enzymatic activity 10 µl of purified enzyme was incubated with 90 µl buffered substrate solution. Substrate solution had 200 µM cholesterol and 400 µM NAD in100 mM Tris-Hcl buffer of pH7.8. The reaction mixture was incubated at 37°C for 20 min. and then 100 µl color reagent was added and incubated in dark, after 30 min OD was taken at 570 nm. Composition of color reagent was 0.4 mg/ml Phenazine methosulphate, 1.6 mg/ml Nitrotetrazolium blue and 10 µl/ml tween 20 in distilled water. A control reaction was set up in same way except the addition of enzyme.

3.2.17. Biochemical characterization of phytase

3.2.17.1. Assay of phytase activity and quantification of the liberated phosphate

To analyze the phyatse enzymatic activity, 2 µl of 400 nM phyLf enzyme was added to 18 µl of buffered substrate solution (final substrate concentration 1 mM in 100 mM sodium acetate buffer, pH 5). The ionic strength of the above mixture was adjusted to 100 mM by addition of NaCl and incubated at 37°C for 20 min. The release of phosphate was estimated by malachite green phosphate assay kit (BioAssay systems, USA). The reaction was stopped by addition of acidic working reagent provided with the kit. For the quantification of released phosphate, a calibration curve of phosphate reagent supplied with the kit was prepared. Enzyme activity unit (U) was expressed as µmoles of phosphate liberated per min.

3.2.17.2. Effect of pH, temperature and ionic strength on phyLf phytase activity and stability

To determine effect of ionic strength on phyLf phytase activity, concentration of NaCl was varied in the reaction mixture from 50 to 500 mM. The optimum pH for phyLf activity was determined by carrying out the above described standard assay using the following buffers (100 mM); glycine-HCl (pH 2.0 and 3.0), sodium acetate buffer (pH 4.5 and 6.0) and Tris-HCl buffer (pH 7.0 and 8.0). Further, the pH tolerance of the enzyme was examined by incubating the enzyme with different pH buffer for 2 h, with subsequent enzyme reactions carried out at an optimum pH of 5.0. The optimum temperature of phyLf was determined by carrying out reactions at temperatures ranging from 30 to 75°C. Thermal stability of the enzyme was studied by incubating the enzyme from 55 to 80°C for 5 and 10 min. Enzyme was brought to RT and followed by enzyme assay. After incubation, the residual phytase activity was assayed according to the standard procedure.

3.2.17.3. Effect of metal ions, inhibitors, detergents and oxidizing agents

The effect of various metal ions on phyLf phytase activity was investigated by pre-incubating the enzyme with 5 and 10 mM of different metal ions at 37°C for 30 to 60 min. The effect of inhibitors (5 mM), chaotropic agents (5 mM) and detergents (5 mM) on the enzyme activity was investigated by pre-incubating with these at 37°C for 30 min. The effect of reactive oxygen species (ROS) on phyLf activity was evaluated by incubating the enzyme with 5 and 10 mM H_2O_2 37°C for 60 min. After each respective pre-incubation, the residual phyLf activity was measured by the standard procedure. A control sample without any pre-treatment was assayed at the same time and its activity was considered 100%.

3.2.17.4. Determination of substrate specificity and kinetic constants

The substrate specificity of phyLf was determined by substituting IP6 in the reaction mixture with different phosphorylated substrates at a final concentration of 1 mM. To determine the affinity of phyLf for IP6, phyLf was incubated with a range of IP6 concentrations (0.2–1.4 mM) at 60°C and pH 5.0, and the steady state kinetic constant for hydrolysis of IP6 was calculated by non-linear regression analysis of Michaelis Menten's plot by GraphPad prism 6.05 (GraphPad Software Inc., CA, USA).

3.2.18. Analysis of IP6 degradation products by HPLC

HPLC samples were prepared by setting up the standard phytase reaction with 5 mM buffered substrate solution and incubated at 50°C for 5 to 6 h. The reaction solution was mixed with mobile phase in 1:1 ratio and filtered with 0.2 µm filters before injection. Phytate/IP6 degradation products were resolved by reverse phase HPLC using liquid chromatography unit (Waters,USA) equipped with UV-visible detector and C-18 reverse phase column (5µ, 4.6*250mm, Sunfire, Mobile phase consisted of 510 ml acetonitrile in 490 ml water, 10 ml of tetrabutylammonium hydroxide (TBNOH), 0.08% formic acid, 200 µl of phytic acid solution (6 mg/ml) and the pH was adjusted to 3.5 by sulfuric acid [129]. Mobile phase was filtered through 0.2 µ filter (Millipore) and pumped through the column at 0.6 ml/min.

3.2.19. Secondary structure prediction

Secondary structure prediction was done by various online servers. Comparison of secondary structures predicted by various servers was done to predict exact features segments of protein sequence. The list of servers used for prediction and analysis of secondary structure are as follows:

Phyre2- http://www.sbg.bio.ic.ac.uk/phyre2/html/page.cgi?id=index

Praline- http://www.ibi.vu.nl/programs/pralinewww/

Jpred- http://www.compbio.dundee.ac.uk/jpred/

PSIpred- http://bioinf.cs.ucl.ac.uk/psipred/

Comparison of predicted secondary structures and template sequence from PDB protein database was done by PRALINE server.

3.2.20. Circular dichroism spectrophotometry

Circular dichroism (CD) spectrum of phyLf was analysed on a Chirascan CD spectrometer (Applied Photophysics, UK) in sodium phosphate buffer (20 mM, pH 7.5). Far-UV (190 – 260 nm) CD spectra of 0.1 mg/ml protein was recorded using quartz cell of 1 mm path length at 1 nm band width and 0.25 s per point. The conformational changes in phyLf upon binding were recorded after incubating the protein with 1 mM and 3 mM IP6 for 10 min on ambient temperature. CD spectra

were analysed using online DichroWeb programme and the values, thus obtained, were expressed in terms of mean residue ellipticity (MRE).

3.2.21. Comparative molecular modeling

For comparative molecular modeling; template structures were selected by comparing the protein sequence with PDB database by using NCBI-BLAST search tool. PSIpred, pGenTHREADER (http://bioinf.cs.ucl.ac.uk/psipred/) tools were also used for template prediction based on fold recognition; Phyre2 was also used for template prediction, which combines various algorithms for prediction of best matching hits as template. Structures showing maximum identity were chosen as template for homology. Homology models were generated by comparative molecular modelling by modeller 9.15. Energy minimization was performed to remove steric clashes by GROMAC simulation suite v4.5.6. Stereochemistry was validated by PROCHECK and MOLPROBITY server.

3.2.22. Production and partial purification of enterocin

Overnight grown culture of *Enterococcus faecium* FH99 in MRS was further subcultured (1%) in 1L of freshly prepared MRS broth and incubated at 30°C for 40 h. After incubation, cells were harvested by centrifugation at 10000 rpm for 15 min at 4°C. The supernatant was collected in a fresh autoclaved glass beaker (Borosil, India) and precipitated with 80% ammonium sulphate at 4°C under stirring conditions. The precipitate so obtained was pelleted by centrifugation at 1000 rpm for 30 mins and dissolved in 1X phosphate buffer saline (PBS). The crude extracellular extract thus obtained was filtered through 3kDa spin column cutoff device (Pall life science, Netherland) as per manufacturer's instruction. The retentate thus obtained was dialysed through 1 kDa membrane against 1X PBS (Spectrum Labs, USA) to remove the salts and low molecular weight impurities. The prepared partially purified enterocin was assessed for its antimicrobial activity by spot assay against *Pediococcus acidilactici* LB42 an indicator strain [130].

3.2.23. Synthesis of enterocin capped silver nanoparticles (En-SNPs)

Enterocin capped silver nanoparticles (En-SNPs) were synthesized by previously known method with slight modification [131]. En-SNPs were synthesized at room temperature by successive addition of freshly prepared 2 mM silver nitrate and 0.6 mM sodium borohydrate solution to the enterocin solution in water. The resultant mixture was exposed to light for 30 min

with subsequent color change from colorless to yellow, indicating the formation of En-SNPs. The optimum concentration of enterocin for the synthesis of En-SNPs was determined by a set of batch experiment with varying concentration of enterocin. The prepared En-SNPs were dialysed using 10 kDa membrane and further characterized using different biophysical techniques. Citrate capped silver nanoparticles (C-SNPs) were synthesized as described in prior literature [132] and used as control. Silver concentration was quantified by using a molar extinction coefficient of $\varepsilon = 2.87 \times 10^{10}\ M^{-1}cm^{-1}$.

3.2.24. Biophysical characterization of En-SNPs

En-SNPs were characterized by different physico-chemical techniques such as UV- visible spectroscopy, zeta potential, dynamic light scattering (DLS), infrared spectroscopy and circular dichroism (CD). Spectroscopy was performed using UV-visible spectrophotometer (Varian, USA). The stability of the NPs was determined by measuring its zeta potential using a Zeta sizer (Malvern, UK). The morphology of nanoparticles was observed using scanning electron microscopy (SEM) and NTEGRE (NTMDT) atomic force microscope (AFM). The samples for SEM were prepared on glass slides and examined on a JEOL JEM-2100F microscope at an accelerating voltage of 200 keV. Infrared absorption measurements were recorded with Thermo Nicolet Nexus Fourier transform infrared (FTIR) spectrophotometer in the mid-IR range.

3.2.25. Determination of minimum inhibitory concentration (MIC)

The minimum inhibitory concentration (MIC) of En-SNPs was determined by micro broth dilution method [133]. Assays were carried out in Mueller-Hinton broth for a number of Gram-positive and Gram-negative bacterial strains. MIC is the lowest concentration of En-SNPs that inhibited the visible growth of microorganisms.

3.2.26. Effect of En-SNPs interaction on bacterial morphology by scanning electron microscope (SEM)

Bacterial cells treated with sub MIC concentration of C-SNPs and En-SNPs were collected by centrifugation at 10000 rpm for 10 min. The cells were fixed with 4% glutaraldehyde and then passed through a gradient of alcohol concentrations (50-100%). The samples were fixed on aluminium stubs and sputtered coated with a thin layer of gold for SEM analysis.

3.2.27. Interaction of En-SNPs with bacterial membrane proteins

To study the interaction of En-SNPs with bacterial membrane, crude membrane proteins were isolated from Gram-negative representative strain *E. coli.* ATCC 25922 (ECMP) and Gram-positive *P. acidilactici* LB42(LBMP) according to the procedure described by Berenson *et.al.* [133]. These membrane preparations were incubated with En-SNPs and fluorescence spectra was recorded in the range of 320-500 nm by exciting the reaction mixture at 295 nm using Carry Eclipse spectrofluorimeter. Stern-Volmer plots were constructed to observe the concentration dependent quenching of membrane preparations. Further, to determine the affinity of this interaction, dissociation constant (Kd) of SNPs with ECMP and LBMP were determined using the equation Y = Bmax X/ (Kd+X) (Graph pad prism 5.02). The formation of a complex between nanoparticles and ECMP/LBMP membrane preparations was studied using resonance light scattering spectrum (RLS). The excitation and emission monochromators of the spectrofluorometer were scanned in synchronous mode from 200–700 nm ($\Delta\lambda$=0 nm). Excitation and emission slit widths were set at 2.5 nm and PMT voltage to 450V.

For all the above studies, membrane preparations (ECMP and LBMP) were incubated with SNPs for thirty min on rocker shaker at 4°C followed by respective measurements.

3.2.28. Haemolysis assays

In accordance with the permission from Institute biosafety committee, haemolysis assays with C-SNPs and En-SNPs preparations in the relevant concentrations were performed using standard methodology: ASTM E2524 – 08 (ASTM, 2008). Blood was collected from human volunteers in evacuated containers (Greiner Bio-one). Human erythrocytes were separated from blood and suspended in 172 mM Tris-Cl buffer (pH 7.6). The haemolysis assays were conducted in 2 ml reactions with 0.125% final haematocrit and a buffer containing the set concentration of agents (SNPs) from 0.05-3.0 µg/ml. 0.1% Triton-X 100 treated erythrocytes were used as a 100% haemolysis standard and the negative control was 172 mM Tris-Cl buffer (pH 7.6). Percent haemolysis was calculated from the fraction of haemoglobin released into the medium by observing the absorbance at 540 nm and was compared with the positive control.

CHAPTER 4

SCREENING OF LACTIC ACID BACTERIA FOR PROBIOTIC PROPERTIES

4.1. Isolation of Lactic acid bacteria

Fermented milk products and infant gut are rich habitats of symbiotic lactic acid bacteria (LAB)[134]. Most of the genera of lactic acid bacteria especially *Lactobacilli* lack monophyletic origin. Primary isolation of LAB was done in MRS medium supplemented with thioglycollate. MRS is a rich selective medium for isolation of lactic acid bacteria, having low pH while thioglycollate was added to generate anaerobic condition. MRS-thioglycollate media allows selective growth of only aerotolerant or microaerophilic fastidious, low pH resistant lactic acid bacteria. Out of 15 selected isolates 8 (NKN51, 53, 54, 58, 60, 63, 64, 65) were selected on MRS-thioglycollate plates incubated aerobically, while four (NKN52, 55, 57, 59) were isolated on MRS-thioglycollate plates incubated anaerobically in gas pack. Three isolates, NKN56, NKN61 and NKN62 were isolated on Bifidoselective medium containing mupirocin (**TOS-propionate-Li-Mupirocin**), in strict anaerobic conditions. Sub lethal concentration of Mupirocin was added to inhibit the non specific growth of microbes since *Bifidobacteria* are mupirocin resistant.

Table 4.1: Colony morphology of LAB isolated from diverse niches.

Strain no.	Colony morphology	Source
NKN51	Large, white, round, smooth, opaque, shining	Yak cheese
NKN52	Small, round, semi-translucent, smooth, glistening	Yak cheese
NKN53	Small, round, semi-translucent, smooth,	Yak cheese
NKN54	Small, round, pale white, shining, smooth	Yak butter
NKN55	Small, round, semi-translucent, smooth, glistening	Yak butter
NKN56	Large, White, opaque, smooth, shining	Infant feces
NKN57	Irregular, rough, translucent,	Infant feces
NKN58	Large, creamy white, opaque, shining	Bovine Butter Milk
NKN59	Small, Rough, opaqe, nonshining, pale white	Yak butter
NKN60	Small, round, creamy, semi translucent, smooth	Bovine Butter Milk
NKN61	Large, White, opaque, smooth, shining	Infant feces
NKN62	Large, White, opaque, smooth, shining	Infant feces
NKN63	Small, pale white, opaque, round, smooth	Bovine Butter Milk

Strain no.	Colony morphology	Source
NKN64	White, round, smooth, opaque, shining	Bovine Curd
NKN65	White, round, smooth, opaque, shining	Bovine Curd

4.2. Morphological analysis by gram staining-

Preliminary identification of bacterial isolates was done by performing Gram staining. As Gram staining classifies bacteria on basis of type of cell wall and most of the symbiotic lactic acid bacteria are Gram positive. Hence Gram staining can facilitate the selection of Gram positive isolates. Based on the Gram staining results as shown in Fig. 4.1, all of the 15 isolates showed typical Gram positive nature/characteristic of LAB with minor differences in stain withholding properties of cell wall among different isolates.

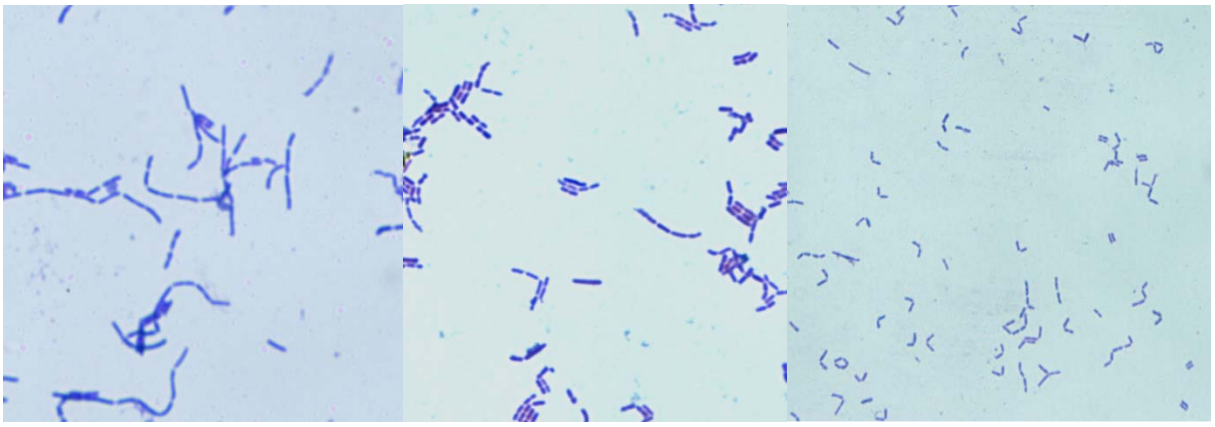

NKN51 NKN52 NKN53

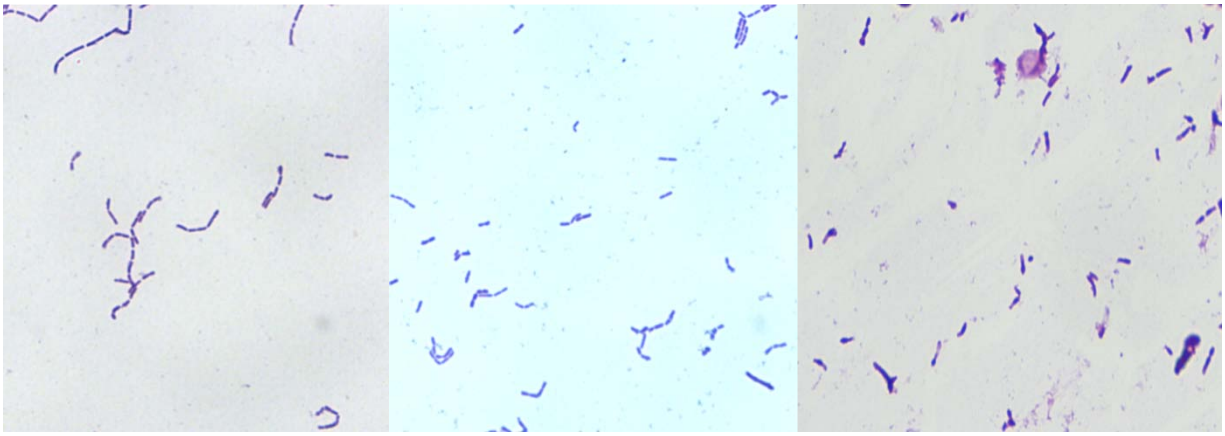

NKN54 NKN55 NKN56

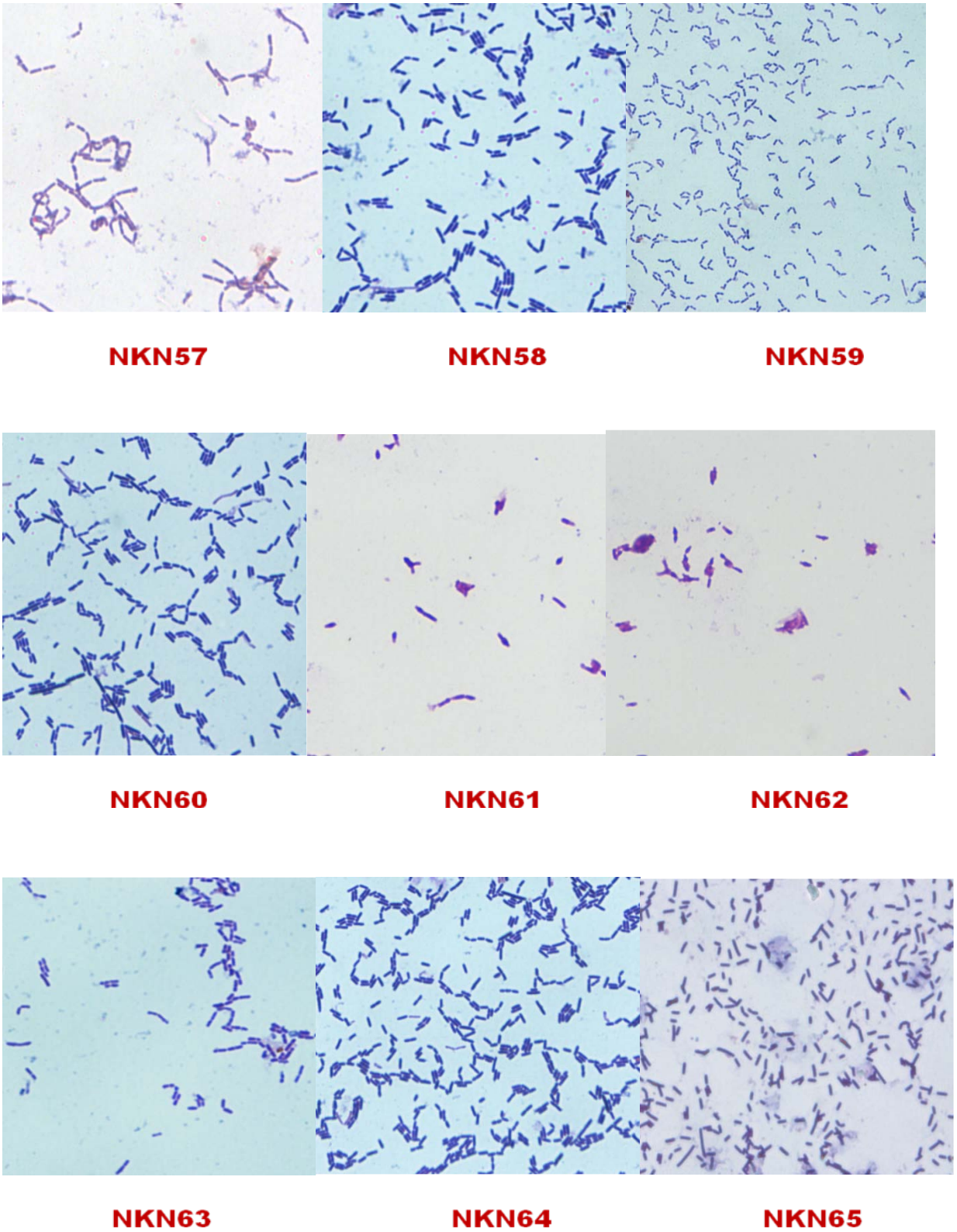

Figure 4.1: Bright field microscopy: Gram-staing of all the isolates from different ecological samples/sources (yalk chesse, yalk butter, infant feces, buttermilk and curd) were microscopically examined under 1000X oil immersion lens showed presence of Gram positive rods.

4.3. Biochemical characterization

4.3.1. Acid production

All of the isolates were examined for acid production on MRS-BCP agar plates, as lactic acid bacteria are non respiratory, fermentative microbes and produce lactic acid as major or secondary end product of fermentation. As shown in Fig 4.2, the MRS-BCP plates demonstrated a strong change in color around the all the isolates selected for this study. This acid production causes a lowering in pH of the MRS-BCP media, which was indicated by the pH indicator dyes bromocresol purple (BCP) as a change in color from red to yellow. All isolates selected for this study were acid producers.

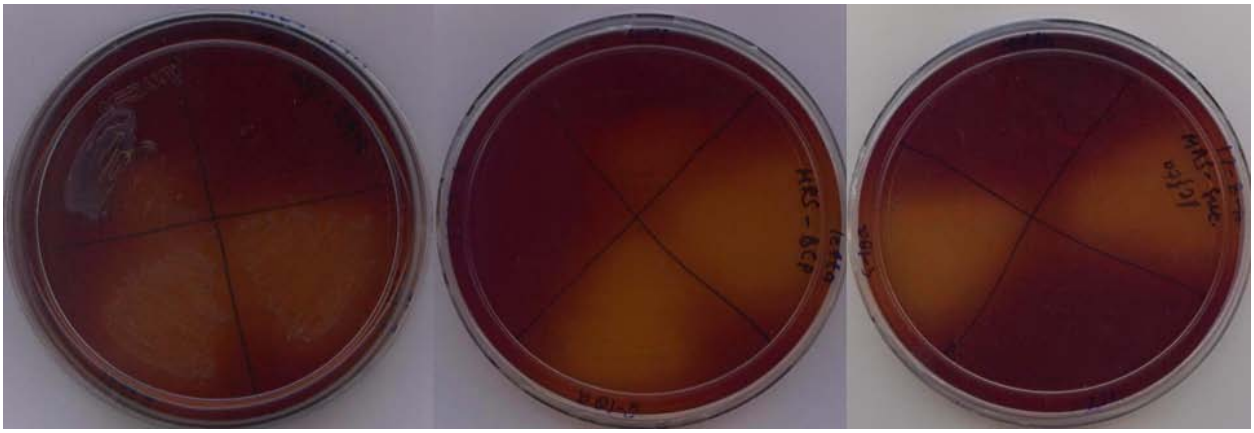

Figure 4.2: Acid production by isolates on MRS-BCP agar.

4.3.2 Catalase test

LAB are known to be non respiratory and fermentative bacteria as they are found in anaerobic or micro-aerobic environment. Although most of the genera of LAB are aerotolerant anaerobes but they lack catalase activity. Catalase production is indicated by bubble formation in presence of H_2O_2 due to degradation of H_2O_2. Out of all the selected isolates screened for catalase activity, none of them demonstrated bubble formation in presence of H_2O_2, classifying the isolates as catalase negative. Therefore, the catalase activity was used as a negative selection strategy for differentiating LAB against the other microbes. In spite of being catalase negative, they have alternative means of detoxifying the ROS such as superoxide dismutases or peroxidases. Thus, the above result gives a preliminary indication that all the isolates belongs to the lactic acid bacteria family.

4.3.3. Microbial identification based on carbon assimilation profile by Biolog

Microbial identification by Biolog is based on the ability of differentiating microbes based on metabolizing all major sources of carbon such as sugars, hexose-phosphates, amino acids, hexose acids, carboxylic acids, esters and fatty acids. Biolog also helps in determining the important physiological conditions such as pH, lactic acid tolerance, reducing power and chemical sensitivity. For identification and analysis of sugar usage profile, the isolates were inoculated in GENIII and anaerobic (AN) 96 well plates with each well consisting of a different carbon sources. Since the LAB requires comparatively rich media for their growth few isolates did not grow well in medium provided with the system, probably because of comparatively nutrient rich medium requirement by LAB.

Table 4.2: Carbon assimilation profile for different fermented milk product isolates using GEN III and anaerobic AN- plates.

SUBSTRATES	**NKN strains**					
	51	**58**	**59**	**60**	**61**	**62**
D-Raffinose	-	-	-	BL	-	-
α-D-Glucose	BL	+	-	+	-	-
D-sorbitol	+	+	-	-	+	+
Gelatin	+	-	+	-	+	+
Pectin	-	-	-	-	-	-
4-Hydroxyphenylacetic acid	+	-	-	-	-	-
Tween 40	-	-	-	BL	-	-
Dextrin	BL	BL	-	-	-	-
α-D-Lactose	BL	+	-	-	-	-
D-Mannose	+	+	-	BL	-	-
D-Mannitol	+	+	+	-	+	+
Glycyl-L-proline	+	-	-	-	-	-
D-Galacturonic acid	+	-	-	BL	-	-
Methyl pyruvate	BL	-	-	-	-	-
¥-Amino butyric acid	BL	-	-	-	-	-
D-Maltose	BL	-	-	+	-	-
D-Melibiose	+	-	+	BL	+	+
D-Fructose	-	+	-	-	-	-
D-Arabitol	+	-	-	-	-	+
L-Alanine	+	-	-	-	-	-
L-Galactonic acid lectone	BL	-	-	-	-	-
D-Lactic acid methyl ester	-	-	-	-	-	-
α -Hydroxy butyric acid	-	-	-	-	-	-
D-Trehalose	-	+	-	-	-	-
β-Methyl D-glucoside	+	-	+	-	-	+
D-Galactose	+	+	+	-	-	+
Myoinositol	BL	-	-	-	-	-

L-Arginine	-	-	-	BL	-	-
L-Gluconic acid	+	+	-	+	-	-
L-Lactic acid	-	-	-	-	-	-
β-Hydroxy-D,L butyric acid	-	-	-	-	-	-
D-Cellobiose	-	+	-	-	-	-
D-Salicin	+	+	+	-	+	+
3-Methyl glucose	+		-	-	+	+
Glycerol	+	+	+	-		+
L-Aspartic acid	-	-	-	-	-	-
D-Glucuronic acid	-		-	BL	-	-
Citric acid	-	-	-	-	-	-
α-Ketobutyric acid	-	-	-	BL	-	-
Gentiobiose	+	-	-	-	-	-
N-Acetyl D-glucosamine	-	+	+	-	-	+
D-Fucose	+	BL	+	BL	+	+
D-Glucose-6-PO_4	+	BL	-	-	-	+
L-Glutamic acid	+	-	+	-	-	-
Glucuronamide	-	BL	-	BL	-	-
α-Ketoglutaric acid	-	-	-	BL	-	-
Acetoacetic acid	-	BL	-	BL	-	-
Sucrose	-	-	-	-	-	+
N-Acetyl β-D-mannosamine	BL	-	+	-	-	+
L-Fucose	+	BL	-	-	+	+
D- Fructose-6-PO_4	+	BL	+	BL	BL	+
L-Histidine	BL	-	-	-	-	-
Mucic acid	-	-	-	-	-	-
D-Malic acid	-	-	-	-	-	-
Propionic acid	BL	-	-	BL	-	-
D-Turanose	-	-	-	-	-	-
N-Acetyl D galactosamine	-	+	-	-	-	-
L-Rhamnose	-	BL	+	-	-	-
D-Aspartic acid	+	-	+	-	-	-
L-Pyroglutamic acid	-	-	-	-	-	-
Quinic acid	-	-	-	-	-	-
L-Malic acid	-	-	-	-	-	-
Acetic acid	+	-	-	BL	BL	+
Stachyose	BL	-	-	-	-	-
N-acetyl Neuraminic acid	-	-	-	-	-	-
Inosine	BL	-	+	-	+	+
D-Serine	BL	-	-	-	-	-
L-Serine	BL	-	-	-	-	-
D-Saccharic acid	BL	-	-	-	-	-
Bromo succinic acid	-	-	-	-	-	-
Formic acid	BL	-	-	-	-	-
Minocycline	-	-	-	-	-	+
Niaproof 4	+	-	+	-	-	-
Tetrazolium blue	-	BL	-	BL	-	-
Potassium tellurite	BL	BL	-	+	-	-
Sodium bromated	BL	-	-	-	-	-
1% Sodium lactate	BL	+	-	-	-	+

Troleandomycin	+	-	-	-	-	+
Lincomycin	-	-	-	-	-	-
Vancomycin	+	+	-	+	-	-
Nalidixic acid	-	+	--	BL	-	-
Aztreonam	BL	+	-	BL	+	+
Fusidic acid	+	BL	+	-	+	+
Rifamycin SV	+	-	-	-	-	+
Guanidine HCL	+	-	+	-	-	-
Tetrazolium violet	-	+	-	BL	-	-
Lithium chloride	-	-	-	-	-	-
Sodium butyrate	-	BL	-	-	-	-

As per biolog data + signifies positive attribute, - signifies negative and BL signifies border line attribute

4.4. 16S rRNA gene sequencing

After biochemical characterization of the bacterial isolates by different methods such as catalase, acid production and carbon assimilation profile the isolates were further identified at genomic level by performing 16S rRNA sequencing. Genomic DNA of isolates NKN51, NKN52, NKN53, NKN54, NKN55, NKN56, NKN57, and NKN63 were extracted as shown in Fig.4.3A and 16S rRNA sequence for each isolate was amplified using universal eubacterial set of primers. Figure 4.3B shows the amplification of a typical ~ 1500 bp 16S rRNA sequences of isolates . Alignment of theses retrieved sequences with nucleotide sequence data base at NCBI with nucleotide BLAST program. Isolates were identified as top hits of the alignment. Table 4.3 shows identification of isolates on the basis of 16S rRNA gene sequences.

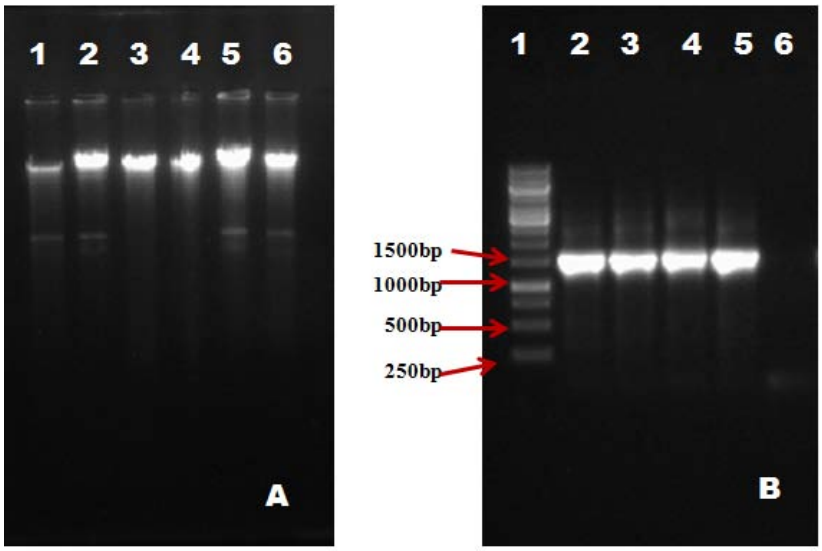

Figure 4.3: A) Eelectrophoresis of genomic DNA samples extracted from isolates (lane1-6) on 1% agarose gel, **B)** Amplification of 16S rRNA sequence from the genomic DNA of the isolates (lane 2-6) using univeral eubacteirial primer set and lane1- 1 kb DNA ladder (Fermentas, USA).

Table 4.3: Identification of lactic acid bacteria from diverse niches on the basis of 16S rRNA gene sequences and Biolog

Strain no.	Identification	Method	% Homology
NKN51	*Lactobacillus fermentum*	16S rRNA	99%
NKN52	*Lactobacillus brevis*	16S rRNA	99%
NKN53	*Weisella paramesenteroides*	16S rRNA	98%
NKN54	*Lactobacillus plantarum*	16S rRNA	97%
NKN55	*Lactobacillus brevis*	16S rRNA	99%
NKN56	*Bifidobacterium longum*	16S rRNA	100%
NKN57	*Lactobacillus gasseri*	16S rRNA	100%
NKN58	*Lactobacillus rhamnosus*	Biolog	-
NKN59	Uncharacterized	Uncharacterized	-
NKN60	*Lactobacillus parabuchneri*	Biolog	-
NKN61	*Bifidobacterium magnum*	Biolog	-
NKN62	*Bifidobacterium pseudocatenulatum*	Biolog	-
NKN63	*Lactobacillus casei*	16S rRNA	100%
NKN64	*Lactobacillus fermentum*	16S rRNA	99%
NKN65	*Lactobacillus fermentum*	16S rRNA	99%

4.5 Screening of isolates for phytase production

Following identification of the fermented milk isolates as LAB, the isolates were screened for phytase production. All the isolates of LAB were plated on MRS-phytate and incubated for growth. The Fig. 4.4 shows hollow zone indicating hydrolysis of phytate on MRS-phytate agar plates against the turbid background of media. The diameter of the zone of hydrolysis exhibited by the isolates directly correlates to their phytase activity. Therefore,NKN51, NKN58, NKN59, NKN60, NKN63, NKN64 and NKN65 displayed very good phytase acitivity as compared to the rest of the isolates. As phytate shows antinutrient properties by chelating metal ions, sugars and proteins and limits their bioavailability in gut [43, 135]. Phytate degradation by lactic acid bacteria will release the bound nutrients and make them freely available for absorption in intestine [2, 51].

Figure 4.4: Screening of fermented milk product isolates for phytase activity:. MRS-phytate agar plates showing zone of phytate hydrolysis by different isolates.

4.6. Screening of isolates for cholesterol assimilation

Cholesterol assimilation is another major mechanism suggested for cholesterol lowering effect of lactic acid bacteria, since it causes direct cholesterol removal from body by converting it into coprostanol, a lesser soluble and hence lesser absorbable form of cholesterol [11, 57, 59]. Out of all isolates NKN51 have showed maximum cholesterol reducing effect in culture medium(~50% of 100µg/ml), beside it NKN58, NKN60, NKN63, NKN64 and NKN65 have also shown good cholesterol reducing effect strictly under anaerobic conditions (figure 4.5). No cholesterol reducing effect was observed in aerobic growth of isolates. NKN51, NKN64 and NKN65 were identified as *Lactobacillus fermentum* by 16S rRNA sequencing. Some of the reports suggest that cholesterol assimilation is correlated with bile salt deconjugation ability of lactic acid bacteria; hence bile deconjugating bacteria would show more cholesterol reduction *in-vitro* [55, 136]. But we did not observe any such effect; as the isolate assimilating cholesterol demonstrated negative bile salt hydrolase activity. It was also observed that the bile salt hydrolase producing isolates NKN52 and

NKN55 showed lower cholesterol assimilating ability when compared to the better cholesterol assimilating isolates (NKN51, 60, 63, 64 and 65). Therefore, this study shows no correlation between bile deconjugation and cholesterol assimilation by lactic acid bacteria especially *Lactobacilli*. Our results are in accordance with observation of Walker and Gilliland (1993). Gut colonization by cholesterol consuming microbes can significantly reduce the re-absorption of dietary and biliary cholesterol in intestine [59]. Similar to the increased bile excretion, increased excretion of cholesterol and other sterol from intestine also shows hypocholsterolemic effect because liver will mobilize more cholesterol through bile in intestine and less will be used in lipoprotein formation for secretion in blood [57, 59]. Direct cholesterol consumption by bacteria shows *in-vitro* cholesterol reducing effect in culture medium [53]. Therefore, these facts encouraged us to examine all the isolates for their *in-vitro* cholesterol reducing potential in culture medium.

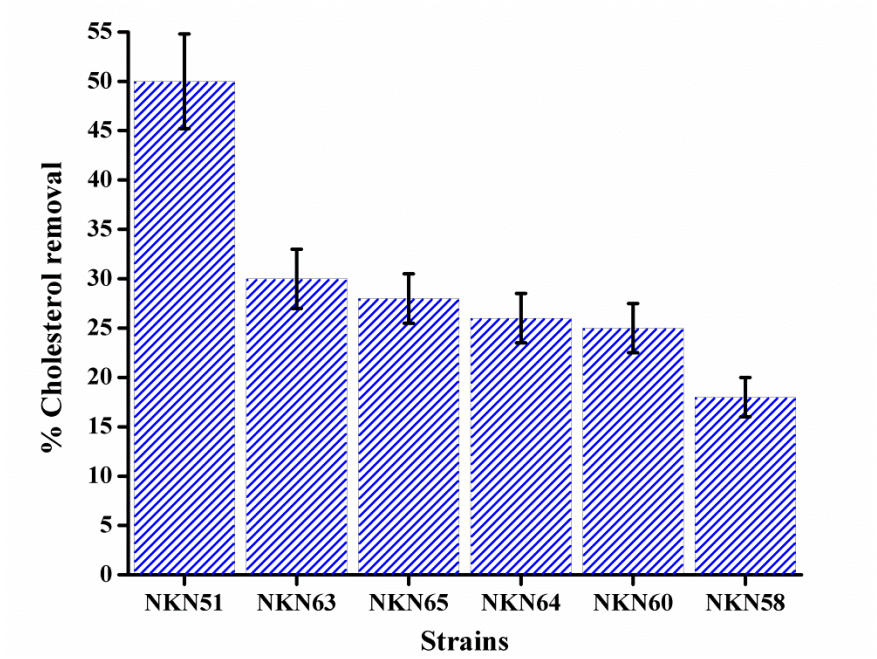

Figure 4.5: *in-vitro* cholesterol reducing effect of different isolates.

4.7. BSH production

Bile salt hydrolase production by symbiotic gut inhabiting bacteria is an important probiotic property as bile hydrolysis causes increased bile excretion. Bile excretion is the major cholesterol disposal mechanism from body. Hence BSH production is proposed as potential mechanism of cholesterol lowering effect of LAB. Out of all isolates only NKN52 and NKN55

were reported to show bile salt hydrolase activity under strictly anaerobic conditions. Both the isolates NKN52 and NKN55 were identified as *Lactobacillus brevis*. BSH production from *Lactobacillus brevis* has been reported by various researchers in earlier studies [137, 138] still functional analysis of gene responsible for this effect is unexplored fom this species.. Figure 4.6 shows zone of precipitation around the colonies of NKN52 and NKN55. *Enterococcus faecium* was taken as positive control (pre-known bile salt hydrolase producing microbe). Since bile salt hydrolase does not cause any *in-vitro* cholesterol reduction, animal studies are prerequisite to study the *in vivo* cholesterol lowering effect of BSH producing microbes. Figure 4.7 shows micrograph of BSH positive and negative isolates under bright field microscope with 40X magnification.

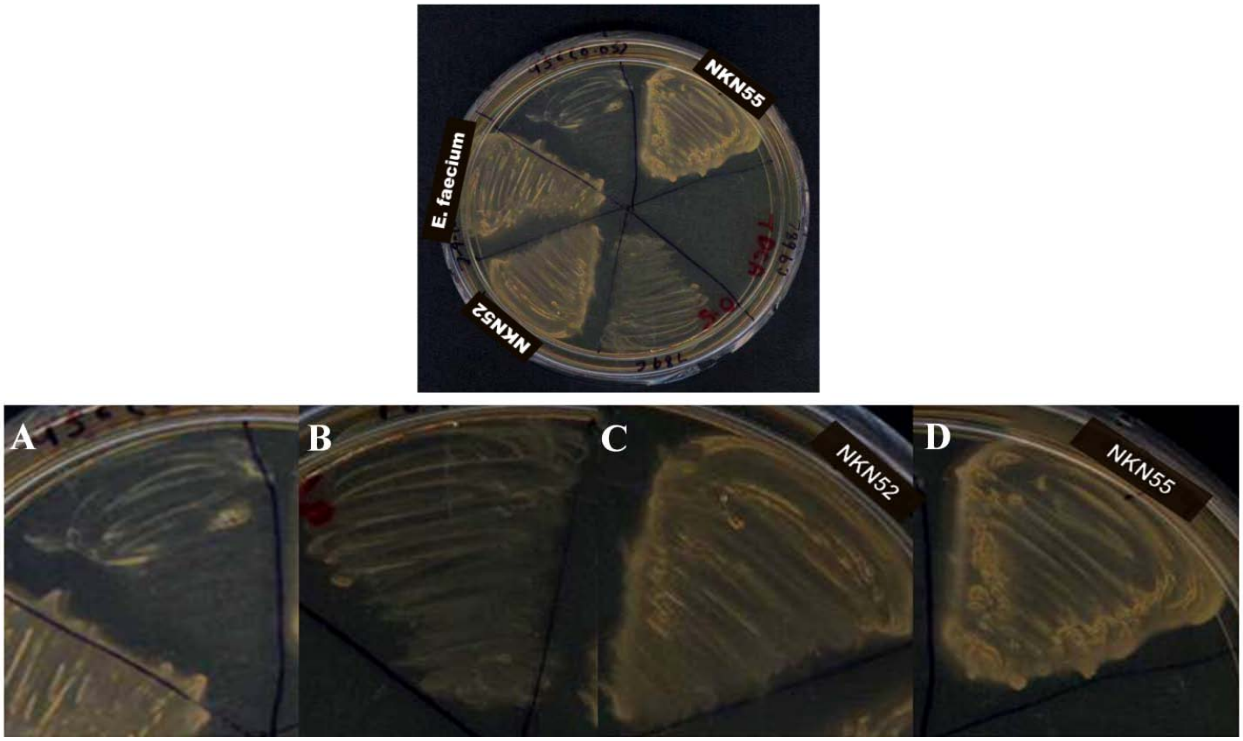

Figur 4.6: Bile salt hydrolase activity of fermented milk product isolates: Zone of bile precipitation indicating BSH activity was seen around the growth of C) NKN52 and D) NKN55 while A) and B) are BSH negative (no zone of precipitation).

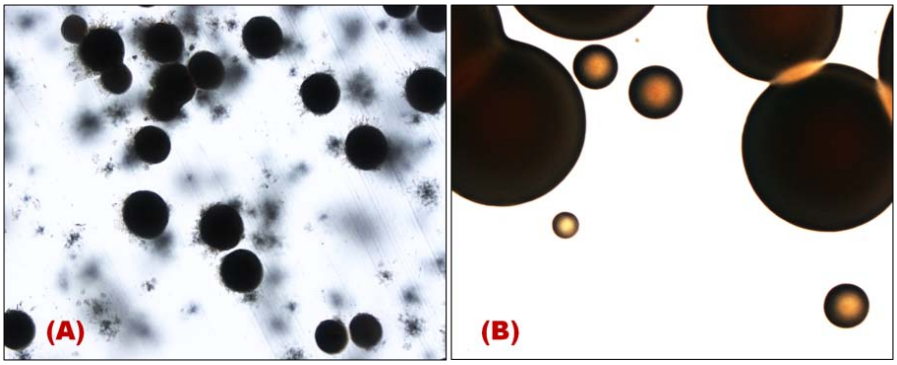

Figure 4.7: Microscopic image of colonies of A) BSH positive and B) BSH negative isolates under 40X magnification showing deconjugated bile precipitate near colonies of BSH producer.

4.8. Asparaginase production

Asparaginase is an antineoplastic agent, especially active against leukemia. Asparaginase production by lactic acid bacteria is high. Out of 15 strains 7 (NKN52, NKN53, NKN55, NKN58, NKN59, NKN60 and NKN63) were found to be positive for asparaginase activity (figure 4.8) while NKN52, NKN55, NKN59 are among top asparaginase producing strains having activities 162.8 U, 191.4 U & 190.4 U respectively. NKN52 and NKN55 both were good asparaginase producers and both were identified as *Lactobacillus brevis* by 16S rRNA sequencing. *Lactobacillus brevis* is foreknown for its probiotic potential and is widely used as probiotic supplement though molecular basis of various probiotic properties are unknown. Previous studies show high antitumorigenic properties of *Lactobacillus brevis* but active principle of the effect is unknown. Asparaginase activity may contribute to the anticancer effect of *Lactobacillus brevis*. Still genetic and molecular studies of the enzyme are necessary to establish the strong basis to the property and measurable effect in different environmental and physiological conditions. Besides NKN52 and NKN55, NKN59 and NKN53 have also shown good aspatraginase production, NKN53 was identified as *Weisella paramesenteroides* by 16S rRNA gene sequencing while NKN59 shows *Weisella* like cell morphology in Gram staining still complete identification of this isolate is remaining. NKN53 is a yak cheese isolate while NKN59 is a yak butter isolate, fairly potent asparaginase production by both isolates suggests anticancer potential of *Weisella*.

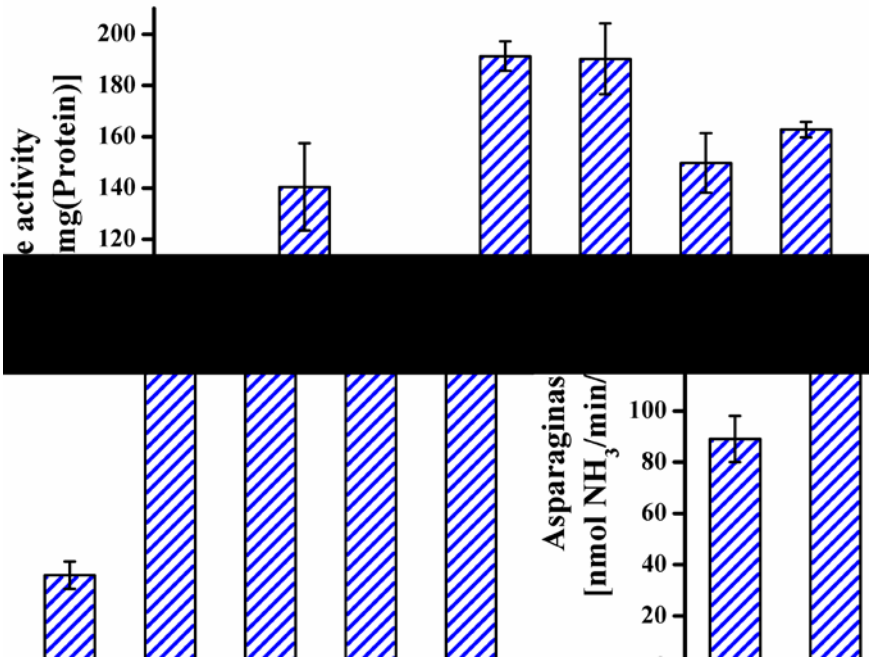

Figure 4.8: Asparaginase production by different isolates.

4.9. Evaluation of probiotic potential of isolates and selection for further studies

15 lactic acid bacteria were isolated from samples collected from diverse locations. Most of them were Gram positive rods belonging to the genera *Lactobacillus*, three were *Bifidobacteria* and two were from genera *Weisella*. Isolates from genera *Lactobacillus* and *Weisella* grown well in presence of oxygen while all the *Bifidobacteria sp*. were obligatory anaerobes. Screening of asparaginase activity has shown good asparaginase production by *Lactobacillus* brevisNKN52, *Lactobacillus* brevisNKN55 and *Weisella paramesenteroides*NKN53. This is the first report of asparaginase activity from the genera *Weisella*. Screening of Probiotic properties of the isolates enabled selection of strains showing multiple health beneficial effects. Out of all isolates *Lactobacillus fermentum*NKN51 have shown good cholesterol assimilation and phytase production while *Lactobacillus* brevisNKN52 and *Lactobacillus* brevisNKN55 have shown good asparaginase and bile salt hydrolase activity. Since there are various reports of probiotic *Lactobacilli* but genetic and molecular basis of the properties are poorly understood, we choose *Lactobacillus fermentum*NKN51 for further genetic and molecular characterizations. The partial 16S rRNA gene nucleotide sequence of *Lactobacillus fermentum* NKN51 has been deposited in the GenBank database under the Accession number KP244308.

CHAPTER 5

MOLECULAR AND BIOCHEMICAL CHARACTERIZATION OF NOVEL PROTEIN TYROSINE PHOSPHATASE LIKE PHYTASE FROM *Lactobacillus fermentum*NKN51

5.1. Sequence analysis -

Out of all classes of phytases, prosite pattern of PTPLP active site was found in genome of *L. fermentum*. Gene LAF_1794 (designated as phyLf herein after) has PTPLP active site pattern i.e. HCXXGXXRT. Comparison of sequence with prokaryotic cluster of orthologous gene database predicted its role in signal transduction and alignment using genomapper placed it with PTPs involved in host microbe interactions (Figure 5.1). While comparison of phyLf with eukaryotic orthologous gene cluster database (by LMBGE server) predicted its role as polyinositol phosphate phosphatase. Further, motif search by Sequence Similarity DataBase of KEGG have shown the presence of PTP like phytase motif in >LAF_1794. These observations led us to select the sequence for designing the primers for PCR amplification of homologous gene from *L. fermentum* NKN51 and analysis of true phytase activity of the protein encoded.

Multiple sequence alignment with PTPLPs revealed that except for phytate binding P-loop rest of the phyLf sequence shows no similarity with previously characterized PTP like phytases (Figure 5.2) Hence, phyLf forms a unique subgroup of class PTPLP. Alignment of phyLf with PDB structure database shows *Mycobacterium* protein tyrosine phosphatase B (MptpB) as closest structure to phyLf. MptpB is also reported to act on polyinositol phosphates, and is involved in host- microbe cross talk [139]. Sequence alignment with non redundant protein data base (BLASTP) shows that various orthologs of phyLf are widely distributed in other *Lactobacilli* and other genera of phylum Firmicutes.

Although, sequence alignment and phylogenetic analysis of phyLf shows more homology with orthologs found in non pathogenic firmicutes (Figure 5.3) but none of them is functionally characterized (Fig. 5.4). Hence, closest (≤39% homology) functio nally characterized homolog is LipA gene in genera *Listeria*. LipA is a PTP which hydrolyzes phosphatidyl inositol poly phosphates and tyrosine phosphates, it is also a MptpB like PTP class of protein and involved in signal transduction between host and microbe [139, 140]. Together, these observations suggest the *in-vivo* function of phyLf in signal transduction for host symbiont cross talk.

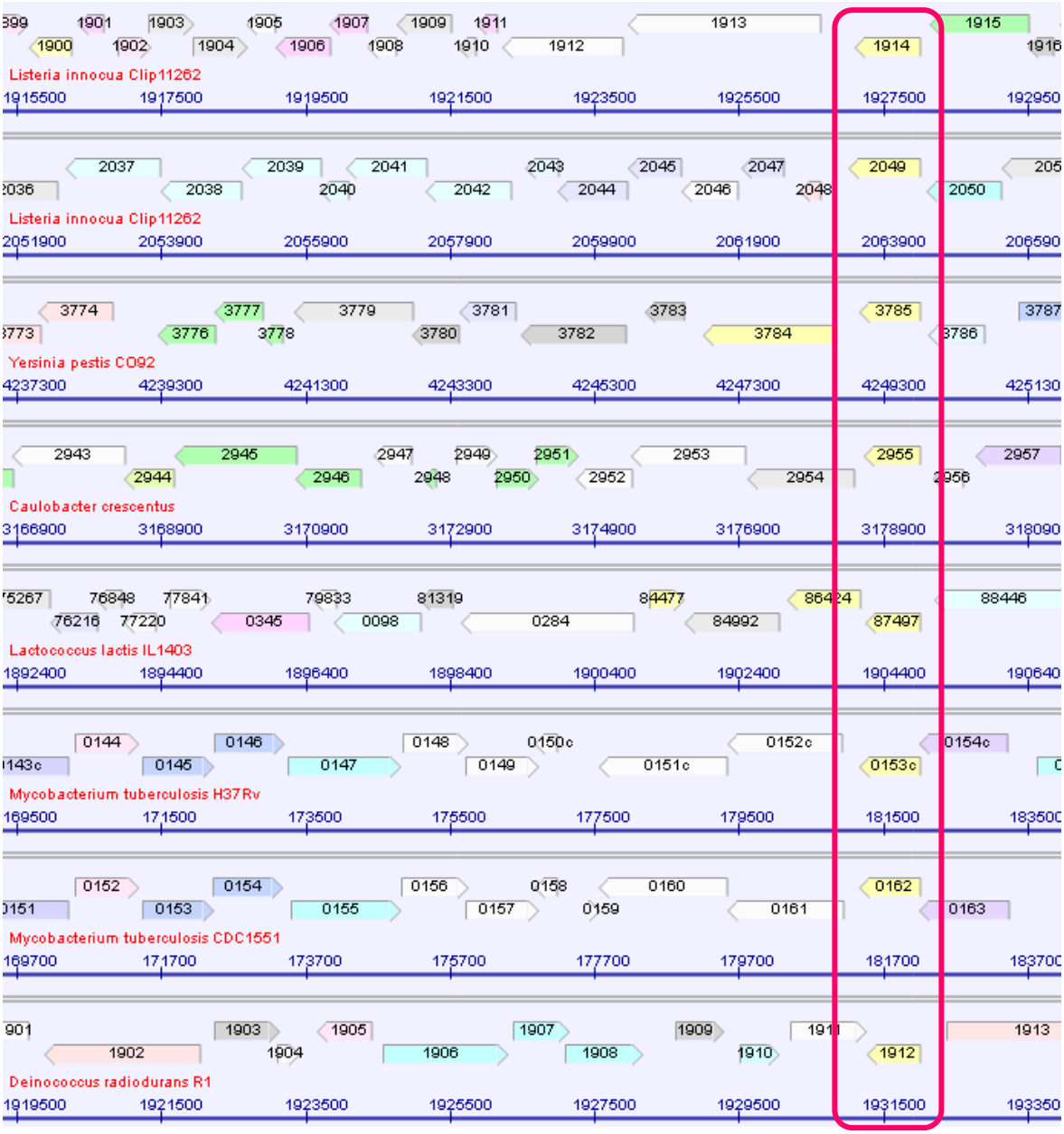

Figure 5.1: Alignment of clusters of phyLf orthologous genes in COG database. Boxed identifiers show phyLf orthologs in gene cluster of respective microbe. Alignment is done by genomapper using LMBGE online server.

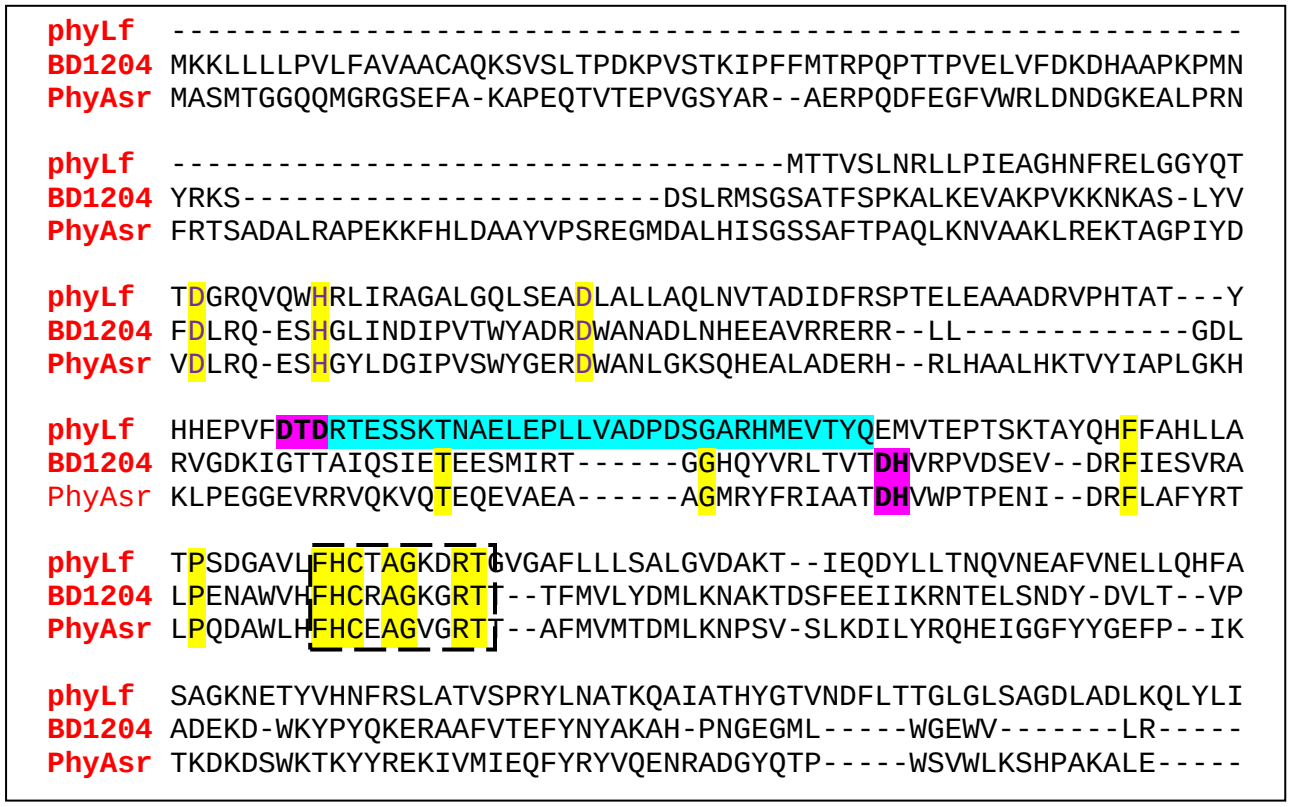

Figure 5.2: Multiple sequence alignment of phyLf with BD1204 (*Bdellovibrio bacteriovorous* PTP like phytase) and phyAsr (*Selenomonas ruminantium* PTP like phytase). Boxed sequence shows active site p-loop patterns of the three proteins. Red highlighted regions show respective acid loops and blue highlight is extra sequence stretch of phyLf between P-loop and acid loop.

```
L. fermentumNKN51 GQLSEADLALLAQLNVTADIDFRSPTELEAAADRVPHTATYHHEPVFDTD 93
L. gastricus      GRLSANDLTYLQQFNLTHDIDLRSPREVNSLPDRVPEGTHFHHEPVFGTD 89
L. suebicus       AHLNEHDLSTLAAIPVTIDIDLRAPEEVKQAPDKLPQTASYYHLPVFKSD 90
L. vaginalis      ARLDQNDLTVLDNIPISLDIDLRAPDEVKKDPDRVPSQAKYYHLPVFEAD 90
L. rueteri        NTLDETDLQVLTSLNVKLDLDFRAPGESDVQPDKVPATAVYHSLPVFQTD 90
Paediococcus      AGLTPEDQQHLSQYGVVADVDFRSKDEQTMAPDRVPVGATYHFLPVFPAD 90
L. brevis         AGLTPEDQQHLSQYGVVADVDFRSKDEQTMAPDRVPVGATYHFLPVFPAD 97
L.gigeriorum      GGLADADIRLLEDYSVKFDVDFRSPEEKSKFPDRVPSGAEYVFAPVFRVD 90
L. brevis         ADLSEADQAFLADYGVKYIVDFRSSEEVTRQPDRVPEGATYEFDPVFSED 92
                    *   *   *    :   :*:*:  *    .*::*  : :   ***  *

L. fermentumNKN51 -RTESSKTNAELEPLLVADPDSGARHMEVTYQEMVTEPTSKTAYQHFFAH 142
L. gastricus      -LTEASKRTSELEPVMNVKPNTGSQHMREVYRLMTELDSATKAYRNFFTY 138
L. suebicus       -ETDASHSDEEIMSRILK-PGNGYQHMLDVYRRMVEVPTAKAAYQRMFEL 138
L. vaginalis      -ETDASHSDEEIAAQMQQ-PGNGYHHMLDVYHRMITTPSAKQAYQKLFNL 138
L. rueteri        -RTDASHSREQIEAEFSDDPTAGYRHMLDVYRDMVTTPQAKQSYQQFFDL 139
Paediococcus      DQTDASATEAELEQRFNGDDQAGYRHMVDVYQKMITLPSAQAAYHDFFAT 140
L. brevis         DQTDASATEAELEQRFNGDDQAGYRHMVDVYQKMITLPSAQAAYHDFFAT 147
L.gigeriorum      -ETQSTKQTDELQRKMNSDPTSGLVEMRRVYRDVIRQRHSQKAYRKFFDA 139
L. brevis         -LTNSSKSIDRLDELSQNDAQFGFDHMLIAYEDMISSESARNAYRKLFAT 141
                    *:::    .:          *  .*  .*. :    :  :*: :*

L. fermentumNKN51 LLA-TPSDGAVLFHCTAGKDRTGVGAFLLLSALGVDAKTIEQDYLLTNQV 191
L. gastricus      LLE-TPEDGAVIFHCQAGKDRTGIGAYLVLSTLGVDQKNIEQDYLLTNQT 187
L. suebicus       LLS-NNPTQASLFHCTAGKDRTGMAAYLILSALQVPEETILKDYLLTNKA 187
L. vaginalis      LL--NNEHGALLFHCTAGKDRTGMAAYLILSALGVEQKIIMEDYLLTNTV 186
L. rueteri        LLN-SDPNSAILFHCTAGKDRTGMGAILLLSALNVDRQISVNDYLLTNQI 188
Paediococcus      LSANDTAQQSVLFHCTAGKDRTGIGAFLALSALNVDPQVIKTDYLLTNQN 190
L. brevis         LSANDTTQQSVLFHCTAGKDRTGIGAFLALSALNVDPQVIKTDYLLTNQN 197
L.gigeriorum      LLANSADDSALLFHCTAGKDRTGMGAIFLLSALNVDEDTIRADYLLTNRA 189
L. brevis         MLANSAENEALIFHCTAGKDRTGFGALLALTALGVPLATIREDYLLTRIT 191
                  :       : :*** *******..* : *::* *       *****.
```

Figure 5.3: Alignment of phyLf homologous protein found in genome of other *Lactobacilli* and *Pediococcus* sp. Conserved active site pattern (HCXXGXXRT) is highlighted in yellow and conserved Aspartate (D) of acid loop is highlited in red.

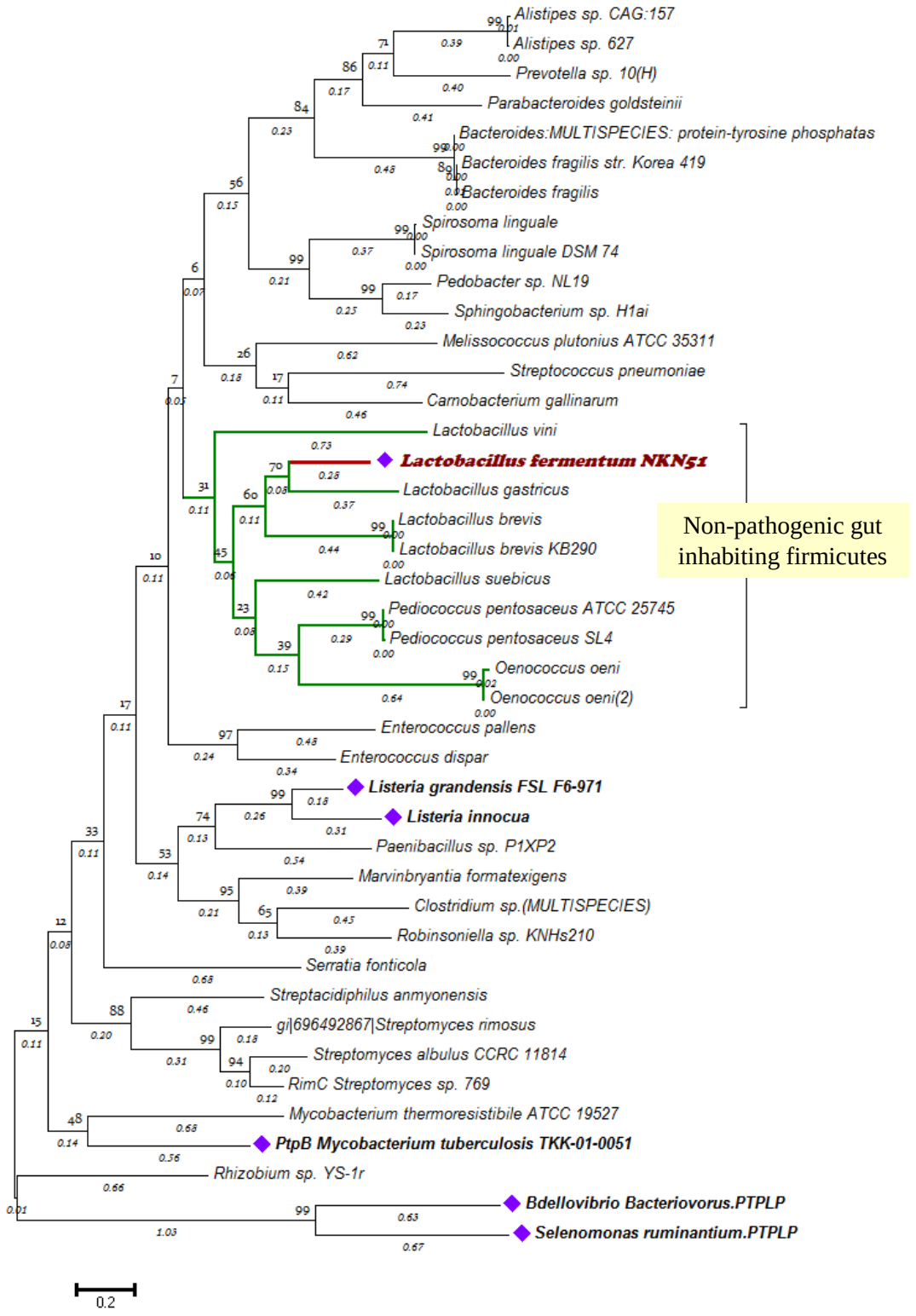

Figure 5.4: Molecular Phylogenetic analysis of phyLf by Maximum Likelihood method**.** The tree shows distribution of phyLf orthologs in nonpathogenic and pathogenic firmicutes, and their

distance from MptpB and previously known PTPLPs of *Bdellovibrio* and *Selenomonas*. Bootstrap values at branch points are expressed as percentage of 500 resamplings. Evolutionary analyses were conducted in MEGA6[126].

5.2. PCR amplification and gene cloning

Genomic DNA of *L. fermentum NKN51* was extracted and phyLf gene was amplified (figure 5.5A). Primers were designed according to predicted protein tyrosine phosphatase from *L. fermentum* IFO3956 (Locus tag: LAF_1794). The nucleotide sequences of phyLf from *Lactobacillus fermentum* NKN51 has been deposited in the GenBank database under the accession number **KT267224**. Amplified gene was successfully cloned in NcoI and HindIII site of pET28a vector. Figure 5.5B shows a diagrammatic representation pET28-phyLf construct. Recombinant plasmid was transformed in *E.coli*DH5α and tranformant were checked for having plasmid with inserts. Figure 5.6 shows double digested recombinant plasmid isolated from *E.coli*DH5α. A band of 798 bp insert was excised out of the plasmid after double digestion. Sequencing of cloned fragment confirmed the cloning of desired gene in proper orientation.

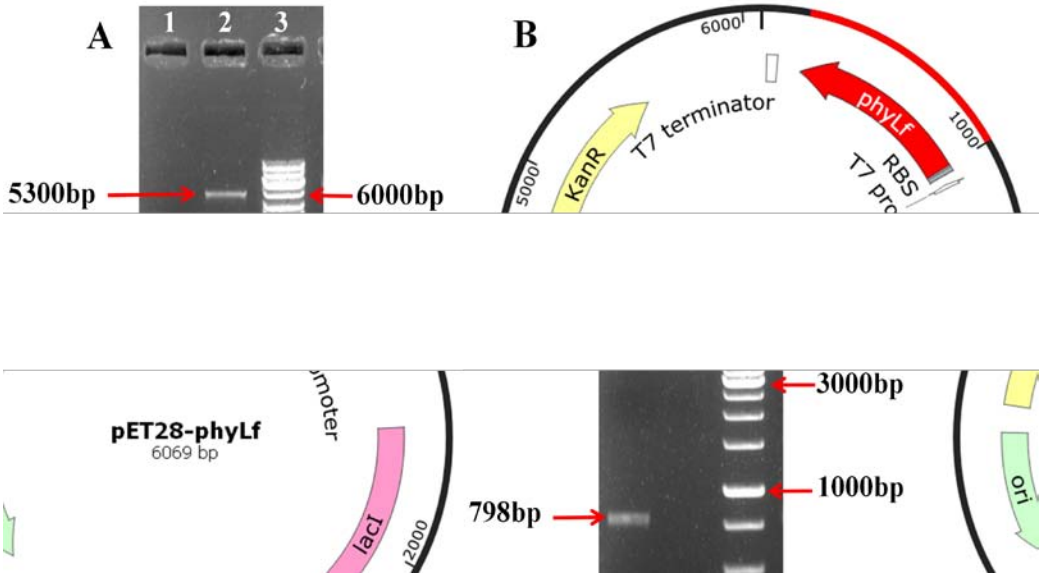

Figure 5.5: Cloning of *phyLf* in pET28a expression vector. (A) Agarose gel electrophoresis of lane1-PCR amplified *phyLf*, lane2-restriction digested (NcoI and HindIII) pET28a vector, lane3-1kb DNA ladder (B) vector map of pET28a-*phyLf* recombinant plasmid.

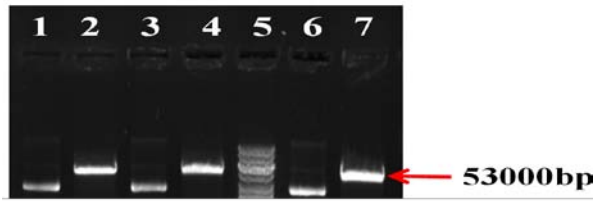

Figure 5.6: Confirmation of successful cloning of *phyLf* in pET28a vector. Undigested recombinant plasmid (lane 1, 3 and 6), NcoI and HindIII restriction digested recombinant plasmids showing presence of *phyLf* insert (798bp) (lane 2, 4 and 7) and 1kb DNA ladder (lane 5).

5.3. Expression, purification and zymographic analysis of recombinant phyLf protein

Analysis of total intracellular protein in SDS-PAGE following induction with L-arabinose have shown overproduction of protein with *M*r of about 29.9 kD. This is consistent with the mass predicted from the sequence of the recombinant protein (predicted *M*r =29,863). Incubation with L-arabinose for periods longer than 4 h was found to significantly reduce the protein yield at 37°C. Therefore culture induced for 4h was taken for further purification. The Ni^{2+}-NTA affinity chromatography was able to produce ~99% homogeneity of phyLf in a single step, as determined by SDS-PAGE and Coomassie Blue-250 staining (Figure 5.7).

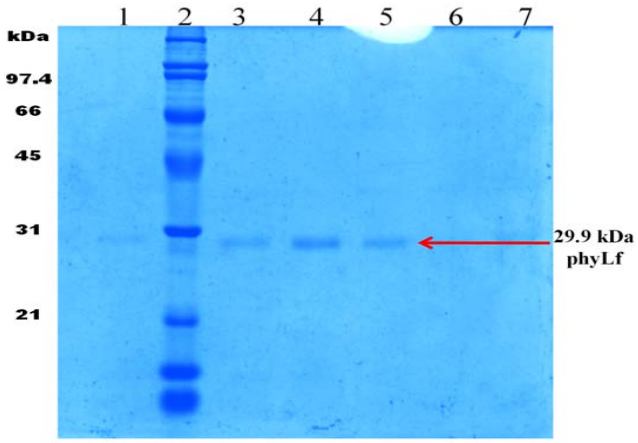

Figure 5.7: Purified fractions after Ni^{2+}-NTA affinity chromatography

Further, purified and concentrated protein by 10KDa filter (Fig 5.8A: lane2) was used for activity analysis. Zymography of purified active protein by in-gel staining of native-PAGE confirmed the phytase activity of phyLf (Figure 5.8B).

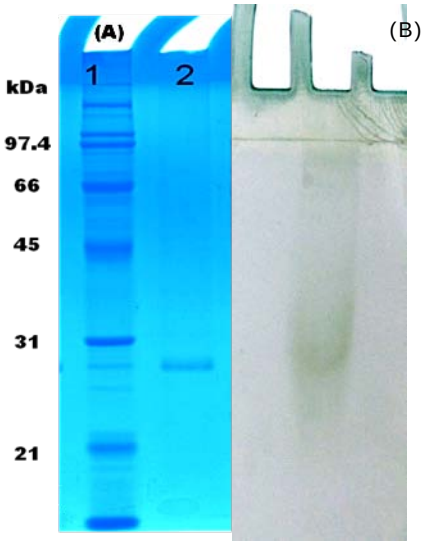

Figure 5.8: Analysis of (A) SDS-PAGE profile of purified phyLf, lane 1 has broad range protein marker, lane 2 has purified phyLf protein and (B) Zymogram developed by in-gel staining of active protein in native PAGE.

5.4. Determination of enzymatic activity and kinetic parameters-

Biochemical characterization of phyLf displayed maximum phytase activity at pH 5.0 and temperature 60 °C. Like previously characterized PTPLPs, phytase activity of phyLf was ionic strength dependent and maximum activity was observed at 100mM ionic strength (Figure 5.9A). Effect of ionic strength on phytase activity clearly showed that electrostatic interactions play important role in mechanism of action as substrate IP6 is also highly negatively charged [41]. PhyLf was fairly active within pH range 3.5 to 6.0 (>60%) (Figure 5.9B), hence, it could be categorized as an acidic phytase, which is a common characteristic of PTP like phytases. Upon preincubation for 2h in different pH buffers phyLf did not lose much activity and it retained ~85% activity throughout the whole pH range from 2 to 8(Figure 5.10A). Optimum temperature for phyLf is 60^{o}C (Figure 5.9C) which is slightly higher than the previously reported PTPLPs. Figure 5.9C shows that enzyme is fairly active from 30^{o}C to 65^{o}C, while rapid decrease (~75%) in activity was observed beyond 65^{o}C. Figure 5.10B shows that upon incubation of phyLf at 55°C for 10 min, 90% activity was retained, while 80% of its original activity was retained after 10 min incubation at 60^{o}C. Incubation at temperatures above 60^{o}C caused a significant activity loss (~75-80%) hence;

Enzyme was stable upto 60^{o}C beyond which activity loss was observed due to heat denaturation. The apparent Km and Kcat for IP6 were 0.7735 mM and 84.31 sec^{-1}, respectively. Specific activity of phyLf for IP6 hydrolysis was 174.5U mg^{-1}. Despite of huge sequence and structural dissimilarity pH, temperature optima and kinetic parameters of phyLf surprisingly falls within range of previously reported PTPLPs [40, 41].

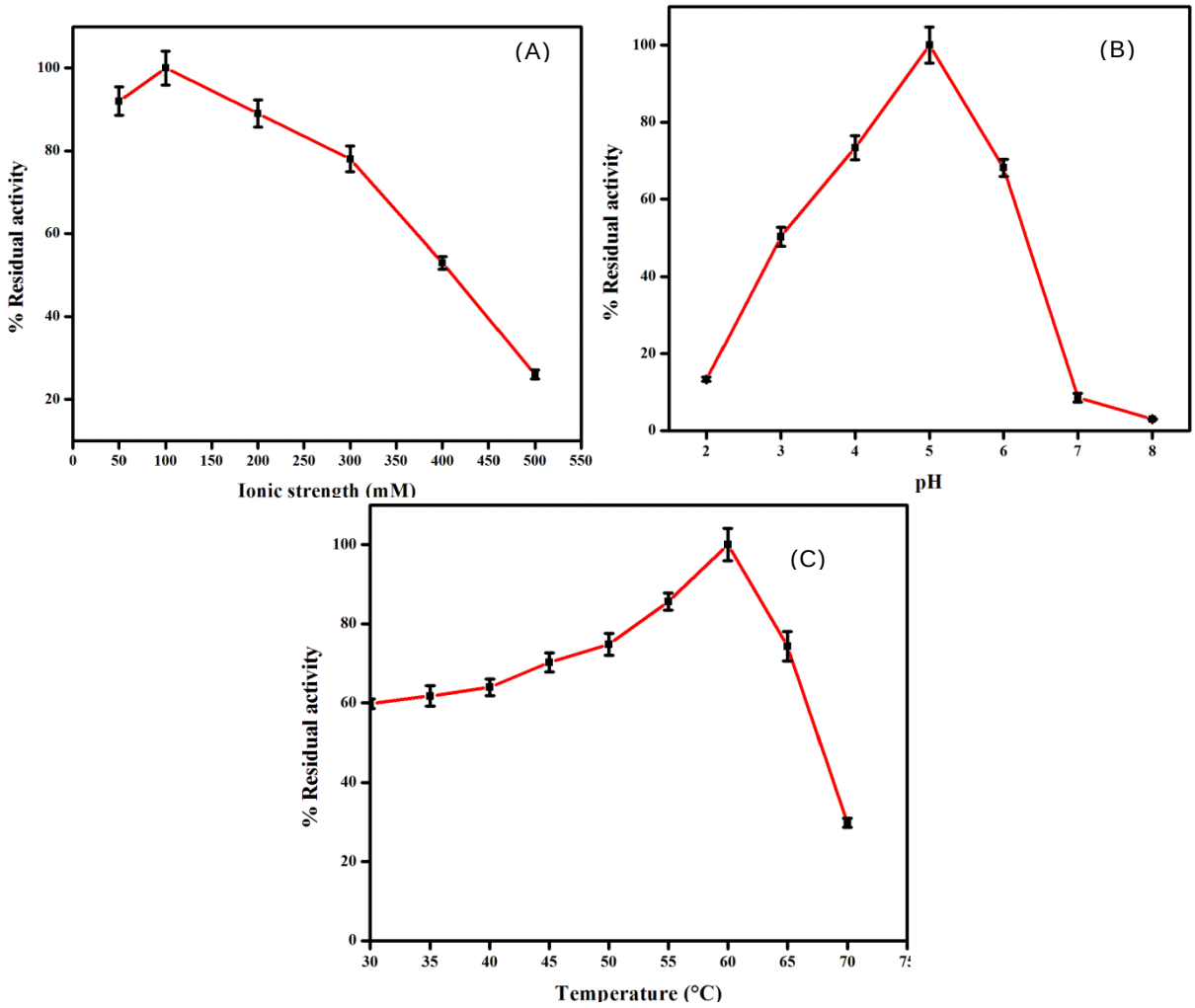

Figure 5.9: Effect of (A) Ionic strength (B) pH and (C) Temperature on phyLf enzyme activity.

Experiments were run in triplicates. Data represents the mean values with error bar representing the standard deviation.

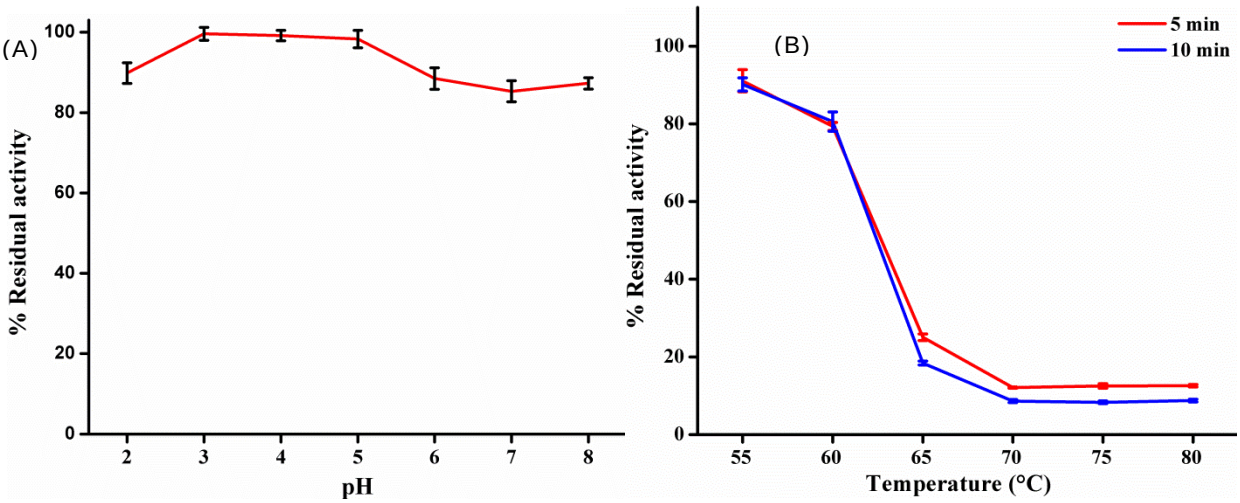

Figure 5.10: (A) Shows pH tolerance of PhyLf over a range of pH 2-8. (B) Shows temperature tolerance of PhyLf from 55 to 80^{o}C.

Evaluation of ability to hydrolyze various phosphorylated compounds exhibited narrow substrate specificty of phyLf (Table 5.1). Maximum phosphatase activity was observed for IP6. Besides IP6, very mild activity was observed for glucose-1-phosphate (14.7%), GTP (9.5%) and ATP (7.8%). But in contrast to MptpB like proteins, almost negligible activity (1.4 %) was observed for phosphotyrosine analog p-nitrophenyl phosphate (pNPP) which is a common substrate of PTPs [5, 140]. Hence, phyLf enzyme activity is highly specific for IP6. High substrate specific nature of phyLf matches with PTP like phytase of *Bdellovibrio bacteriovorus* [40]. This property establishes phyLf as a true phytase.

Table 5.1: Hydrolysis of different phosphorylated compounds by phyLf.

Substarte (1mM)	Relative activity (%)
Phytate	100.0±0.80
Ribose 5 Phosphate	ND
Glucose1 Phosphate	14.7±1.51
Phosphoenol Pyruvate	1.4±0.51
Fructose1,6 Phosphate	ND
Paranitro Phenyl Phosphate	0.4±0.30
ATP	7.8±1.11
GTP	9.5±1.20
Glucose 6 Phosphate	4.9±1.20

The data represents the mean values with ± standard deviation of triplicate experiments. ND shows no detectable catalytic activity.

The study of the effect of metal ions on phyLf activity showed that the enzyme activity was almost unaffected by Ca^{++}, Hg^{++}, Mg^{++} and Co^{++}, while Ag^{++} showed stimulatory effect (Table 5.2). On the other hand, Fe^{++}, Mn^{++} and Zn^{++} and sodium vanadate, an eminent inhibitor of PTPs, almost completely inhibit the enzyme activity.

Table 5.2: Effect of metal ions on phytate hydrolysis by phyLf.

Metal Ions	**% Residual activity**	
	5mM	10 mM
Phytate (Control)	100.00	100.00
$AgNO_3$	151.66 ± 4.72	90.89 ±1.80
$ZnCl_2$	22.55 ±0.91	3.14 ±0.15
$HgCl_2$	92.85 ±2.03	45.38 ±1.35
$CaCl_2$	101.20 ±3.93	65.52 ±1.50
Vanadate	4.38 ±0.18	ND
$MgCl_2$	90.56 ±3.42	83.68±2.71
$CoCl_2$	87.90 ±3.66	70.98±1.15
$FeCl_3$	7.80 ±0.27	6.08 ±0.17
$MnCl_2$	71.24 ±1.15	19.42 ±0.82
$CuCl_2$	7.24 ±0.25	3.01 ±0.12

The data represents the mean values with ± standard deviation of triplicate experiments. ND shows no detectable catalytic activity.

The effect of different inhibitors, detergent, chelating agent and chaotropic agent was analysed on phyLf activity (Table 5.3). phyLf was insensitive or moderately sensitive to DTT, BME, idoacetamide, EDTA and urea, even after 30 min of incubation. Resistance to DTT and BME even after presence of cysteine) at active site is a surprising property. This may be due to the presence of only single cysteine residue in phyLf sequence hence, formation of intrachain disulfide bond is practically impossible. Incubation with 5mM SDS for 30 min caused ~70% activity loss, while incubation with 5mM sodium fluoride for 30 min caused nearly complete activity loss. PTPLP is a least studied class of phytases hence not much data are available to compare the effect of inhibitors, detergent, chelating agent and chaotropic agents on enzyme activity in literature.

Table 5.3: Effect of inhibitors on phytate hydrolysis by phyLf.

Inhibitors	**% Residual activity**
Phytate (Control)	100 .00 ±0.36
SDS	0.96 ±0.03
Iodoacetamide	80.59 ±1.99
BME	97.03 ±2.12
Urea	95.42 ±1.14
NaF	32.94 ±1.71
DTT	95.65 ±2.43
EDTA	93.92 ±2.48

The data represents the mean values with ± standard deviation of triplicate experiments

5.5. HPLC analysis of degradation products

HPLC analysis of enzyme activity showed that IP5 as major degradation product from IP6 (Fig. 5.11). Small amount of IP4 was also detected but pattern of peaks smaller than IP5 was inconsistent. Since, UV-visible detector shows comparatively low sensitivity towards inositol poly phosphates (IPPs), low amount of products would not be recorded. Therefore if there would be low amount of products smaller than IP5, that amount would not be detected. Although high catalytic activity of phyLf indicates strong possibility of formation of smaller IPPs than IP5.

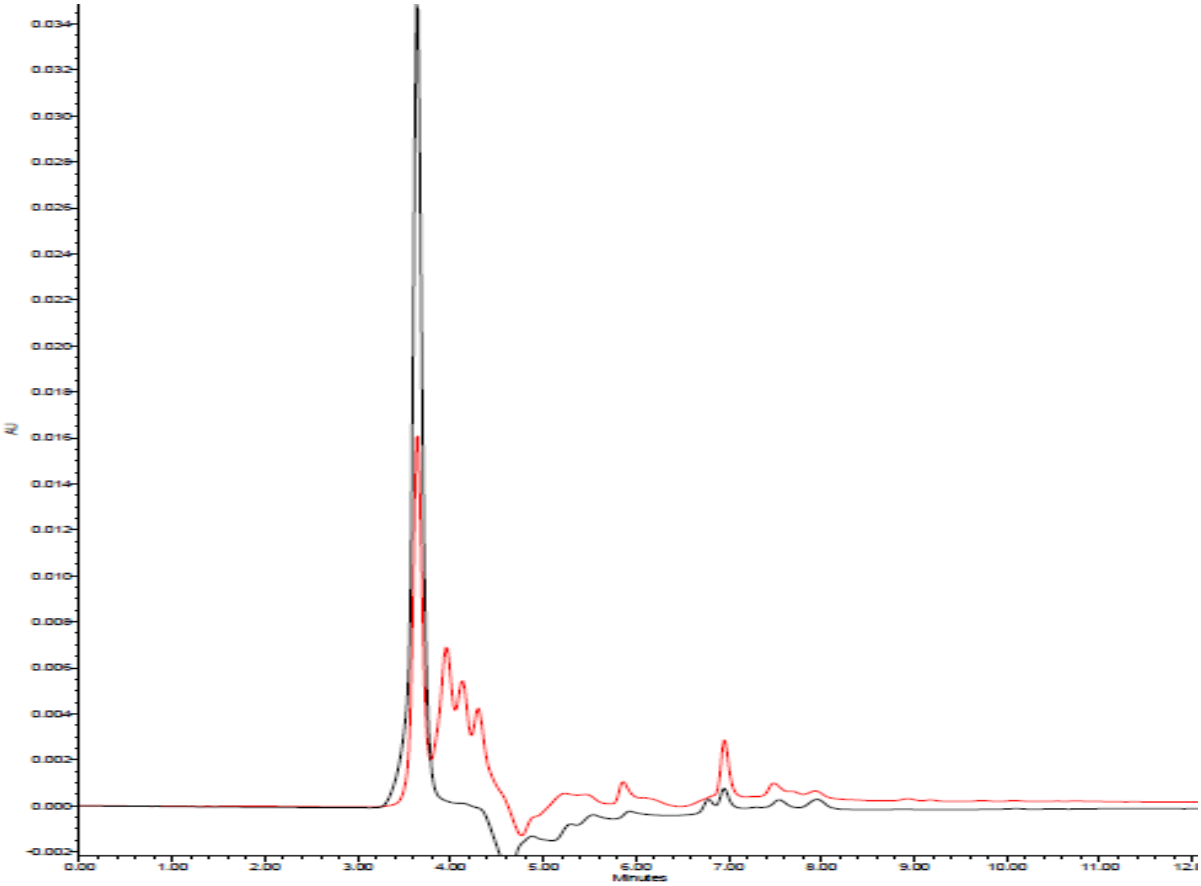

Figure 5.11: Reverse phase HPLC analysis of the IP6 hydrolysis products by phyLf. Overlapping of substrate chromatogram (Black) with reaction product chromatogram (Red) shows longer retention time of less phosphorylated/polar product and degradation of IP6 (black) into reaction products (Red).

5.6. Analysis of protein secondary structure

In-silico secondary structure prediction by various programs (PSIpred, Jpred, PHYRE2, PRALINE etc.) showed that phyLf was mainly a helical protein consisted of several α helices and

4 β strands. Like ptpB, phyLf have two extra sequence insertions in comparison to most other PTPs [5] first insertion is upsteam to phytate binding loop connecting β3 to α4. This region is preceded by general acid loop, which is DTD (from 91 to 93 amino acid) in phyLf not WPD or FPD like other PTPs [5]. Second insertion is downstream to P-loop, which is predicted to form two large α helices [5]. Both of the insertions in phyLf are smaller than the ptpB. (Figure 5.13).

Negative peak from~205 to 250 nm in CD spectrum of native protein indicated predominantly helical secondary structure. A gradual change in CD-spectrum has been observed in presence of increasing concentration of IP6 which indicates structural rearrangement in phyLf on substrate binding (Figure 5.12). In agreement with CD spectrum analysis, *In-silico* prediction also illustrates higher percentage of α-Helix (~50%) than β-sheet(~10%) in phyLf secondary structure (Fig. 7).

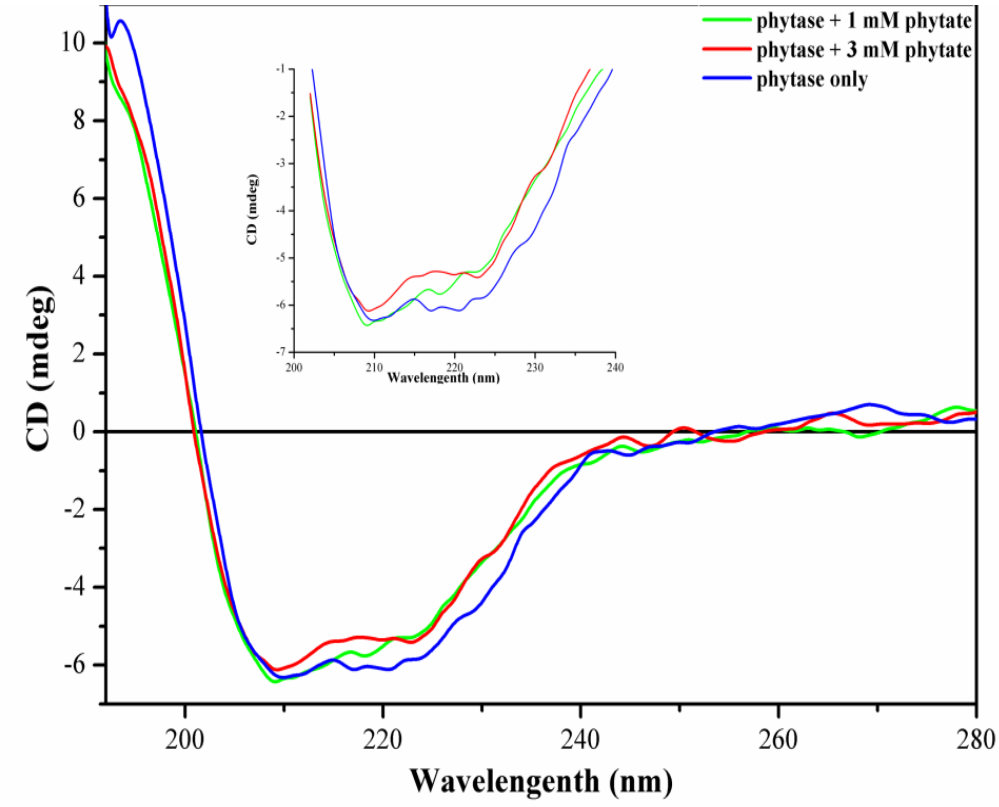

Figure 5.12: CD spectra analysis of native phyLf and in presence of 1mM and 3mM phytate. Inset shows gradual change in spectra in presence of increasing concentration of substrate

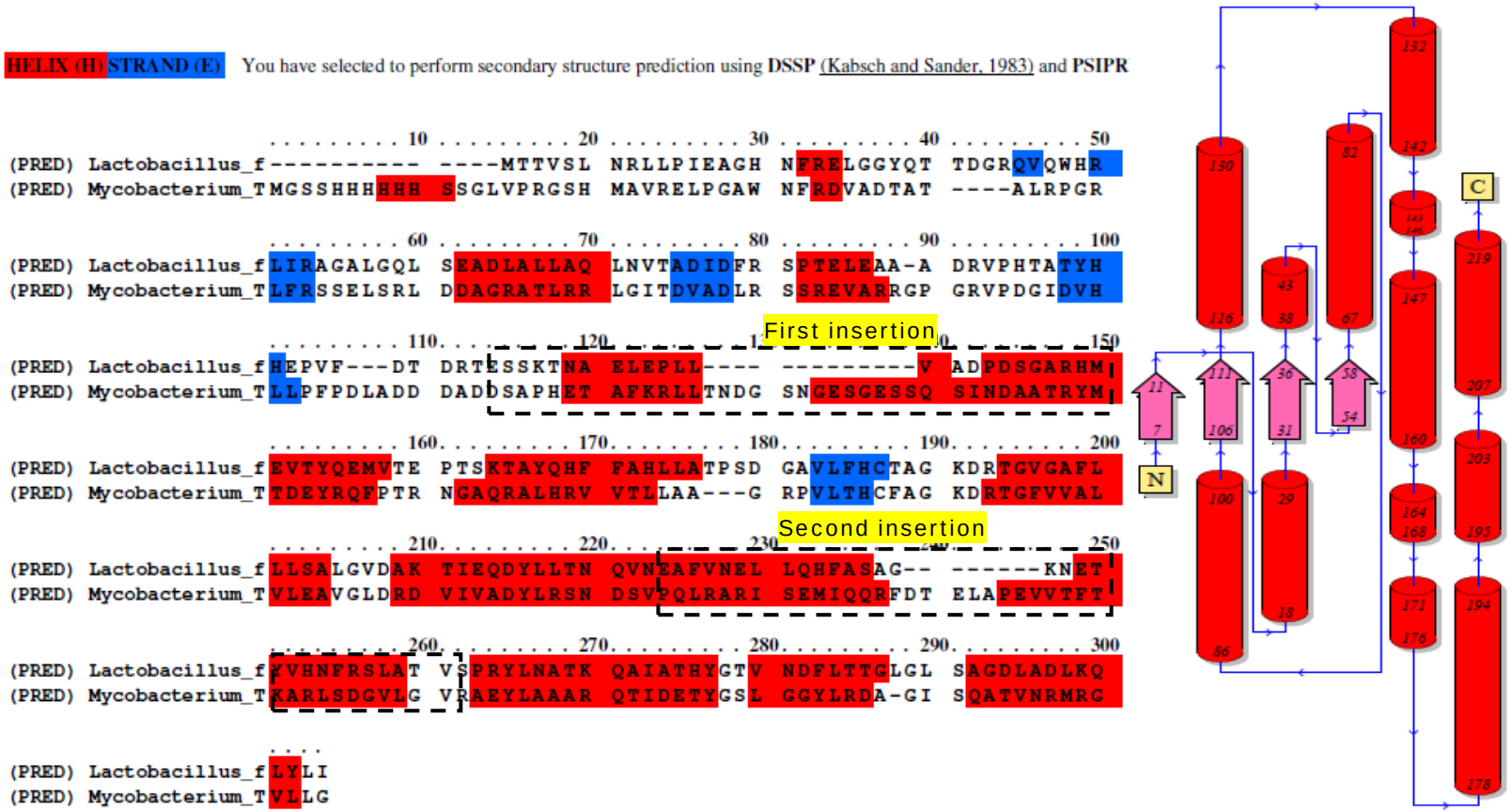

Figure 5.13 (A) Alignment of phyLf (from *Lactobacillus*) predicted secondary structure with MptpB (from *Mycobacterium*) secondary structure by PRALINE server. (B) Topology of spatial arrangement of secondary structure elements in phyLf homology model, analyzed by PDBsum

5.7. Three-dimensional structure analysis of the protein

Alignment of phyLf with PDB structure database shows *Mycobacterium* MptpB as closest structure**.** PTP class of proteins are known to exhibit strong structural conservation of catalytic domains even after little sequence homology [5] As PTP1B and YopH, two representative conventional PTPs, share only about 20% sequence homology, but high structural similarity (Barford et al., 1994; Stuckey et al., 1994). There is not much sequence similarity (~29%) but alignment of predicted secondary structure of phyLf with MptpB secondary structure shows good conservation of secondary structure folds (Fig. 5.13), Also it matches well with predicted secondary structures of close orthologs of the gene in non-pathogenic firmicutes. Collectively, these results corroborate with select MptpB as template for homology modelling of phyLf.

phyLf backbone atoms trace similar path as template ptpB, overall phyLf have central 4 parallel stranded β sheet, surrounded by several α helices (Fig. 5.14A). PTP active site comprises phosphate binding P-loop and mobile general acid (GA) loop (Fig.5.15A). Universal ptp feature core β sheet, active site P- loop and following helix is conserved in phyLf (Fig 5.15 D). Order of β strands in central β sheet is β-1, β-4, β-2 and β-3 (Fig. 5.14 A). Unlike other conventional PTPs phyLf lacks antiparallel β -strands surrounding central β - sheet and have additional α helices. Like ptpB, phyLf have two large insertions in comparison to other bacterial PTPs although both are smaller than ptpB's. First insertion immediately follows general acid loop. GA loop have conserved aspartate(93) residue which works as proton donor to the phosphate bound substrate. GA loop preceds first insertion which forms a disordered loop. Modelling of this portion is perplexing as crystal structure of corresponding portion of the template is not properly solved. This loop has conserved serine residues in the end which may enhance the flexibility of loop. This region is predicted to form a helix (Fig. 5.13). This region is followed by P-loop harbouring active site cysteine (156), which acts as nucleophile and binds with Phosphorous. P-loop is followed by second long insertion which makes long helical ptpb like lid over active site (Fig. 5.14B), although lid is smaller in phyLf than ptpB but it covers active site. Lid has to move out of the way for substrate binding. As the length of both insertions is smaller in phyLf than ptpB, substrate binding pocket is comparatively larger in phyLf. CD analysis of protein in presence of increasing substrate concentrations shows a gradual decrease in percentage of helix which eventually increases percentage of β-sheets. It indicates a structural change in phyLf for substrate binding.

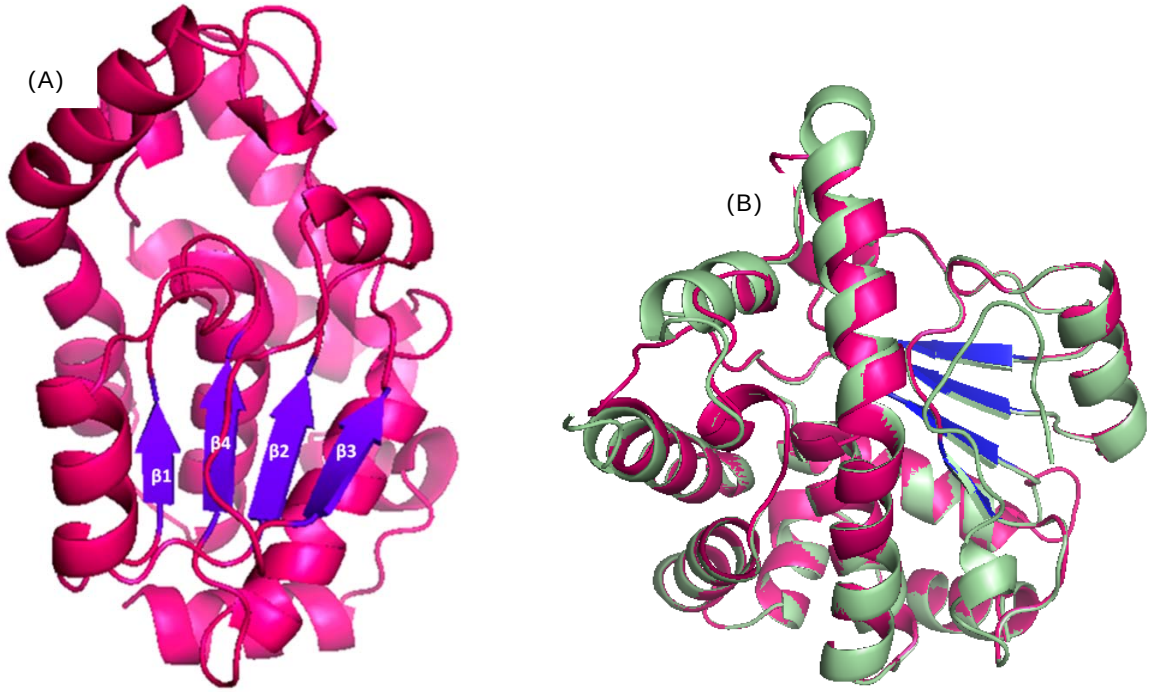

Figure 5.14: (A) Overall predicted 3D structure of phyLf showing central β-sheet comprising of 4 parallel β-strands and surrounding α-helices. (B) Superimposition of phyLf homology model (pink) with MptpB (PDB ID: 1YWF) structure (green), showing large helical cap covering active site.

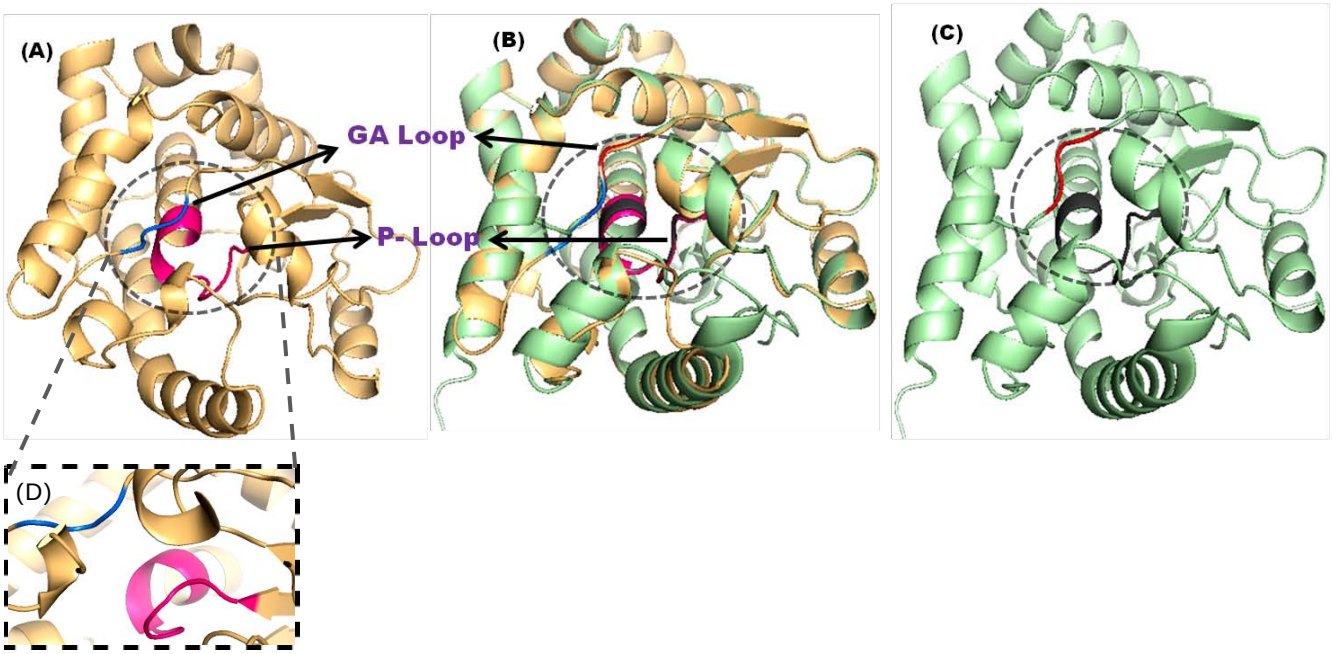

Figure 5.15: The stereo view of substrate binding pocket of (A) phyLf (B) superimposition of phyLf and MptpB structure and (C) MptpB . (D) Enlarged view of phyLf active site showing P-loop in pink (comprising core β strand, phosphate binding loop and following helix) and general acid or GA loop in blue.

5.8. Reactive oxygen species tolerance of protein

Active site cysteine nucleophile of PTPs is generally sensitive to oxidation *in-vivo* by ROS causing inactivation or regulation of protein [5]. phyLf exhibited high tolerance for oxidative inactivation by H_2O_2. Figure 5.16 shows Only 25% activity is lost after 60 min treatment with 10 mM H_2O_2 at pH 5.0 while *Mycobacterial* ptpB, recorded to have highest H_2O_2 tolerance in literature, looses 37% activity after treatment with 250 µM H_2O_2 for 20 min. at pH 7.5, Grundner et al.(2005) [5] suggested high tolerance of ptpB for H_2O_2 is due to closed active site by cap region helix in absence of substrate, which makes active site cysteine unavailable for oxidation. Other PTPs lack long cap helix henceforth active site cysteine is exposed for oxidation by ROS. phyLf also have long additional sequence after P-loop which is predicted to form helical cap over active site in 3D structure analysis. In addition this cap region in phyLf shows similarity with superoxide dismutase C-terminal domain when aligned with PDB structures. As resistance to oxidative inactivation in different PTPs in various reports does not provide very firm data for quantitative comparison but phyLf qualitatively shows exceptionally high resistance to H_2O_2 inactivation among all known PTPs till date.

If phyLf is helpful in gut colonization of *Lactobacillus* like its orthologs in other bacteria (lipA, ptpB) then it needs to be highly tolerant to H_2O_2. Various *Lactobacilli* are known to stimulate ROS generation in the host cells. Certain peptides of *Lactobacilli* interact with formyl peptide receptors (FPR) and activates NOX mediated ROS genetration, while gut inhabiting Gram negative microbes were unable to do so. *Alam et al*. has reported that redox signaling regulates commensal mediated mucosal homeostasis and restitution[141]. Since H_2O_2 is a strong oxidizing agent and can readily cause oxidative inactivation of cysteine phytase, high H_2O_2 tolerance in phyLf is a desirable character.

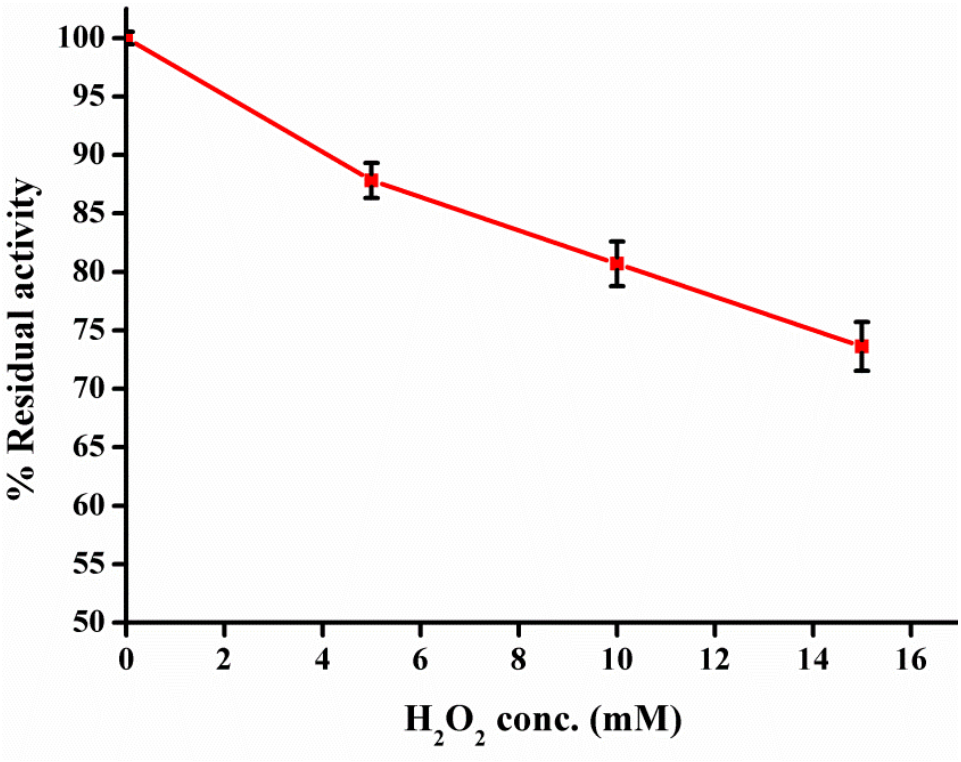

Figure 5.16: Effect of H_2O_2 on phyLf enzyme activity

CHAPTER 6

INVESTIGATION ON CHOLESTEROL ASSIMILATION ABILITIES OF *Lactobacillus fermentum* NKN51

6.1. Effect of cholesterol on growth in M17 medium

Screening of LAB isolates on MRS supplemented with 0.2% thioglycollate led to the selection of cholesterol reducing bacterium, *Lactobacillus fermentum* NKN51. Further, to understand the fate of cholesterol during growth, due to auxotrophic nature of lactobacillus, M17 medium supplemented with cholesterol and thioglycollate (0.1%) was used for the study. The growth profile of *Lactobacillus fermentum* NKN51 in M17-thioglycolate broth supplemented with cholesterol showed better growth as compared to the control (M17-thioglycolalte without cholesterol; Fig 6.1). A maximum difference of 26% growth was observed at 6 h which gradually decreases to 9% at 24 h as shown in Table 6.1. Log phase started after 6 hrs of inoculation while maximum growth was observed at 20 h.

A slight but observable increase in growth of *L. fermentum NKN51* was noticed in M17 medium after addition of cholesterol even in the absence of thioglycollate. According to previous studies, cholesterol is incorporated in cell wall and/or cell membrane [136]. There are no reports of increase in growth of *Lactobacillus* due to the presence of cholesterol. Nevertheless, considerable increase in growth of *Lactobacillus fermentum* NKN51 by incorporation of cholesterol in nutritionally scarce medium indicates that part of cholesterol supports bacterial growth (Fig. 6.1).

Table. 6.1: The growth difference at different interval of time for *Lactobacillus fermentum* NKN51 in presence and absence of cholesterol in M17-thioglycollate medium.

Time (h)	% growth increase
6	26±0.5
12	25±0.48
18	14±0.29
24	9±0.15

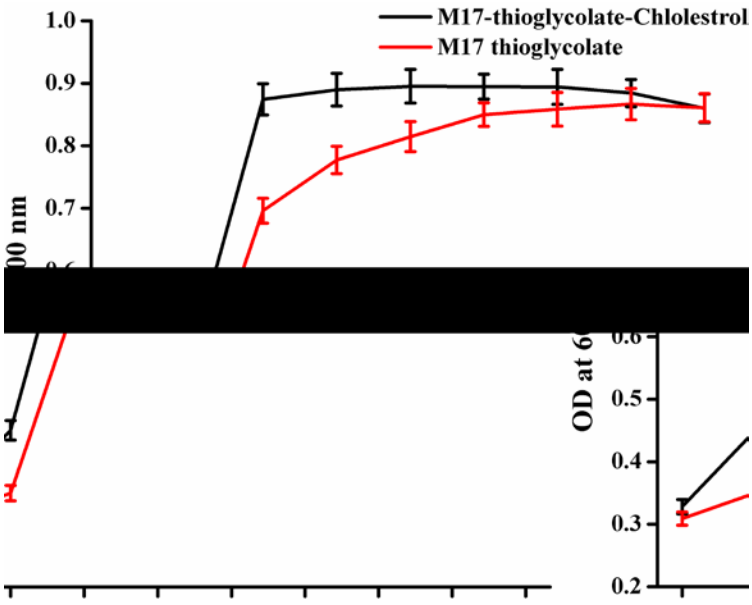

Figure 6.1: The effect of growth of *Lactobacillus fermentum* NKN52 in M17-thioglycollate medium supplemented with cholesterol. A clear difference in growth was observed in cholesterol supplemented M17-thioglycollate broth (black line) when compared with M17-thioglycollate broth alone.

6.2. Flow cytometric analysis on consumption of fluorescent cholesterol by *Lactobacillus fermentum* NKN51

The uptake of cholesterol is apparent from the growth profile of *Lactobacillus fermentum* NKN51 in presence of cholesterol. This analysis of the results prompted us to confirm the above observation. *Lactobacillus fermentum* NKN51 was allowed to grow in M17-thioglycollate medium in the presence of NBD-cholesterol (15µg/ml). After growth of 24 h, the bacterial cells were analyzed by flow cytometer for the uptake of cholesterol. The results in the Fig. 6.2 show a distinct shift in the fluorescence peak for cells grown in presence of NBD-cholesterol (pink) in comparison to the control samples without NBD cholesterol. As NBD-cholesterol is a fluorescent molecule with excitation at 469 nm (blue) and emission at 538 nm (yellowish-orange), thereby its assimilation by the cells results in emission of fluorescence in the PE bandpass filter range (X-axis of Fig. 6.2) upon excitation. Therefore a shift in the fluorescence intensity of cells grown in NBD-cholesterol clearly suggests and confirms the assimilation of cholesterol by *Lactobacillus fermentum* NKN51. These observations give strength to the hypothesis of *in-vivo* cholesterol assimilation by lactic acid bacteria and thus, possibly results in hypocholesterolemic effect.

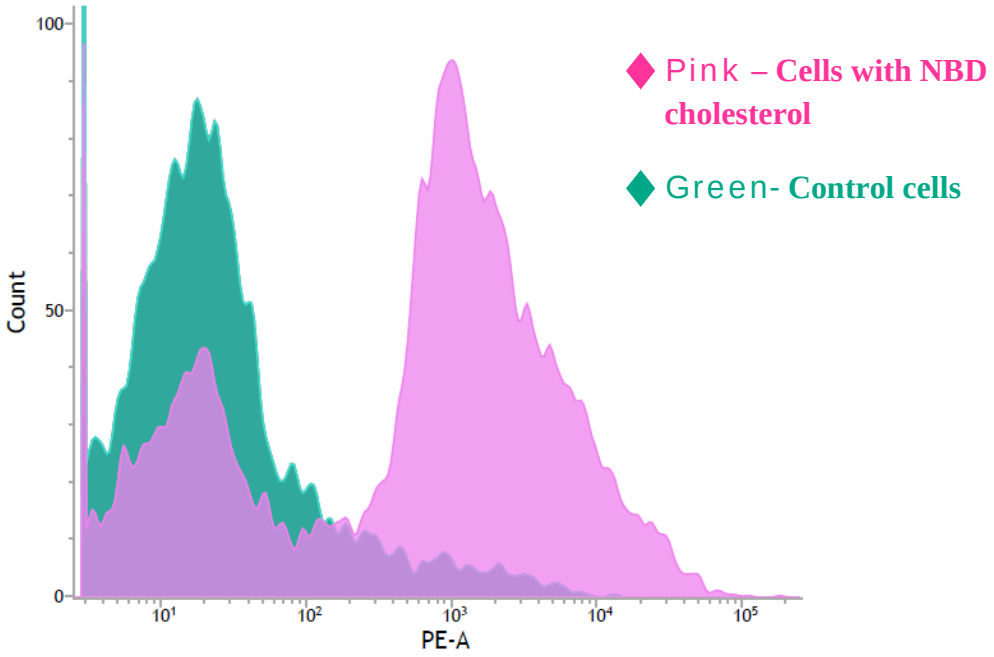

Figure 6.2: Flow cytometric analysis of cholesterol assimilation ability of *Lactobacillus fermentum* NKN51. A shift in fluorescence peak for cells grown in NBD-cholesterol (pink) indicates assimilation of cholesterol as compared to the control cells without NBD-cholesterol (green).

6.3. Pathway analysis

Exact mechanism of cholesterol consumption is not known for gut inhabiting symbiotic flora and very few reports are available for mechanistic exploration [11, 58]. Based on the current knowledge of cholesterol degradation mechanism in symbiotic bacteria only one study has reported direct cholesterol conversion into coprostanol by lactobacilli (path II, Fig. 6.3), involving cholesterol reductase activity but no protein or gene sequence responsible for this enzymatic activity has been described [7]. All other reports suggested indirect cholesterol conversion into coprostanol by intermediate formation of cholestenone and coprostanone.[11, 58]

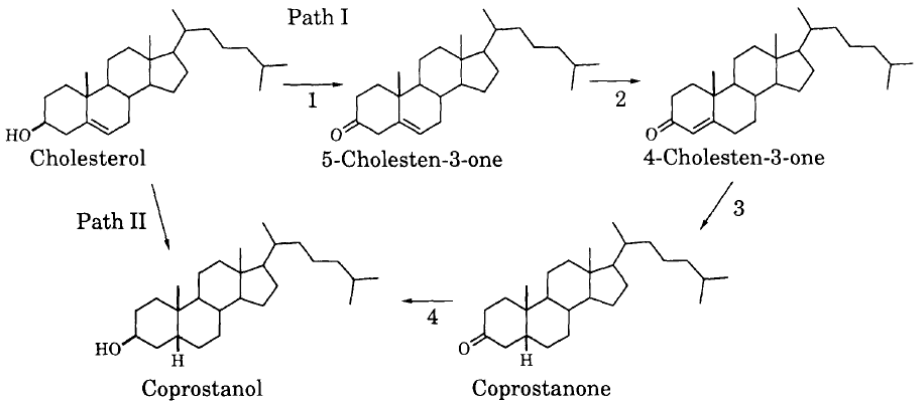

Figure 6.3: Pathway proposed for cholesterol conversion into coprostanol by gut microflora. [11]

First step in the indirect pathway (path I, fig.6.3) is conversion of cholesterol to cholestenone, which is also first step in cholesterol degradation by non lactic acid bacteria like *Brevibacillus, Mycobacterium, Rhodococcus* etc. which completely degrades cholesterol as carbon source into carbon dioxide (CO_2). (Fig. 6.4)

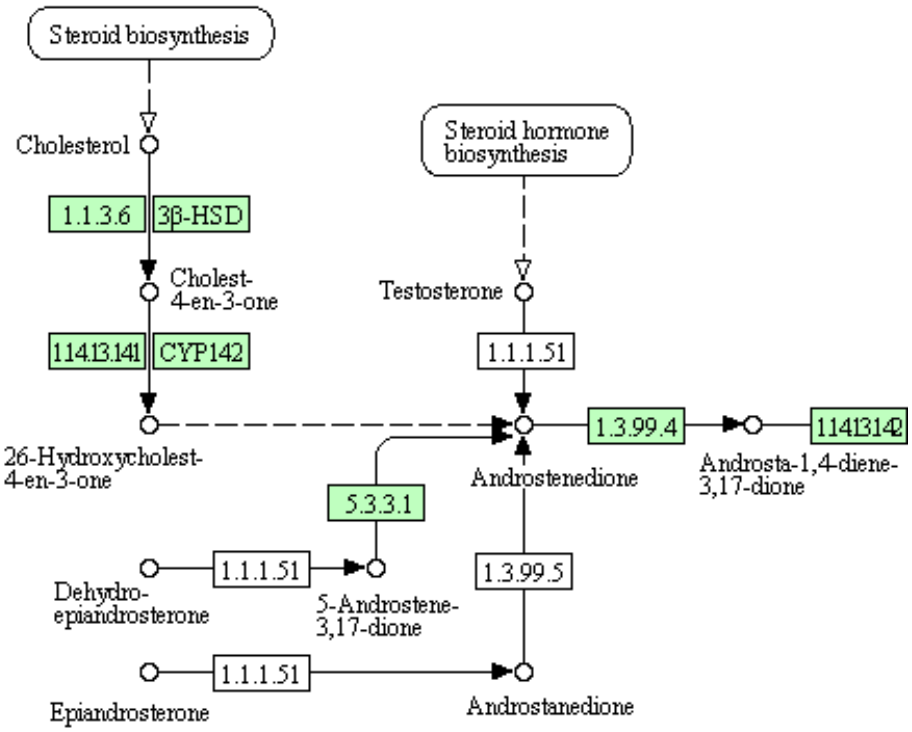

Figure 6.4: Pathway invoved in complete mineralization of cholesterol

(source of figure: http://www.genome.jp/kegg/pathway/map/map00140.html)

Enzymes involved in the conversion of cholesterol to cholestenone in non-lactic acid bacteria are cholesterol oxidase and 3β-hydroxysteroid dehydrogenase. Hence, we searched genomic DNA of *Lactobacillus fermentum* for putative enzymes of these classes.

6.4. Search for cholesterol metabolizing genetic locus in *Lactobacillus fermentum* NKN51

Cholesterol oxidases are FAD dependent enzymes, involved in oxic degradation of cholesterol to generate H_2O_2 after cofactor regeneration. Therefore, presence of cholesterol oxidase is very unlikely as cholesterol consumption is on anaerobic process in *Lactobacilli* [60]. Bacterial 3β-hydroxysteroid dehydrogenases (3βHSD) uses NAD or NADP as cofactor and are members of short chain dehydrogenase family (SDR) of proteins. They have common Rossman fold, cofactor binding N-terminal prosite pattern TGXXGXXG and atypical substrate binding site which is usually YXXXK but YXXXN in fungal HSDs [142]. Therefore, these

patterns of 3βHSD were searched in the genome of *L. fermentum*. Gene > LC40_0723 (designated as *hsdlf* herein after) was predicted as a putative 3β hydroxysteroid dehydrogenase, and has both N-terminal cofactor binding motif and conserved YXXXK motif as shown in Fig. 6.5. This gene was further selected to study 3β-hydroxysteroid dehydrogenase activity of the encoded polypeptide and its role in cholesterol assimilation by *Lactobacillus fermentum* NKN51.

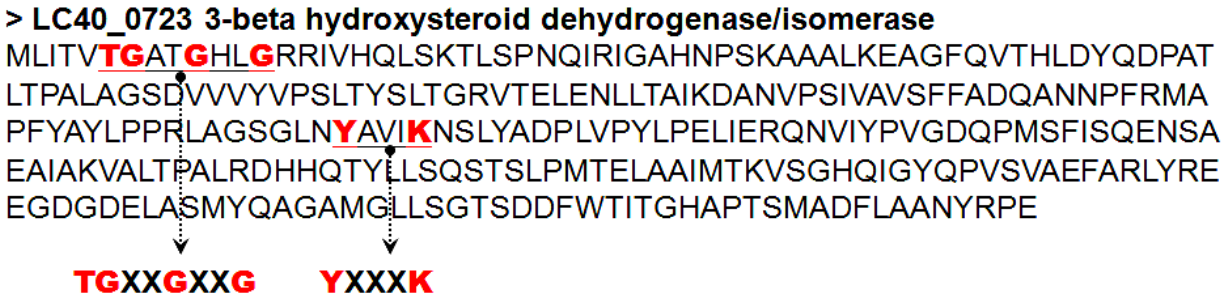

Figure 6.5: Amino acid sequence of 3βHSDLf showing N- terminal co-factor binding site and conserved active site motif.

Motif id	From	To	Definition	E value	Score
pf:RmlD_sub_bind	1	23	RmlD substrate binding domain	0.71	-
pf:DapB_N	2	71	Dihydrodipicolinate reductase, N-terminus	0.12	-
pf:NAD_binding_10	3	186		4.9e-15	-
pf:NmrA	3	226	NmrA-like family	5.3e-12	-
pf:Epimerase	3	72	NAD dependent epimerase/dehydratase family	0.00032	-
pf:Polysacc_synt_2	3	45	Polysaccharide biosynthesis protein	0.011	-
pf:Saccharop_dh	4	71	Saccharopine dehydrogenase	0.0005	-
pf:adh_short	4	66	short chain dehydrogenase	0.02	-
pf:3Beta_HSD	5	79	3-beta hydroxysteroid dehydrogenase/isomerase family	2.6e-07	-
pf:NAD_binding_4	5	51	Male sterility protein	0.0046	-
pf:TrkA_N	7	66	TrkA-N domain	0.00025	-
pf:B12-binding	39	114	B12 binding domain	0.15	-
pf:Cys_Met_Meta_PP	40	117	Cys/Met metabolism PLP-dependent enzyme	0.069	-

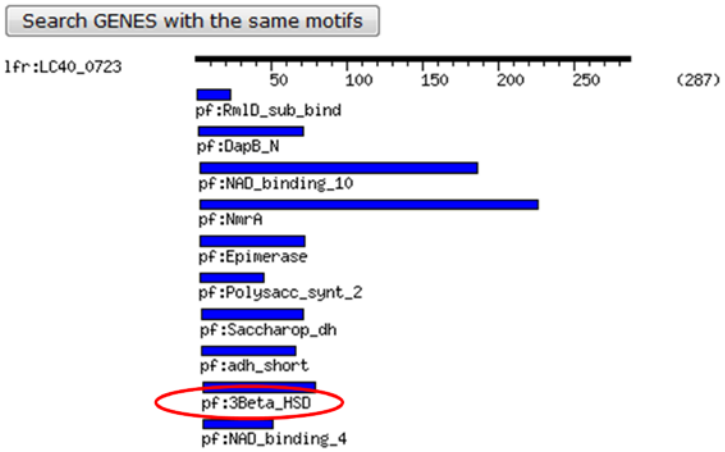

Figure 6.6: 3βHSD motif predicted in the selected protein sequence (hsdLf), by Kyoto encyclopedia of genes and genomes or KEGG. (http://www.genome.jp/kegg/)

6.5. Phylogenetic analysis

Alignment of 3βhsdLf amino acid sequence with protein database using NCBI-pBLAST program showed its orthologs in other *Lactobacillus* species with the nearest orthologs being *Lactobacillus reuteri* and *Lactobacillus hominis*. The above multiple sequence alignment data, with few selective previously reported cholesterol dehydrogenase from other bacteria were used for constructing a phylogenetic tree by MEGA6 software [126].

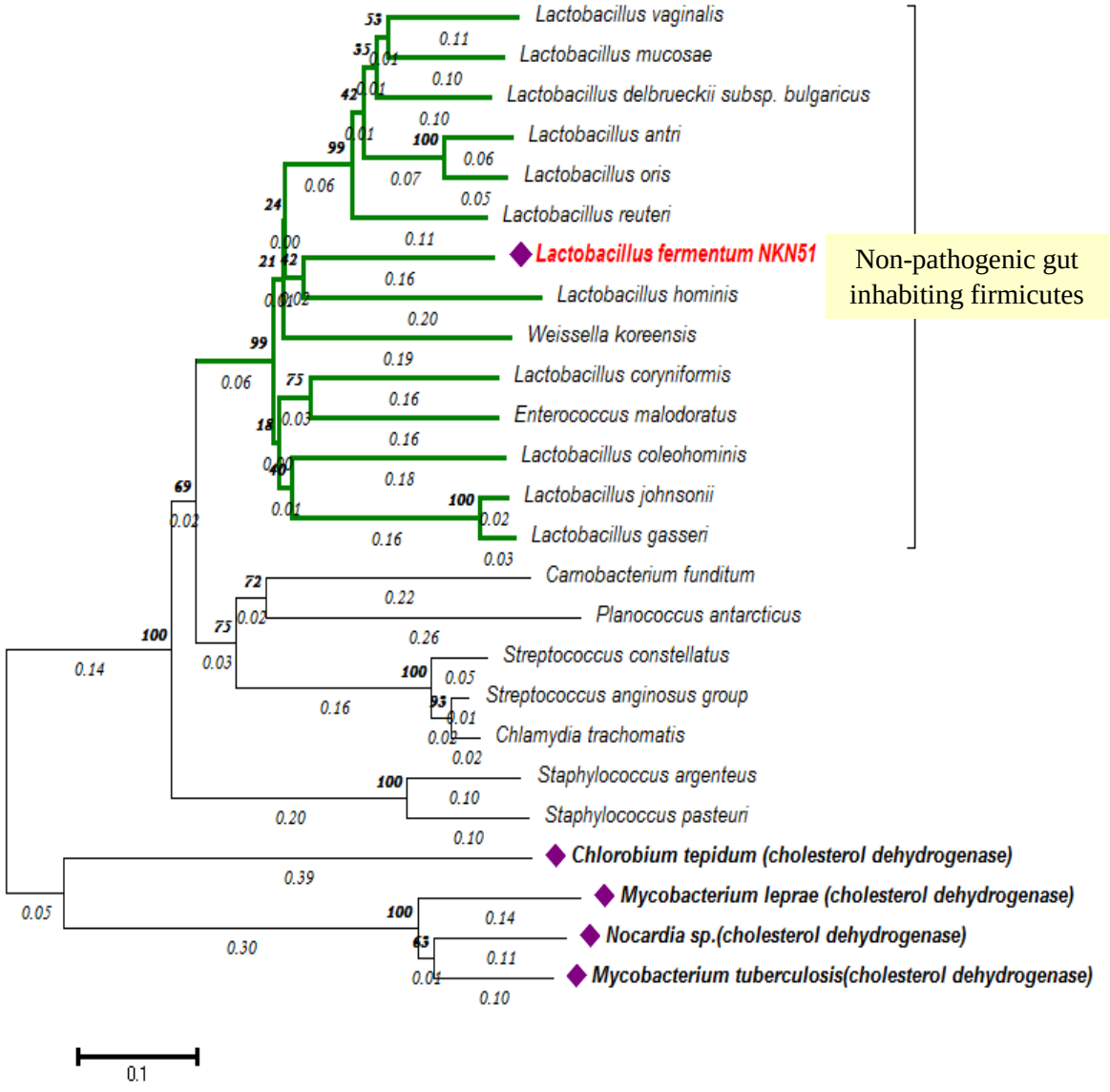

Figure 6.7: Maximum likelyhood tree for phylogenetic analysis of 3βHSDLf from *L. fermentum* with its orthologs found in non pathogenic firmicutes and previously known cholesterol dehydrogenases.

6.6. Multiple sequence alignment by COBALT

Multiple sequences alignment of 3βhsdLf protein sequence with existing and predicted cholesterol dehydrogenases was done by COBALT program. The alignment in Fig. 6.9 showed some unexpected results, as the active site (YXXXK) pattern of 3βHSDLf in *Lactobacillus fermentum* NKN51 was found to be at a different position (highlighted in yellow color) from the active site (YXXXK) of the rest of the cholesterol dehydrogenase. Along with this, a sequence pattern (YXXXR) slightly different from the active site was in alignment with the active site of the rest of cholesterol dehydrogenases sequences. If the position of this site falls at the same place in secondary or tertiary structure, then the active site pattern of 3βHSDLf is slightly modified, replacement of lysine (K) with arginine (R) will not affect the function of the protein to large extent because both are basic amino acids. However, it can affect the kinetics of the reaction. Ge´raldine *et al* 2012 [142] suggested that tyrosine (Y) of active site (YXXXK) binds the substrate, whereas lysine (K) of the active site likely reduces the pKa of tyrosine due to its basic nature. Similarly, the presence of arginine (R) in 3βHSDLf of *Lactobacillus fermentum* NKN51 can also reduce the pKa of tyrosine contributing phenomenal to oxidoreducase nature of enzyme [142].

Phylogenetic tree based on COBALT gave the same result as shown by MEGA6 of 3βHSDLf from *Lactobacillus fermentum* NKN51 being closest to *Chlorobium tepidum* (Fig. 6.8).

Figure 6.8: Alignment of 3βHSDLf with previously reported cholesterol dehydrogenases by COBALT program box 1 shows co factor binding site and box 2 shows active site.

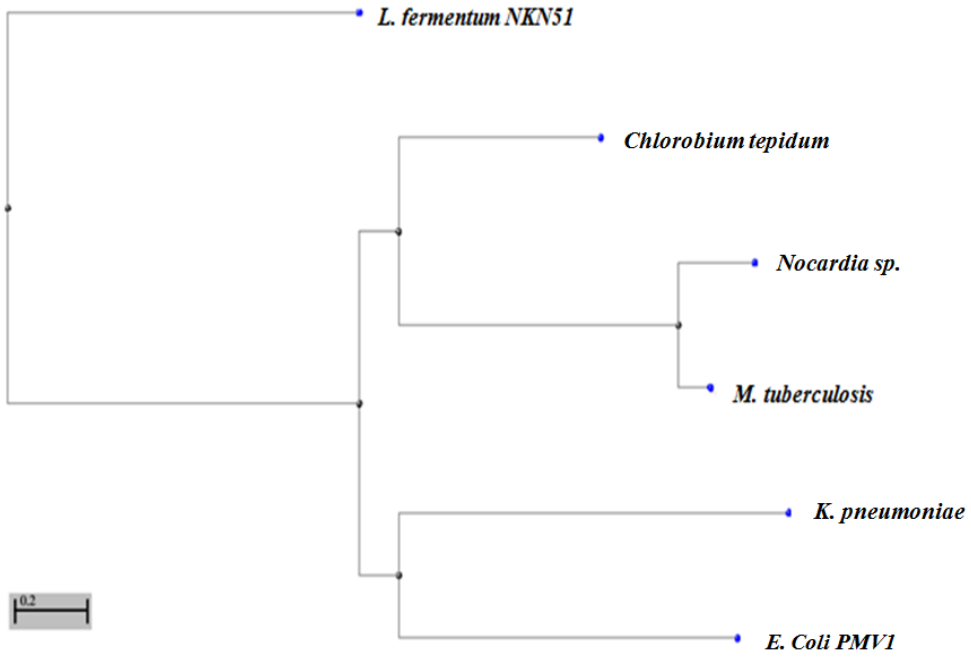

Figure 6.9: Distance tree of 3βHSDLf with established cholesterol dehydrogenases by COBALT software. 3βhsdLf from *Lactobacillus fermentum* NKN51 displayed/showed closest evolutionary relationship with cholesterol dehydrogenase sequence of *Chlorobium tepidum*

6.7. Cloning and expression of putative 3βhsd in pET28a

Based on the bioinformatics search results, we decided to investigate 3βHSDLf of *Lactobacillus fermentum* NKN51 as a probable candidate for genetic locus responsible for cholesterol assimilation. Selected gene encoding for 3βHSDLf protein was PCR amplified from genomic DNA of *L. fermentum* NKN51 and size of the amplified product was checked on 1% agarose gel as shown in Fig. 6.10. A The amplified product (864bp) was double digested with *NdeI* and *HindIII* and ligated with pET28a vector digested with similar enzymes to yield a recombinant construct pET28a-*hsdLf* (Fig. 6.10 B). The recombinant plasmid was transformed in *E. coli* DH5α and the plasmid isolated from transformants was checked for the presence of hsdlf insert, by double digestion. Figure 6.11 shows that the ~864 bp fragment was excised out of recombinant plasmid after double digestion. Sequencing of recombinant plasmid (pET28a-*hsdLf*) confirmed the cloning of desired gene in proper orientation and with expected nucleotide sequence.

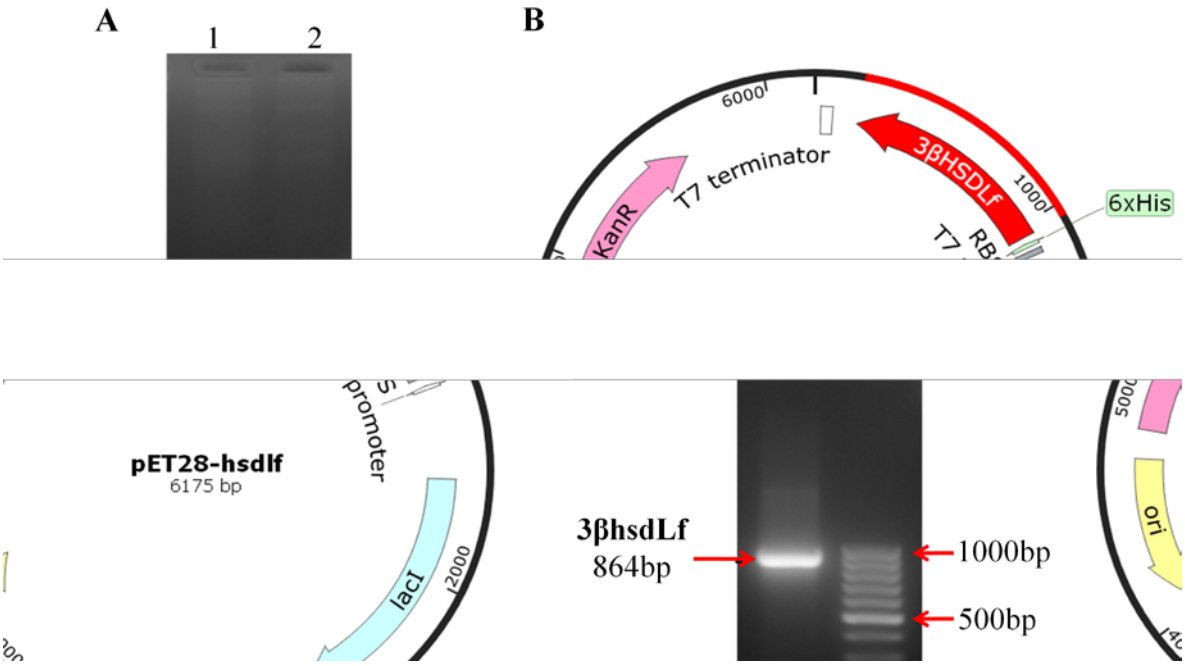

Figure 6.10: Cloning of *hsdLf* in pET28a expression vector. (A) Agarose gel electrophoresis (1%) of lane1-PCR amplified *hsdLf*, lane2- 1kb DNA ladder (B) vector map of pET28a-*hsdLf* recombinant plasmid.

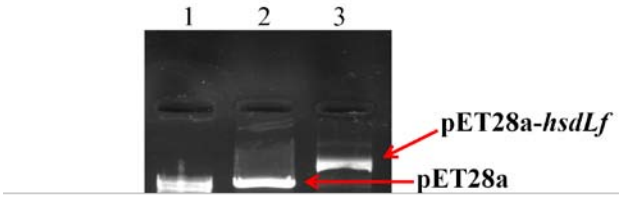

Figure 6.11: Confirmation of successful cloning of *hsdLf* in pET28a vector. Lane 1- 1kb DNA ladder, lane 2- *NcoI* and *HindIII* digested recombinant plasmid showing presence of 864bp of *hsdLf*, lane 3- Undigested recombinant plasmid

6.8. Expression and purification

For over expression of 3βHSDLf, pET28-hsdlf construct was transformed in *E. coli* BL21AI cells. Tranformants were induced with 0.75% arabinose and expression of the protein was checked by preparing the induced and uninduced samples by boil prep and run on 12%

SDS PAGE. Lane 1 and 2 of Fig 6.12 shows uninduced and induced protein samples. A band of *Mr* 30kD was observed in induced sample indicating the over-expression of protein. This over expressed protein was purified by Ni-NTA affinity column (Fig. 6.12) and the purified fractions were pooled and passed through 10kDa centrifugal device to exchange of buffer for imidazole removal and to concentrate the protein. Purified concentrated protein was checked on 12% SDS PAGE. Lane 3 of Fig 6.12 shows purified protein

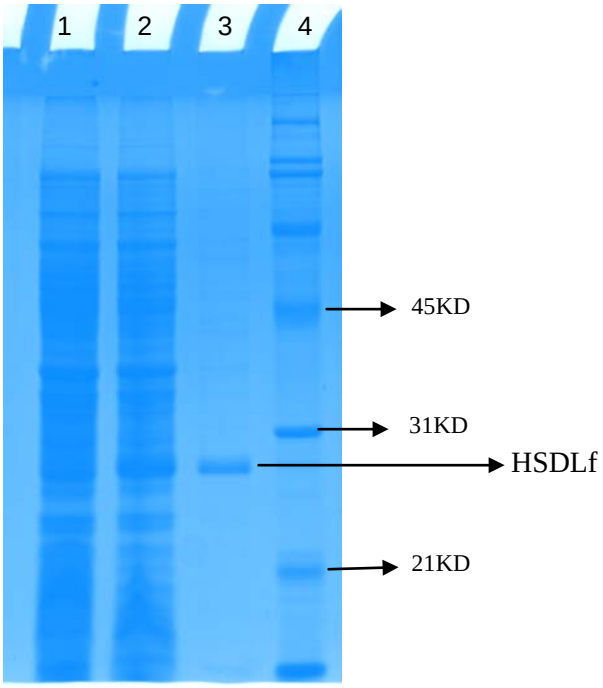

Figure 6.12: Expression and purification of 3βHSDLf in *E. coli* BL21AI on SDS PAGE; Lane 1 and Lane 2 shows protein from uninduced and induced samples respectively. Lane 3 has purified 3βHSDLf and lane 4 is broad range protein marker (Bio-Rad).

6.9. Functional analysis

Functional analysis of purified protein was done by zymography and biochemical analysis of 3βhsdLf enzyme activity against cholesterol as substrate.

6.9.1. Zymography

Fig 6.13 shows zymogram of hsdlf, a dark blue color band appeared after gel development with cholesterol and chromogenic reagents [127]. In-gel activity assay was done by gel electrophoresis of purified protein on native PAGE at 4^{o}C. After electrophoresis, gel was incubated in pH 8.0 tris-HCl buffer containing the substrate cholesterol, NAD and color developing reagents (phenazine methosulphate and tetrazolium blue). The reaction of enzyme with cholesterol in presence of NAD removes hydrogen from cholesterol and reduces NAD to

NADH, this NADH reacts with tetrazolium blue to form colored formazone, while phenazine methosulphate acts as activator of the reaction. Gel was immersed in solution and incubated in dark at 37^{o}C for 1h or until the band appeared.

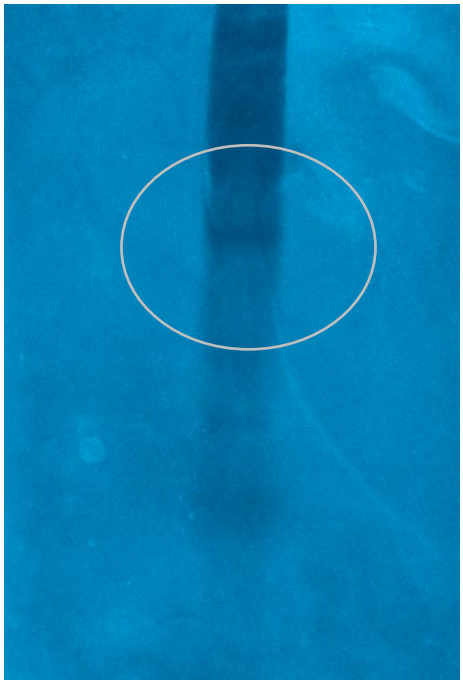

Figure 6.13: Zymograph of 3βHSDLf *in gel* activity staining in native PAGE. Circled region shows the developed band of 3βhsdLf.

6.9.2. Priliminary analysis of Enzyme activity

Besides zymography, enzyme activity was also checked by biochemical analysis of cholesterol conversion by 3βhsdLf in the presence of NAD. And the NADH formed in reaction was analysed by adding phenazine methosulphate and tetrazolium blue containing color reagent in reaction mixture. After 30 min of addition of color reagent, OD of the reaction was checked at 570 nm. An increase in OD of the enzymatic reaction was observed in comparison to the control reaction. Control reaction was processed in similar way except the addition of enzyme. A 50% increase in OD of the enzyme reaction was observed in comparison to the control reaction, at 570 nm, indicating formazone formation due to enzyme reaction. Although detailed biochemical analysis of the enzyme is still remaining but cholesterol dehydrogenase activity of 3βhsdLf is confirmed zymography and preliminary biochemical analysis.

6.10. *In-silico* Secondary structure analysis

Secondary structure analysis of 3βHSDLf was done by various online servers PHYRE, PRALINE, JPRED and PSIPRED. Results of all of the methods predicts a typical NAD

binding Rossmann fold like pattern of alternative β-α-β-α-β-α–β-α which usually forms central beta sheet of parallel or antiparallel beta strands surrounded by α helices in Short chain Dehydrogenases. As observed in multiple alignment of 3βHSDLf with known cholesterol dehydrogenases, active site pattern of HSDLf is YXXXR in place of YXXXK, The PHYRE result of secondary structure prediction in Fig. 6.14 shows that (136)YXXXK(140) site of 3βHSDLf forms a beta sheet (β6) while in other HSDs it forms α helix, but (124)YXXXR(128) site upstream to it, forms an α helix (α5), further location of the site was confirmed by presence of conserved serine residue, like other cholesterol dehydrogenases, on the preceding beta sheet (β5) to the active site containing α helix. Same prosite pattern (YXXXR) is found in 3βhsdLf orthologs in other *Lactobacillus* species.

Also the results concurs with our hypothesis of (YXXXR) pattern of hsdLf likely being the active site pattern, as the one amino acid change of lysine (K) with arginine (R) showed no effect on the secondary structure of the active site of 3βHSDLf falling into the region of alpha helix similar to the rest of the cholesterol dehydrogenases in comparison. Another evidence of YXXXR of 3βHSDLf being the active site comes from the presence of conserved residue of serine (S) present in the beta sheet (β6) of 3βHSDLf upstream of the alpha helix harboring the active site seen in the ortholog of other LAB (Fig. 6.15).

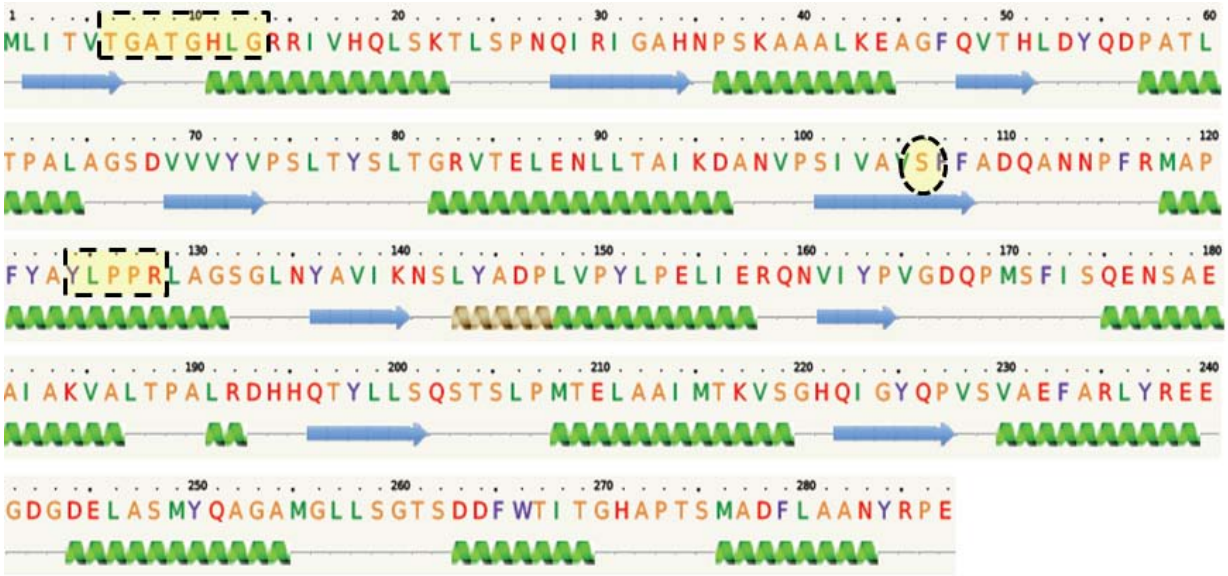

Figure 6.14: Secondary structure prediction of hsdLf by online server PHYRE showing the presence of hsdLf active site pattern (YXXXR) of the desired region of alpha helix.

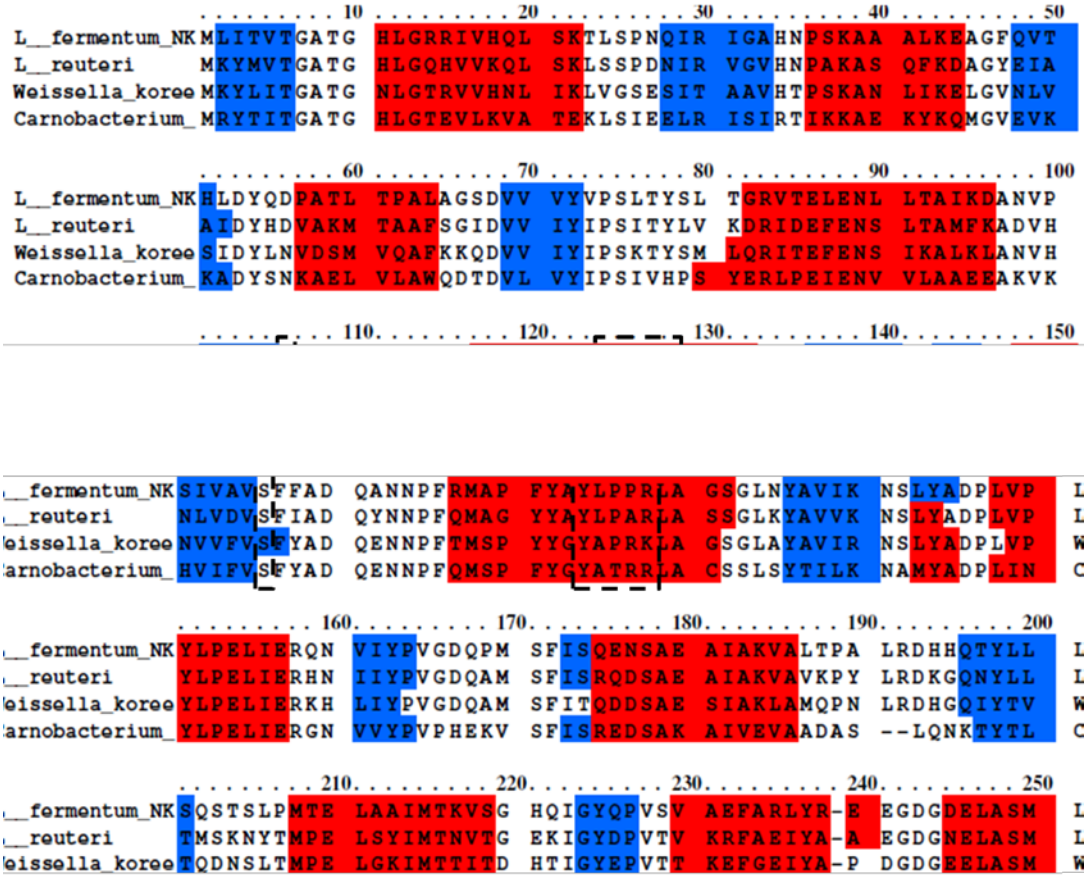

Figure 6.15: Alignment of predicted secondary structures of 3βHSDLf and its orthologs in lactic acid bacteria. Red highlighted region shows α-helix and blue highlight shows β-strands. Structures were predicted by DSSP and PSIpred and aligned by PRALINE server.

Cholesterol assimilation by LAB has remained an enigma. Discovery and functional characterization of cholesterol degrading enzyme will go a long way in establishing the ability of LAB for cholesterol reduction followed by their performance in fermented food products. The discovery of 3βHSDLf in *Lactobacillus fermentum* NKN51 is the first step in this direction. Cloning and expression of the genetic locus responsible for 3βHSDLf has opened the path for further detailed kinetic characterization of the enzyme. It will be very important to assess the degradation products of cholesterol in the presence of 3βHSDLf so that the fate of this undesirable molecule in dairy products can be followed.

CHAPTER 7

NANO BASED STRATEGIES FOR PATHOGEN CONTROL

7.1. Nanoparticle characterization and evaluation of enterocin capping

Batch experiments with different compositions of the preparatory mixture were carried out to determine the optimum concentration of enterocin which can efficiently form SNPs with typical absorption spectrum. The typical UV-vis absorption spectrum of the resulting solution displays characteristic surface plasmon resonance band of SNP's at 400 nm (Fig 7.1).

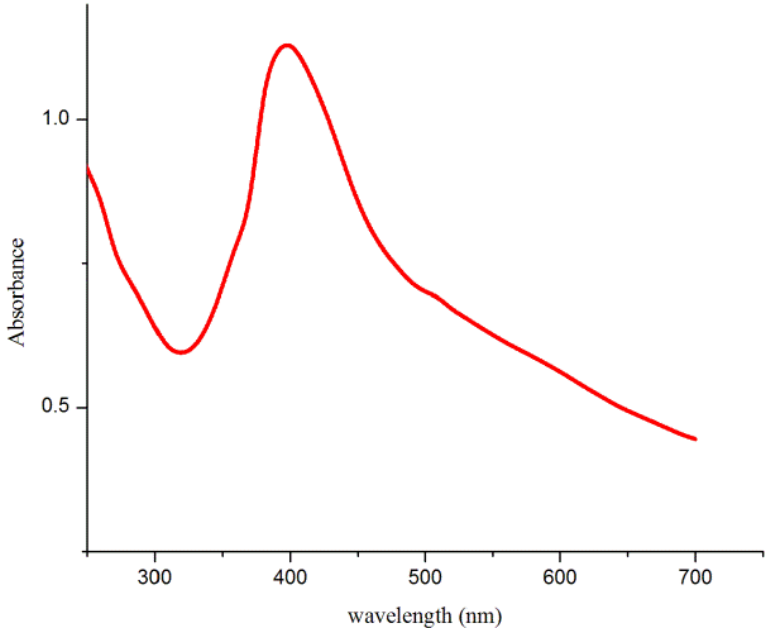

Figure7.1: UV-vis spectrum of En-SNPs exhibiting a SPR band at 400nm.

The En-SNPs formed were mono dispersed, spherical, with mean diameter of 30-40 nm as confirmed by SEM (Fig. 7.2) and AFM (Fig. 7.3A and 7.3B). The zeta potential of the nanoparticles formed was approximately -34.8 mV (Fig. 7.4) while zeta potential for C-SNPs was recorded to be -23mV (data not shown) indicating better stability of En-SNPs over C-SNPs. Size of En-SNPs as collected by Dynamic light scattering (DLS) was approximately 325 nm which could be attributed to the capping of enterocin on nanoparticles (Fig. 7.5).

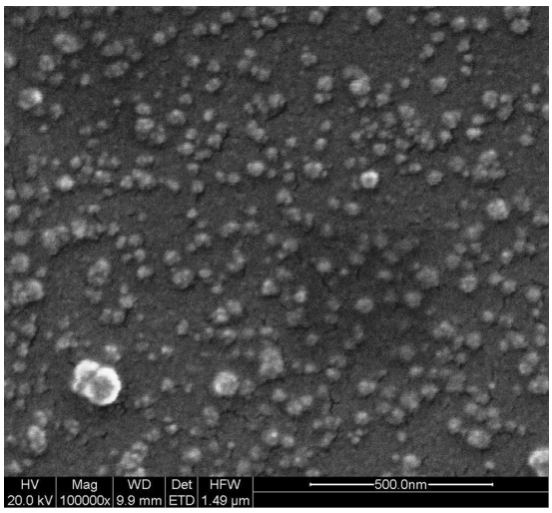

Figure 7.2: Scanning electron micrograph of En-SNPs showing spherical nanoparticles in the size range 30-40nm.

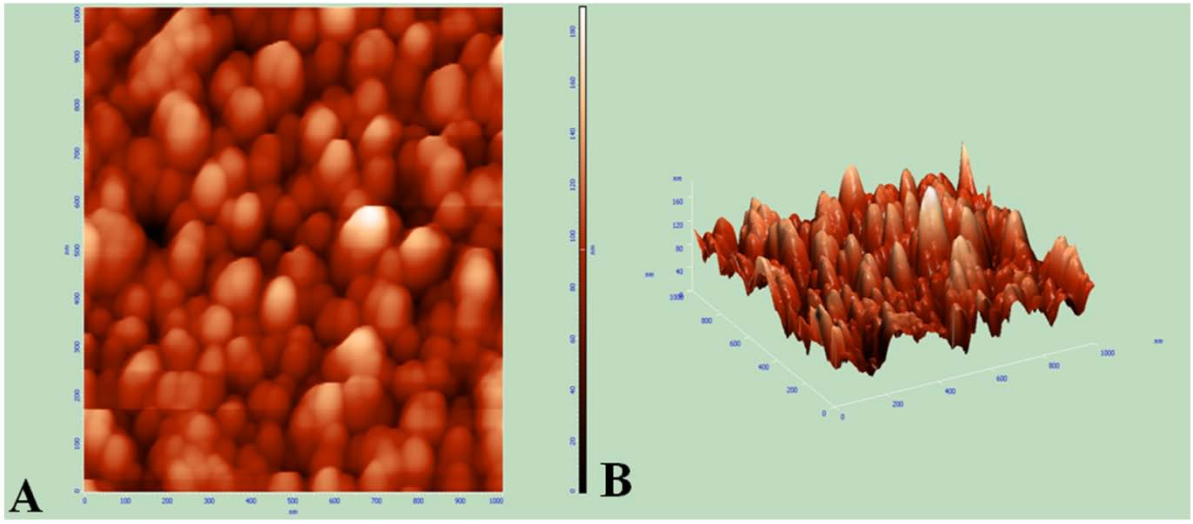

Figure 7.3: - Atomic force micrograph of En-SNPs (A-normal view and B-3D view)

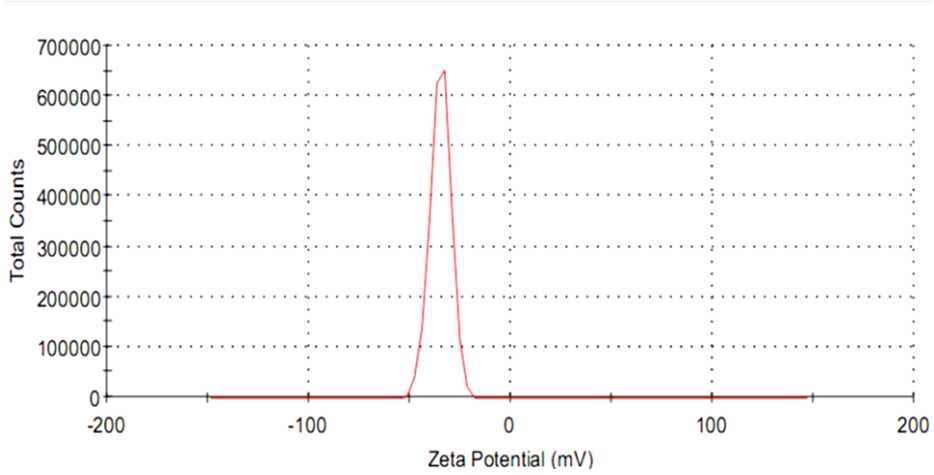

Figure 7.4: Zeta potential of En-SNPs having an average value of -34.8mV, elucidating their fair stability.

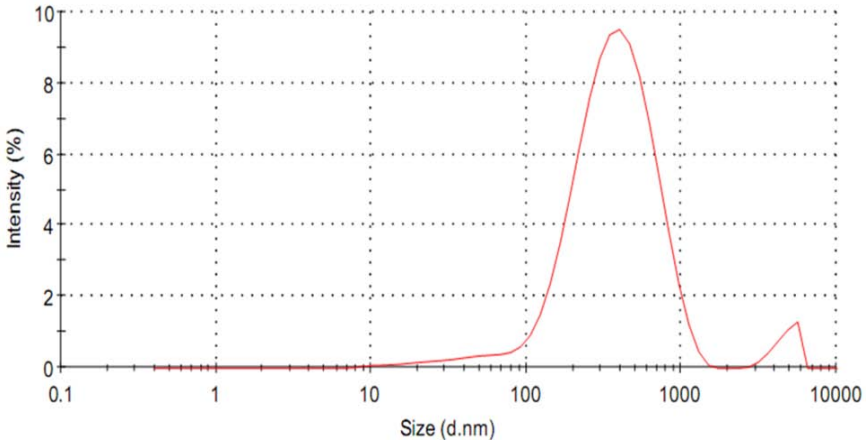

Figure 7.5: Dynamic light scattering spectra of En-SNPs unveiling an average size of 325 nm owing to the capping of enterocin on SNPs.

The capping of enterocin on SNPs was confirmed by FTIR (Fig. 7.6). The spectrum of En-SNPs was identical to the spectrum of free enterocin. Results obtained inveterate that no major alterations occur in the structure of enterocin as a result of its association with SNPs during synthesis. Changes in the protein secondary and tertiary structures alter hydrogen bonding between the CO and NH groups in the peptide backbone which results in deviation of the primary, secondary or tertiary amine bands between 1200 and 1700 cm^{-1}[143]. No such considerable shifts were observed in this IR region between En-SNPs and free enterocin. In both cases there was an unusual peak at 1636 cm^{-1} representing the amide group.

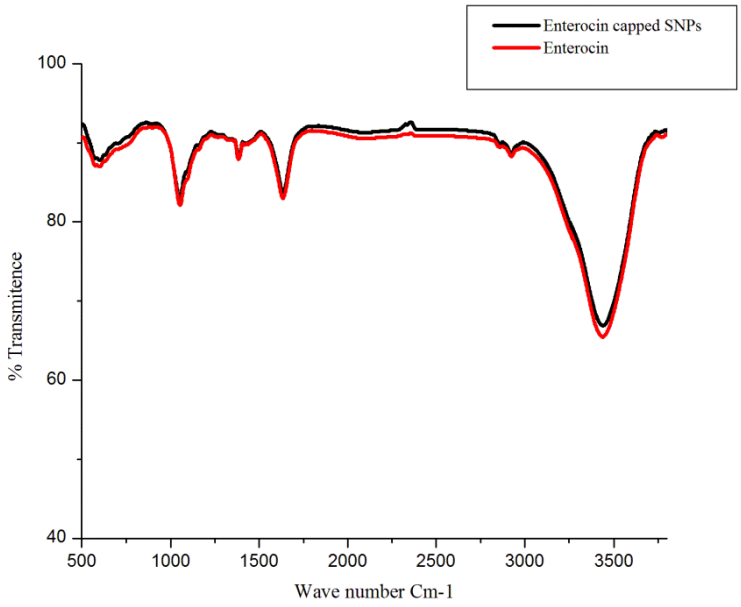

Figure 7.6: Fourier transfer infra-red (FTIR) spectrum of En-SNPs conferring capping of enterocin on silver NPs

Further confirmation of enterocin capping was achieved by circular dichroism. Most importantly, circular dichroism analysis elucidates that the enterocin retained its secondary structure even after capping onto the NPs. In particular, a negative peak at ~200 nm (peptide π-

π* transition), typical of helix structures [144] was detected in the spectra of both free peptide in water and En-SNPs. No such peak was observed in case of C-SNPs (Fig. 7.7), which were used as a control.

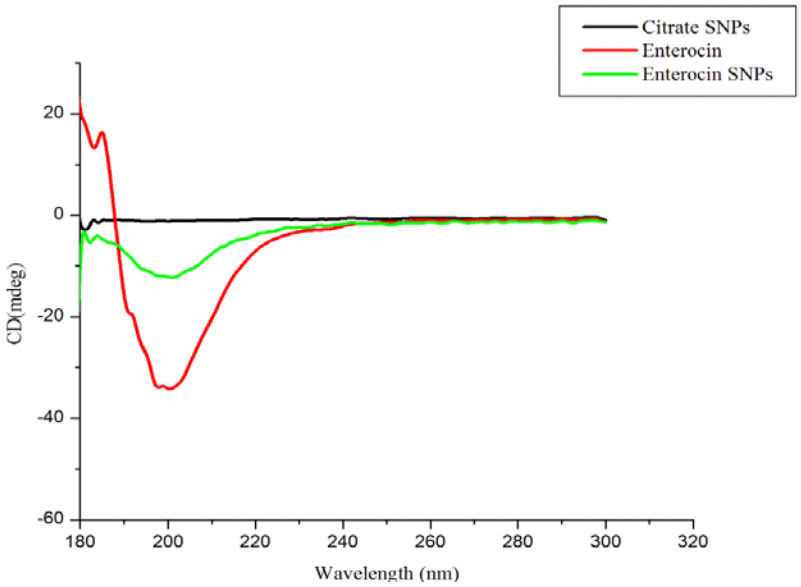

Figure7.7: Circular Dichroism (CD) Spectra displaying presence of α-helix in En-SNPs and enterocin, revealing efficient capping on SNPs without any alterations of its secondary structure.

7.2. Antibacterial activity

The potential of antibacterial activity was determined in terms of MIC. Lower MICs correspond to stronger antibacterial activities. MIC against the tested Gram-positive and Gram-negative strains are mentioned in Table 7.1. The MIC values suggest that En-SNPs are approximately 2 to 16 folds more inhibitory as compared to same concentration of C-SNPs against a range of bacterial pathogens tested. There was significant enhancement in the degree of inhibition in case of *B. cereus and L. monocytogenes.* On the contrary, *K. pneumoniae* was inhibited more effectively by C-SNPs as compared to enterocin capped SNPs.

Table7.1: Minimum inhibitory concentrations (MIC's) of Ent-SNPs and C-SNPs against tested bacterial pathogens.

S. No.	Bacterial Strains Used	MIC of citrate capped SNPs (pg/ml)	MIC of enterocin capped SNPs (pg/ml)
1	*E. coli ATCC 25922*	3.75	0.93
2	*B. cereus*	No inhibition up to 10 pg/ml	3.75
3	*K. pneumoniae*	3.75	7.50
4	*L. monocytogenes*	15	0.93
5	*M. luteus*	0.93	0.23
6	*P. acidilactici LB42*	0.93	0.23
7	*S. flexneri*	1.87	0.93
8	*S. aureus*	3.75	1.87

7.3. Evaluation of bacterial morphology on interaction of En-SNPs with bacteria by SEM

To study the interaction of En-SNPs with bacterial strains, one representative from Gram-negative (*E. coli* ATCC 25922) and another from Gram-positive (*S. aureus*) were taken. SEM was performed to observe changes in bacterial membrane integrity on interaction with En-SNPs. There was significant loss of membrane integrity when the bacterial strains were treated with sub lethal concentrations of En-SNPs. However there was slight damage to membrane by C-SNPs. Enterocin is predicted to interact with components of bacterial membrane [145] and is also expected to facilitate interaction of bacteria with SNPs, leading to damage, followed by death of the bacterial cells. *E.coli* cells became elongated and deformed when treated with C-SNPs or En-SNPs which indicates a typical stress response. *S. aureus* cells formed clumps and showed loss of membrane integrity in response to C-SNPs and En-SNPs. Membrane damage was more severe in case of En-SNPs which can be attributed to the combined inhibitory effect of enterocin and NP component of En-SNPs. (Fig. 7.8)

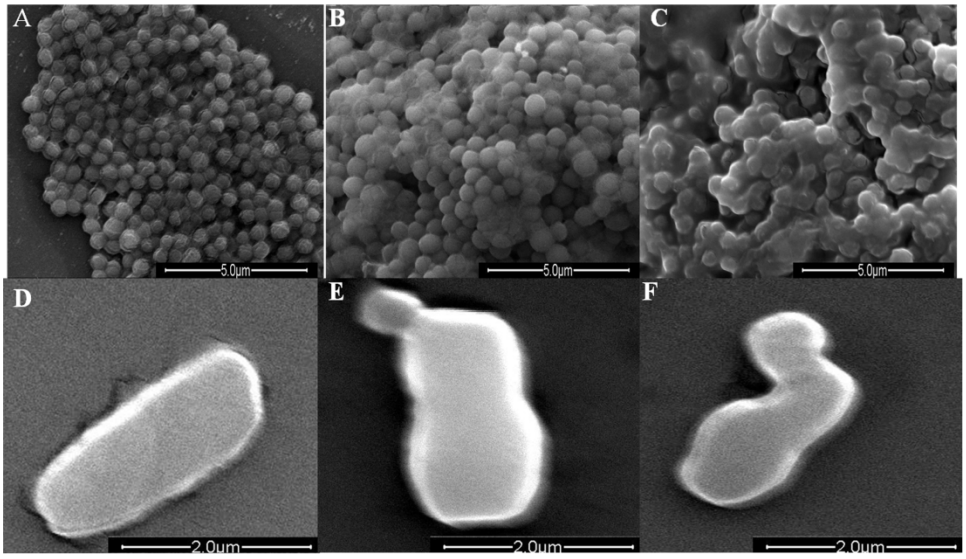

Figure 7.8: Interaction of En-SNPs with bacteria as observed through SEM (Upper panel *S. aureus* A- untreated, B-treated with C-SNPs, C- treated with En-SNPs; Lower panel *E.coli* D-untreated, E-treated with C-SNPs, F- treated with En-SNPs).

7.4. Interaction of enterocin SNPs with bacterial membrane proteins

SEM results revealed significant damage to bacterial cells; in order to elucidate the interaction between En-SNPs and bacteria, protein interaction studies were performed using fluorescence spectroscopy. Alteration in tryptophan (trp) fluorescence (for trp present in the bacterial membrane proteins) was measured as a function of protein-NP interaction. When *E.coli* and *P. acidilactici* LB42 membrane preparations were incubated with C-SNPs and En-

SNPs in HEPES buffer, a typical trend was observed. In the presence of En-SNPs, trp fluorescence was quenched up to a great extent in comparison to quenching with C-SNPs (Fig. 7.9). It is evident from the emission spectra that, trp fluorescence of ECMP (*E. coli.* ATCC 25922 membrane protein) and LBMP (*P. acidilactici* LB42 membrane protein) decreases as the concentration of En-SNPs is increased (Fig. 7.10). A similar trend was observed in an earlier study when SNPs interact with bovine serum albumin (BSA).[146]

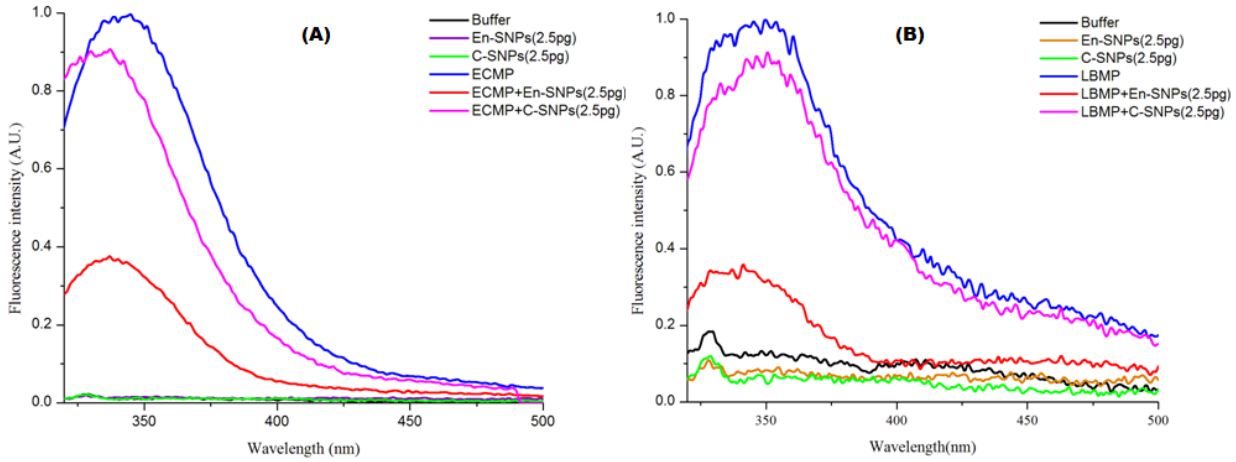

Figure 7.9: Fluorescence spectra displaying quenching as observed on interaction of membrane preparations with C-SNPs and En-SNPs (A-ECMP, B-LBMP).

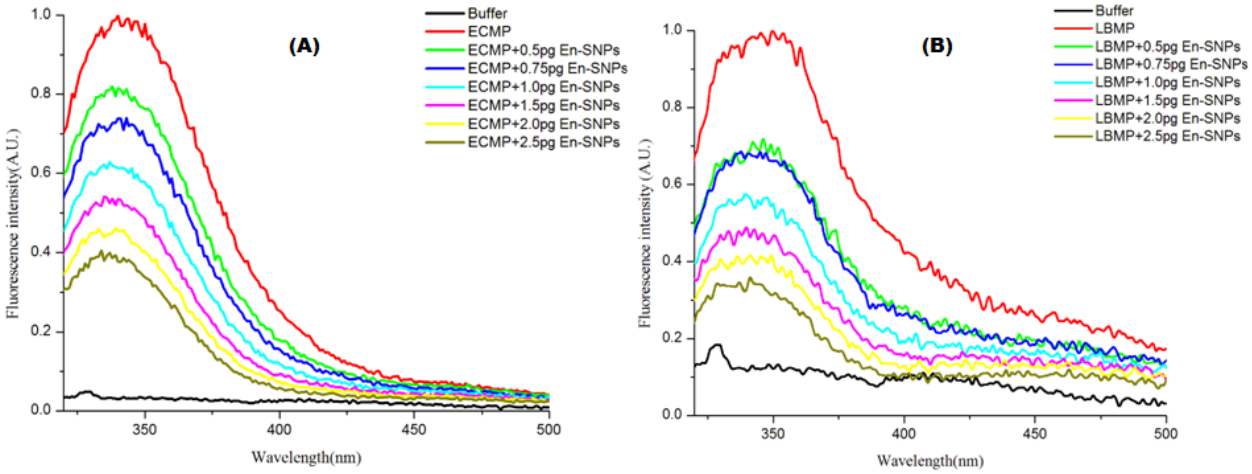

Figure 7.10: Fluorescence studies depicting concentration dependent quenching of membrane preparations on interaction with En-SNPs (A-ECMP, B-LBMP).

The quenching phenomenon was further studied by Stern-Volmer plot. En-SNPs interact with ECMP/LBMP in a concentration dependent manner as a linear Stern-Volmer plot (Fig. 7.11) was obtained which is characteristic of a single class of fluorophores, equally accessible to the quencher molecule. [52]

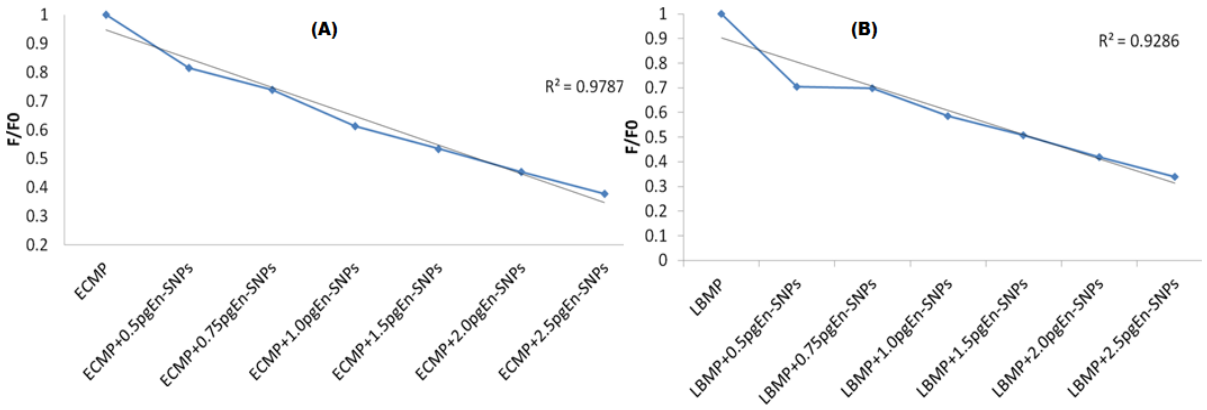

Figure 7.11: Fluorescence studies depicting concentration dependent quenching of membrane preparations on interaction with En-SNPs (A-ECMP, B-LBMP).

To measure the binding affinity, different concentrations of En-SNPs and C-SNPs (0-1200fM) were incubated with ECMP and LBMP and the dissociation constant Kd was calculated (Fig. 7.12). In case of ECMP Kd was higher (86fM) than LBMP (62fM) which is attributed to inherent ability of enterocin to bind Gram-positive bacteria. However, C-SNPs exhibit lower affinity to both Gram-positive and Gram-negative bacterial membrane preparations in comparison to En-SNPs (Kd values ECMP-535.5fM, LBMP-991.6fM; data not shown). In order to study the formation of a complex between nanoparticles and ECMP/LBMP membrane preparations RLS was performed. RLS spectra revealed that as a result of ECMP/LBMP interaction with C-SNP/En-SNPs formation of aggregates occurs which is exhibited by enhanced fluorescence intensity (Fig.7.13).

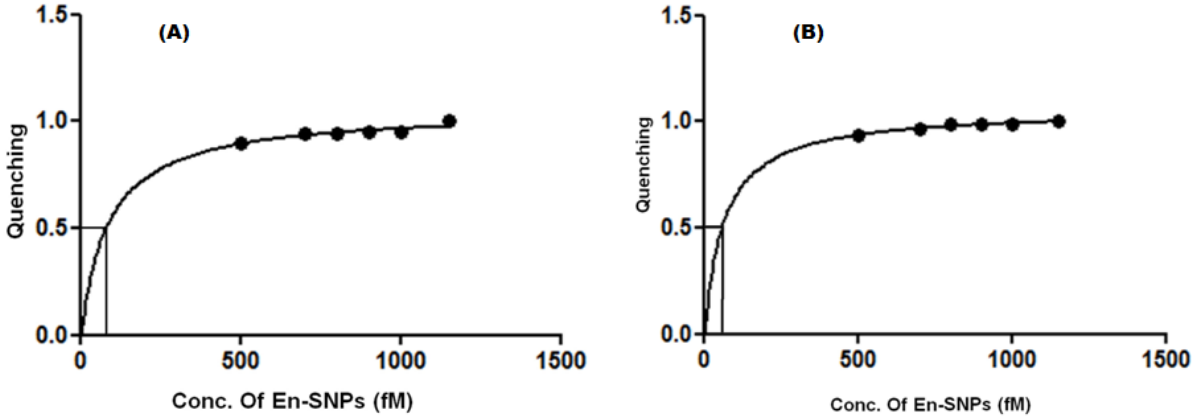

Figure 7.12: Apparent dissociation constants as obtained using nonlinear regression in Graph-pad prism 5.02 (A-ECMP, B-LBMP).

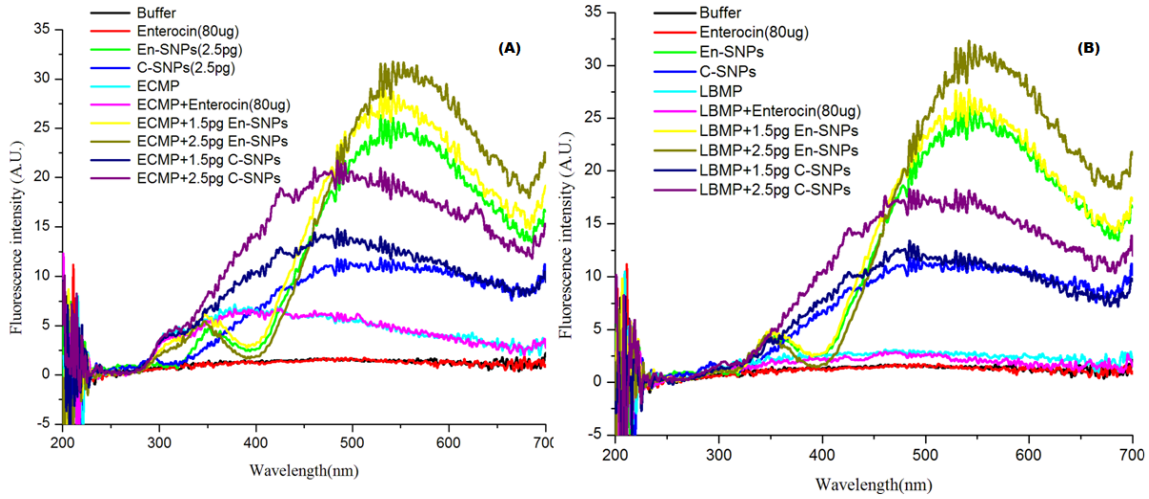

Figure 7.13: Resonance Light Scattering (RLS) showing formation of complexes (A-ECMP, B-LBMP).

The fluorescence value is higher in case of En-SNPs as compared to C-SNPs and can be attributed to the formation of a larger complex in presence of En-SNPs (peak at about 520nm) as compared to C-SNPs (peak at 490nm). The results obtained here are in agreement with observation by Mariam *et.al*. [146]. The results of the interaction studies further support the stronger interaction of En-SNPs over C-SNPs and also elucidate that En-SNPs interact with bacterial membranes to exert their inhibitory effect.

7.5. Haemolysis assays

No haemolysis of RBCs was observed in case of En-SNPs up to a concentration of 3µg/ml. At the same concentration C-SNPs showed partial haemolysis as compared to controls. (Fig. 7.14)

Figure 7.14: En-SNPs show no haemolysis of RBCs which are completely destroyed by Triton X-100 (A-positive control Triton X-100,100% haemolysis; B-1µg En-SNPs; C-2µg En-SNPs; D-3µg En-SNPs; E-negative control buffer Tris-Cl, 0% haemolysis).

A number of research groups have reported the antibacterial potential of some antibacterial peptides but there is no report on antibacterial action mediated through food grade antibacterial peptides attached to SNPs. Ruden *et. al.*[147] reported synergistic action of silver NPs and polymyxin when these were used in combination. Recently Soohyang *et. al.* reported the antibacterial property of polymyxin conjugated gold nanoparticles and quantum dots.[148]

Antibacterial peptides are known to interact with bacterial membranes whose structure and chemical composition are well studied. Owing to the presence of outer membrane, Gram-negative pathogens show resistance to a variety of drugs. This outer membrane is primarily composed of lipids which includes phospholipids present in inner leaflet and lipopolysaccharide (LPS) in outer leaflets of the asymmetric bilayer. LPS provides selective permeability to Gram-negative bacteria. Enterocin, a cationic peptide shows impressive antibacterial activity against Gram-positive bacteria due to its interaction with anionic lipids (dimyristoylphosphatidylcholine). On the other hand SNPs show great degree of inhibition of Gram-negative bacteria as compared to Gram-positive bacteria [149]. It is evident from the MIC data that En-SNPs show significant antibacterial activity on both Gram-positive and Gram-negative bacteria which could be attributed to enterocin capping on SNPs. Though En-SNPs are more potent antibacterials for Gram-positive bacteria, the antibacterial activity against Gram-negatives is due to the major contribution from SNPs with enterocin potentiating its antibacterial effect.

The increased activity of En-SNPs is likely due to the presence of a large number of enterocin molecules on the surface of SNPs. When these conjugates interact with the bacterial surface, they give ample opportunity to both enterocin and SNPs to interact with bacteria simultaneously. The FTIR and CD data revealed that there was no major perturbation in enterocin structure. The bacteriocin maintains its structure after capping on to the SNPs, keeping its antibacterial action intact. The results clearly indicates En-SNPs are more potent antibacterial agents in comparison to C-SNPs. Preliminary toxic studies also indicate that En-SNPs are not haemolytic which conjectures their use as food preservatives to tackle food borne bacterial pathogens. More toxicological studies need to be undertaken before the application of enterocin coated nanoparticles in food products is made available.

CHAPTER 8

CONCLUSION

Probiotic bacteria are associated with several properties which are claimed to provide beneficial effects on their hosts. However, most of these properties have not been subjected to detailed scientific scrutiny. The aim of the present investigation was to study chosen probiotic properties of lactic acid bacteria at molecular level so that the gap between claimed probiotic properties and scientific evidence can be narrowed. The investigation started by isolation of fifteen lactic acid bacterial isolates from various ecological niches and their probiotic potential was analysed by screening of four important health beneficial properties; viz. phytase production, cholesterol reduction, bile salt hydrolase production and asparaginase production. Following isolates were found positive for probiotic attributes-

	Phytase production	**Cholesterol reduction**	**Bile salt hydrolase production**	**Asparaginase production**
NKN51	+	+	-	-
NKN52	-	-	+	+
NKN53	-	-	-	+
NKN54	-	-	-	-
NKN55	-	-	+	+
NKN56	-	-	-	-
NKN57	-	-	-	-
NKN58	+	+	-	+
NKN59	+	-	-	+
NKN60	+	+	-	+
NKN61	-	-	-	-
NKN62	-	-	-	-
NKN63	+	+	-	+
NKN64	+	-	-	-
NKN65	+	-	-	-

Out of all isolates, NKN51 was selected for further molecular and biochemical characterization of probiotic properties, due to its high phytase activity and good cholesterol reducing ability. However NKN52 and NKN55 also hold great potential as probiotic bacteria as they can show anticancer effect due to asparaginase activity and cholesterol reducing effect due to bile salt deconjugation.

To study molecular basis of phytase activity of NKN51, a novel phytase of class protein tyrosine phosphatase has been identified, cloned, expressed and purified. Biochemical characterization of the protein product (phyLf) confirmed its phytase activity. phyLf is a novel phytase of class protein tyrosine phosphatase. It is the first phytase gene reported from probiotic genera *Lactobacillus.* HPLC analysis, zymography and biochemical characterization show high substrate specificity for IP6 and impressive catalytic activity. Its high resistance towards oxidative inactivation imparts it advantage to function in vicinity of *Lactobacilli*, as various *Lactobacillus* are known to accumulate H_2O_2 , also *in-vivo* H_2O_2 is generated by host cells as a defence mechanism. Apart from making available the phosphate to the *Lactobacillus* from the environment, phyLf seems to play a crucial role in host-microbe interaction. Various orthologs of phyLf are widely distributed in *Lactobacilli* and other non-pathogenic firmicute genera. The predicted role of phyLf in signal transduction and involvement of orthologous proteins LipA and mptpB in host-microbe signal transduction collectively indicates a possibility of phyLf in cross kindom cell signaling. Since the substrate specificities of phyLf differ from LipA and MptpB, we speculate that phyLf lies at the interphase of PTPLP and MptpB like proteins and its role in host microbe cross talk could be determined precisely by further analysis of host response toward variation in expression levels of phyLf in *Lactobacillus* and its effect on gut colonization by *Lactobacillus*.

In third part of this work, cholesterol reducing effect of the NKN51 was investigated. Although cholesterol reducing effect of symbiotic flora has been reported by various groups, yet exact fate of cholesterol in such probiotic strains is not established. We also observed improvement in growth of *Lactobacillus fermentum* NKN51 in presence of cholesterol under nutrient deficient conditions. Studies of cholesterol uptake using fluorescently labelled cholesterol showed that the *L. fermentum* NKN51 accumulates cholesterol probably in cell wall. These results provide strong experimental proof for cholesterol assimilation by *Lactobacillus fermentum* NKN51, and suggest that assimilation could be the reason of cholesterol lowering effect of probiotics in gut. Further to explore the mechanistic insight of the process, putative genes involved in assimilation or conversion of cholesterol were searched in the genome of *Lactobacillus fermentum* which led to identification of a genetic locus coding for

a novel 3β hydroxysteroid dehydrogenase (3βHSDLf) enzyme. The genetic locus was amplified, cloned, expressed and purified enzyme was partially characterized. Although the detailed biochemical characterization of 3βHSDLf is still remaining yet zymographic analysis and preliminary biochemical assays for cholesterol dehydrogenation have proved that the recombinant enzyme is functional and is involved in cholesterol metabolism. As this is the first step of genetic study of cholesterol conversion in lactic acid bacteria, this study paves way for further detailed characterization of the enzyme and down-stream pathway.

In the last part of this thesis, the problem of food spoilage by undesirable bacteria was addressed. Due to multiple modes of action against bacterial pathogens, inability of the bacteria to develop resistance against silver is well established. In the present investigation, we have increased the potency of silver by synthesizing bio-functionalized silver nanoparticles using a facile method and have characterized them using various biophysical and analytical techniques. Antibacterial peptides produced by food grade bacteria offer great advantages when combined with NPs. In fourth part of the study we demonstrated an approach using a bacteriocin 'enterocin' and showed antibacterial potential of En-SNPs exhibiting various advantages over normal SNPs. The process of enterocin capped SNP synthesis was done without use of hazardous chemicals. This nanobiotic approach assumes a new dimension ready to fight bacterial pathogens and could be an efficient weapon for food borne bacterial pathogens.

REFERENCES

1. KUMAR, V. and S. AGRAWAL, *Short Communication: An insight into protein sequences of PTP-like cysteine phytases.* EDITORIAL BOARD, 2014: p. 102.
2. Askelson, T.E., et al., *Evaluation of phytate-degrading Lactobacillus culture administration to broiler chickens.* Applied and environmental microbiology, 2014. **80**(3): p. 943-950.
3. Tamayo-Ramos, J.A., et al., *Novel Phytases from Bifidobacterium pseudocatenulatum ATCC 27919 and Bifidobacterium longum subsp. infantis ATCC 15697.* Applied and environmental microbiology, 2012. **78**(14): p. 5013-5015.
4. Stentz, R., et al., *A bacterial homolog of a eukaryotic inositol phosphate signaling enzyme mediates cross-kingdom dialog in the mammalian gut.* Cell reports, 2014. **6**(4): p. 646-656.
5. Grundner, C., H.-L. Ng, and T. Alber, *Mycobacterium tuberculosis protein tyrosine phosphatase PtpB structure reveals a diverged fold and a buried active site.* Structure, 2005. **13**(11): p. 1625-1634.
6. Ooi, L.-G. and M.-T. Liong, *Cholesterol-lowering effects of probiotics and prebiotics: a review of in vivo and in vitro findings.* International journal of molecular sciences, 2010. **11**(6): p. 2499-2522.
7. Lye, H.-S., et al., *The improvement of hypertension by probiotics: effects on cholesterol, diabetes, renin, and phytoestrogens.* International journal of molecular sciences, 2009. **10**(9): p. 3755-3775.
8. Kellogg, T.F., *Steroid balance and tissue cholesterol accumulation in germfree and conventional rats fed diets containing saturated and polyunsaturated fats.* Journal of lipid research, 1974. **15**(6): p. 574-579.
9. Lye, H.-S., G. Rusul, and M.-T. Liong, *Removal of cholesterol by lactobacilli via incorporation and conversion to coprostanol.* Journal of dairy science, 2010. **93**(4): p. 1383-1392.
10. Lin, M.-Y. and T.-W. Chen, *Reduction of cholesterol by Lactobacillus acidophilus in culture broth.* Journal of Food and Drug Analysis, 2000. **8**(2).
11. Ren, D., et al., *Mechanism of cholesterol reduction to coprostanol by Eubacterium coprostanoligenes ATCC 51222.* Steroids, 1996. **61**(1): p. 33-40.
12. O'Hara, A.M. and F. Shanahan, *The gut flora as a forgotten organ.* EMBO reports, 2006. **7**(7): p. 688-693.

13. Mazmanian, S.K., J.L. Round, and D.L. Kasper, *A microbial symbiosis factor prevents intestinal inflammatory disease.* Nature, 2008. **453**(7195): p. 620-625.
14. Duary, R., et al., *Randomly amplified polymorphic DNA profiles of Lactobacillus isolates from human faecal samples.* International Journal of Probiotics and Prebiotics, 2009. **4**(1): p. 55-64.
15. Artis, D., *Epithelial-cell recognition of commensal bacteria and maintenance of immune homeostasis in the gut.* Nature Reviews Immunology, 2008. **8**(6): p. 411-420.
16. Kaushik, J.K., et al., *Functional and probiotic attributes of an indigenous isolate of Lactobacillus plantarum.* PloS one, 2009. **4**(12): p. e8099.
17. Caricilli, A.M., A. Castoldi, and N.O.S. Câmara, *Intestinal barrier: a gentlemen's agreement between microbiota and immunity*. World journal of gastrointestinal pathophysiology, 2014. **5**(1): p. 18.
18. Näse, L., et al., *Effect of Long–Term Consumption of a Probiotic Bacterium, Lactobacillus rhamnosus GG, in Milk on Dental Caries and Caries Risk in Children.* Caries research, 2001. **35**(6): p. 412-420.
19. Hatakka, K., et al., *Effect of long term consumption of probiotic milk on infections in children attending day care centres: double blind, randomised trial.* Bmj, 2001. **322**(7298): p. 1327.
20. Reid, G., et al., *Potential uses of probiotics in clinical practice.* CLINICAL microbiology Reviews, 2003. **16**(4): p. 658-672.
21. Ouwehand, A.C., S. Salminen, and E. Isolauri, *Probiotics: an overview of beneficial effects.* Antonie Van Leeuwenhoek, 2002. **82**(1-4): p. 279-289.
22. Lei, K., *THE EFFICACY OF PROBIOTICS IN THE TREATMENT OF IRRITABLE BOWEL SYNDROME.* Modern Preventive Medicine, 2011. **17**: p. 015.
23. Braat, H., et al., *Lactobacillus rhamnosus induces peripheral hyporesponsiveness in stimulated CD4+ T cells via modulation of dendritic cell function.* The American journal of clinical nutrition, 2004. **80**(6): p. 1618-1625.
24. Rosenfeldt, V., et al., *Effect of probiotic Lactobacillus strains in children with atopic dermatitis.* Journal of Allergy and Clinical Immunology, 2003. **111**(2): p. 389-395.
25. Cooke, G., J. Behan, and M. Costello, *Newly identified vitamin K-producing bacteria isolated from the neonatal faecal flora.* Microbial ecology in health and disease, 2006. **18**(3-4): p. 133-138.

26. Strozzi, G.P. and L. Mogna, *Quantification of folic acid in human feces after administration of Bifidobacterium probiotic strains.* Journal of clinical gastroenterology, 2008. **42**: p. S179-S184.
27. Hamilton-Miller, J., *The role of probiotics in the treatment and prevention of Helicobacter pylori infection.* International journal of antimicrobial agents, 2003. **22**(4): p. 360-366.
28. McFarland, L.V., *Meta-analysis of probiotics for the prevention of antibiotic associated diarrhea and the treatment of Clostridium difficile disease.* The American journal of gastroenterology, 2006. **101**(4): p. 812-822.
29. Kumar, M., et al., *Cholesterol-lowering probiotics as potential biotherapeutics for metabolic diseases.* Experimental diabetes research, 2012. **2012**.
30. Khalesi, S., et al., *Effect of probiotics on blood pressure a systematic review and meta-analysis of randomized, controlled trials.* Hypertension, 2014. **64**(4): p. 897-903.
31. Amalaradjou, M.A.R. and A.K. Bhunia, *Bioengineered probiotics, a strategic approach to control enteric infections.* Bioengineered, 2013. **4**(6): p. 379-387.
32. Gruninger, R.J., *Structure and mechanism of protein tyrosine phosphatase-like phytases*. 2009, Lethbridge, Alta.: University of Lethbridge, Dept. of Chemistry and Biochemistry, c2009.
33. Macbeth, M.R., et al., *Inositol hexakisphosphate is bound in the ADAR2 core and required for RNA editing.* Science, 2005. **309**(5740): p. 1534-1539.
34. Frederick, J.P., et al., *An essential role for an inositol polyphosphate multikinase, Ipk2, in mouse embryogenesis and second messenger production.* Proceedings of the National Academy of Sciences of the United States of America, 2005. **102**(24): p. 8454-8459.
35. Gontia-Mishra, I. and S. Tiwari, *Molecular characterization and comparative phylogenetic analysis of phytases from fungi with their prospective applications.* Food Technology and Biotechnology, 2013. **51**(3): p. 313-326.
36. Kumar, V., et al., *In Silico characterization of histidine acid phytase sequences.* Enzyme research, 2012. **2012**.
37. Mullaney, E.J. and A.H. Ullah, *The term phytase comprises several different classes of enzymes.* Biochemical and biophysical research communications, 2003. **312**(1): p. 179-184.
38. Kumar, V., et al., *Cloning, Sequencing, and In Silico Analysis of-Propeller Phytase Bacillus licheniformis Strain PB-13.* Biotechnology research international, 2014. **2014**.

39. Yanke, L., L. Selinger, and K.J. Cheng, *Phytase activity of Selenomonas ruminantium: a preliminary characterization.* Letters in applied microbiology, 1999. **29**(1): p. 20-25.
40. Gruninger, R.J., et al., *Structural and Biochemical Analysis of a Unique Phosphatase from Bdellovibrio bacteriovorus Reveals Its Structural and Functional Relationship with the Protein Tyrosine Phosphatase Class of Phytase.* PloS one, 2014. **9**(4): p. e94403.
41. Puhl, A.A., R. Greiner, and L.B. Selinger, *A protein tyrosine phosphatase-like inositol polyphosphatase from Selenomonas ruminantium subsp. lactilytica has specificity for the 5-phosphate of myo-inositol hexakisphosphate.* The international journal of biochemistry & cell biology, 2008. **40**(10): p. 2053-2064.
42. Chaudhry, R., et al., *Lesson of the week: a foodborne outbreak of organophosphate poisoning.* BMJ: British Medical Journal, 1998. **317**(7153): p. 268.
43. Kumar, V., et al., *Dietary roles of phytate and phytase in human nutrition: A review.* Food Chemistry, 2010. **120**(4): p. 945-959.
44. Rao, D., et al., *Molecular characterization, physicochemical properties, known and potential applications of phytases: an overview*. Critical reviews in biotechnology, 2009. **29**(2): p. 182-198.
45. Lucca, P., R. Hurrell, and I. Potrykus, *Genetic engineering approaches to improve the bioavailability and the level of iron in rice grains.* Theoretical and Applied Genetics, 2001. **102**(2-3): p. 392-397.
46. Yoon, S.-M., et al., *Transgenic microalgae expressing Escherichia coli AppA phytase as feed additive to reduce phytate excretion in the manure of young broiler chicks.* Applied microbiology and biotechnology, 2011. **91**(3): p. 553-563.
47. Mudge, S.R., F.W. Smith, and A.E. Richardson, *Root-specific and phosphate-regulated expression of phytase under the control of a phosphate transporter promoter enables Arabidopsis to grow on phytate as a sole P source.* Plant Science, 2003. **165**(4): p. 871-878.
48. Singh, A., et al., *Effect of phosphate and meat (pork) types on the germination and outgrowth of Clostridium perfringens spores during abusive chilling.* Journal of Food Protection®, 2010. **73**(5): p. 879-887.
49. Singh, B. and T. Satyanarayana, *Improved phytase production by a thermophilic mould Sporotrichum thermophile in submerged fermentation due to statistical optimization.* Bioresource technology, 2008. **99**(4): p. 824-830.

50. Vohra, A. and T. Satyanarayana, *Phytases: microbial sources, production, purification, and potential biotechnological applications.* Critical reviews in biotechnology, 2003. **23**(1): p. 29-60.
51. Zuo, R., et al., *Phytase gene expression in Lactobacillus and analysis of its biochemical characteristics.* Microbiological research, 2010. **165**(4): p. 329-335.
52. Zamudio, M., A. González, and J. Medina, *Lactobacillus plantarum phytase activity is due to non-specific acid phosphatase.* Letters in applied microbiology, 2001. **32**(3): p. 181-184.
53. Pereira, D.I. and G.R. Gibson, *Effects of consumption of probiotics and prebiotics on serum lipid levels in humans.* Critical reviews in biochemistry and molecular biology, 2002. **37**(4): p. 259-281.
54. Kumar, R., et al., *Molecular Cloning and Sequence Analysis of Bile Salt Hydrolase Gene (bsh) from Lactobacillus plantarum MBUL90 Strain of Human Origin.* Food Biotechnology, 2010. **24**(3): p. 215-226.
55. Gilliland, S., C. Nelson, and C. Maxwell, *Assimilation of cholesterol by Lactobacillus acidophilus.* Applied and Environmental Microbiology, 1985. **49**(2): p. 377-381.
56. Walker, D.K. and S.E. Gilliland, *Relationships among bile tolerance, bile salt deconjugation, and assimilation of cholesterol by Lactobacillus acidophilus.* Journal of dairy science, 1993. **76**(4): p. 956-961.
57. Gérard, P., *Metabolism of cholesterol and bile acids by the gut microbiota.* Pathogens, 2013. **3**(1): p. 14-24.
58. Björkhem, I. and J.Å. Gustafsson, *Mechanism of microbial transformation of cholesterol into coprostanol.* European Journal of Biochemistry, 1971. **21**(3): p. 428-432.
59. Madden, U.A., *Use of Eubacterium coprostanoligenes to decrease plasma cholesterol concentration in hypercholesterolemic rabbits and the cholesterol content of fermented meats.* 1995.
60. Chiang, Y.-R., et al., *Study of anoxic and oxic cholesterol metabolism by Sterolibacterium denitrificans.* Journal of bacteriology, 2008. **190**(3): p. 905-914.
61. Stiles, M.E., *Biopreservation by lactic acid bacteria.* Antonie van leeuwenhoek, 1996. **70**(2-4): p. 331-345.
62. Malik, R., et al. *Development of bacteriocin based biopreservative for preservation of paneer (an Indian soft cheese).* in *Central theme, technology for all: sharing the knowledge for development. Proceedings of the International Conference of*

Agricultural Engineering, XXXVII Brazilian Congress of Agricultural Engineering, International Livestock Environment Symposium-ILES VIII, Iguassu Falls City, Brazil, 31st August to 4th September, 2008. 2008. International Commission of Agricultural Engineering (CIGR), Institut fur Landtechnik.

63. Amalaradjou, M. and A.K. Bhunia, *Modern approaches in probiotics research to control foodborne pathogens.* Adv Food Nutr Res, 2012. **67**: p. 185-239.
64. Bhunia, A., M. Johnson, and B. Ray, *Purification, characterization and antimicrobial spectrum of a bacteriocin produced by Pediococcus acidilactici.* Journal of Applied Bacteriology, 1988. **65**(4): p. 261-268.
65. Chen, H. and D. Hoover, *Bacteriocins and their food applications.* Comprehensive reviews in food science and food safety, 2003. **2**(3): p. 82-100.
66. Cleveland, J., et al., *Bacteriocins: safe, natural antimicrobials for food preservation.* International journal of food microbiology, 2001. **71**(1): p. 1-20.
67. Deegan, L.H., et al., *Bacteriocins: biological tools for bio-preservation and shelf-life extension.* International dairy journal, 2006. **16**(9): p. 1058-1071.
68. Nes, I.F., et al., *Biosynthesis of bacteriocins in lactic acid bacteria.* Antonie van Leeuwenhoek, 1996. **70**(2-4): p. 113-128.
69. Landers, T.F., et al., *A review of antibiotic use in food animals: perspective, policy, and potential.* Public health reports, 2012. **127**(1): p. 4.
70. McManus, P.S., et al., *Antibiotic use in plant agriculture.* Annual Review of Phytopathology, 2002. **40**(1): p. 443-465.
71. Mantovani, H., A. Cruz, and A. Paiva, *Bacteriocin activity and resistance in livestock pathogens.* Science against microbial pathogens: Communicating current research and technological advances. Formatex Research Center, Badajoz, 2011: p. 853-863.
72. Kjos, M., I.F. Nes, and D.B. Diep, *Mechanisms of resistance to bacteriocins targeting the mannose phosphotransferase system.* Applied and environmental microbiology, 2011. **77**(10): p. 3335-3342.
73. Hastings, J., et al., *Characterization of leucocin A-UAL 187 and cloning of the bacteriocin gene from Leuconostoc gelidum.* Journal of Bacteriology, 1991. **173**(23): p. 7491-7500.
74. Quadri, L., et al., *Chemical and genetic characterization of bacteriocins produced by Carnobacterium piscicola LV17B.* Journal of Biological Chemistry, 1994. **269**(16): p. 12204-12211.

75. Garneau, S., N.I. Martin, and J.C. Vederas, *Two-peptide bacteriocins produced by lactic acid bacteria.* Biochimie, 2002. **84**(5): p. 577-592.
76. Khehra, M.S., et al., *Biodegradation of azo dye CI Acid Red 88 by an anoxic–aerobic sequential bioreactor.* Dyes and Pigments, 2006. **70**(1): p. 1-7.
77. Khehra, M.S., et al., *Comparative studies on potential of consortium and constituent pure bacterial isolates to decolorize azo dyes.* Water Research, 2005. **39**(20): p. 5135-5141.
78. Khehra, M.S., et al., *Decolorization of various azo dyes by bacterial consortium.* Dyes and Pigments, 2005. **67**(1): p. 55-61.
79. Duncan, T.V., *Applications of nanotechnology in food packaging and food safety: barrier materials, antimicrobials and sensors.* Journal of colloid and interface science, 2011. **363**(1): p. 1-24.
80. Ahamed, M., et al., *Green synthesis, characterization and evaluation of biocompatibility of silver nanoparticles.* Physica E: Low-dimensional Systems and Nanostructures, 2011. **43**(6): p. 1266-1271.
81. De, M., P.S. Ghosh, and V.M. Rotello, *Applications of nanoparticles in biology.* Advanced Materials, 2008. **20**(22): p. 4225-4241.
82. Roco, M.C., C.A. Mirkin, and M.C. Hersam, *Nanotechnology research directions for societal needs in 2020: retrospective and outlook.* Vol. 1. 2011: Springer Science & Business Media.
83. Currall, S.C., et al., *What drives public acceptance of nanotechnology?* Nature Nanotechnology, 2006. **1**(3): p. 153-155.
84. Siegrist, M., et al., *Laypeople's and experts' perception of nanotechnology hazards.* Risk Analysis, 2007. **27**(1): p. 59-69.
85. Le, D.M., et al., *Biorefining of wheat straw: accounting for the distribution of mineral elements in pretreated biomass by an extended pretreatment–severity equation.* Biotechnology for biofuels, 2014. **7**(141).
86. Tsai, C.-T. and A.S. Meyer, *Enzymatic cellulose hydrolysis: Enzyme reusability and visualization of β-Glucosidase immobilized in calcium alginate.* Molecules, 2014. **19**(12): p. 19390-19406.
87. Luo, J., et al., *Functionalization of a Membrane Sublayer Using Reverse Filtration of Enzymes and Dopamine Coating.* ACS applied materials & interfaces, 2014. **6**(24): p. 22894-22904.

88. Siegrist, M., et al., *Perceived risks and perceived benefits of different nanotechnology foods and nanotechnology food packaging.* Appetite, 2008. **51**(2): p. 283-290.
89. Dahl, J.A., B.L. Maddux, and J.E. Hutchison, *Toward greener nanosynthesis.* Chemical reviews, 2007. **107**(6): p. 2228-2269.
90. Hussain, I., et al., *Preparation of acrylate-stabilized gold and silver hydrosols and gold-polymer composite films.* Langmuir, 2003. **19**(11): p. 4831-4835.
91. Albrecht, M.A., C.W. Evans, and C.L. Raston, *Green chemistry and the health implications of nanoparticles.* Green Chemistry, 2006. **8**(5): p. 417-432.
92. Alivisatos, P., *The use of nanocrystals in biological detection.* Nature biotechnology, 2004. **22**(1): p. 47-52.
93. Ahearn, D., L. May, and M. Gabriel, *Adherence of organisms to silver-coated surfaces.* Journal of industrial microbiology, 1995. **15**(4): p. 372-376.
94. Zhao, G. and S.E. Stevens Jr, *Multiple parameters for the comprehensive evaluation of the susceptibility of Escherichia coli to the silver ion.* Biometals, 1998. **11**(1): p. 27-32.
95. Nadworny, P.L., et al., *Anti-inflammatory activity of nanocrystalline silver in a porcine contact dermatitis model.* Nanomedicine: nanotechnology, biology and medicine, 2008. **4**(3): p. 241-251.
96. Tian, J., et al., *Topical delivery of silver nanoparticles promotes wound healing.* ChemMedChem, 2007. **2**(1): p. 129-136.
97. Atiyeh, B.S., et al., *Effect of silver on burn wound infection control and healing: review of the literature.* burns, 2007. **33**(2): p. 139-148.
98. Panáček, A., et al., *Silver colloid nanoparticles: synthesis, characterization, and their antibacterial activity.* The Journal of Physical Chemistry B, 2006. **110**(33): p. 16248-16253.
99. Pal, S., Y.K. Tak, and J.M. Song, *Does the antibacterial activity of silver nanoparticles depend on the shape of the nanoparticle? A study of the gram-negative bacterium Escherichia coli.* Applied and environmental microbiology, 2007. **73**(6): p. 1712-1720.
100. Sharma, V.K., R.A. Yngard, and Y. Lin, *Silver nanoparticles: green synthesis and their antimicrobial activities.* Advances in colloid and interface science, 2009. **145**(1): p. 83-96.
101. Pillai, Z.S. and P.V. Kamat, *What factors control the size and shape of silver nanoparticles in the citrate ion reduction method?* The Journal of Physical Chemistry B, 2004. **108**(3): p. 945-951.

102. Wang, H., et al., *Preparation of silver nanoparticles by chemical reduction method.* Colloids and Surfaces A: Physicochemical and Engineering Aspects, 2005. **256**(2): p. 111-115.
103. Zhu, J., et al., *Shape-controlled synthesis of silver nanoparticles by pulse sonoelectrochemical methods.* Langmuir, 2000. **16**(16): p. 6396-6399.
104. Farazuddin, M., et al., *Amoxicillin-bearing microparticles: potential in the treatment of Listeria monocytogenes infection in Swiss albino mice.* Bioscience reports, 2011. **31**: p. 265-272.
105. Adwan, G. and M. Mhanna, *Synergistic effects of plant extracts and antibiotics on Staphylococcus aureus strains isolated from clinical specimens.* Middle-East Journal of Scientific Research, 2008. **3**(3): p. 134-139.
106. Kwong, T., et al., *5S clavam biosynthesis is controlled by an atypical two-component regulatory system in Streptomyces clavuligerus.* Antimicrobial agents and chemotherapy, 2012. **56**(9): p. 4845-4855.
107. Tahlan, K., et al., *Two sets of paralogous genes encode the enzymes involved in the early stages of clavulanic acid and clavam metabolite biosynthesis in Streptomyces clavuligerus.* Antimicrobial agents and chemotherapy, 2004. **48**(3): p. 930-939.
108. Damm, C., H. Münstedt, and A. Rösch, *The antimicrobial efficacy of polyamide 6/silver-nano-and microcomposites.* Materials Chemistry and Physics, 2008. **108**(1): p. 61-66.
109. Neal, A.L., *What can be inferred from bacterium–nanoparticle interactions about the potential consequences of environmental exposure to nanoparticles?* Ecotoxicology, 2008. **17**(5): p. 362-371.
110. Strohal, R., et al., *Nanocrystalline silver dressings as an efficient anti-MRSA barrier: a new solution to an increasing problem.* Journal of Hospital Infection, 2005. **60**(3): p. 226-230.
111. Zhang, W., X. Qiao, and J. Chen, *Synthesis of silver nanoparticles—effects of concerned parameters in water/oil microemulsion.* Materials Science and Engineering: B, 2007. **142**(1): p. 1-15.
112. Mohanpuria, P., N.K. Rana, and S.K. Yadav, *Biosynthesis of nanoparticles: technological concepts and future applications.* Journal of Nanoparticle Research, 2008. **10**(3): p. 507-517.

113. Eby, D.M., H.R. Luckarift, and G.R. Johnson, *Hybrid antimicrobial enzyme and silver nanoparticle coatings for medical instruments.* ACS applied materials & interfaces, 2009. **1**(7): p. 1553-1560.
114. Taglietti, A., et al., *Antibacterial activity of glutathione-coated silver nanoparticles against gram positive and gram negative bacteria.* Langmuir, 2012. **28**(21): p. 8140-8148.
115. Nam, K.T., et al., *Peptide-mediated reduction of silver ions on engineered biological scaffolds.* Acs Nano, 2008. **2**(7): p. 1480-1486.
116. Mei, L., et al., *Bioconjugated nanoparticles for attachment and penetration into pathogenic bacteria.* Biomaterials, 2013. **34**(38): p. 10328-10337.
117. Golubeva, O.Y., et al., *Synthesis and study of antimicrobial activity of bioconjugates of silver nanoparticles and endogenous antibiotics.* Glass Physics and Chemistry, 2011. **37**(1): p. 78-84.
118. Jaiswal, S., et al., *Enhancement of the antibacterial properties of silver nanoparticles using β-cyclodextrin as a capping agent.* International journal of antimicrobial agents, 2010. **36**(3): p. 280-283.
119. Wei, Q., et al., *Norvancomycin-capped silver nanoparticles: synthesis and antibacterial activities against E. coli.* Science in China Series B: Chemistry, 2007. **50**(3): p. 418-424.
120. Boshoff, H.I., et al., *Biosynthesis and Recycling of Nicotinamide Cofactors in Mycobacterium tuberculosis AN ESSENTIAL ROLE FOR NAD IN NONREPLICATING BACILLI.* Journal of Biological Chemistry, 2008. **283**(28): p. 19329-19341.
121. Tahlan, K., et al., *Initiation of actinorhodin export in Streptomyces coelicolor.* Molecular microbiology, 2007. **63**(4): p. 951-961.
122. Tahlan, K., et al., *SQ109 targets MmpL3, a membrane transporter of trehalose monomycolate involved in mycolic acid donation to the cell wall core of Mycobacterium tuberculosis.* Antimicrobial agents and chemotherapy, 2012. **56**(4): p. 1797-1809.
123. Singh, A., et al., *Dynamic predictive model for the growth of salmonella spp. in liquid whole egg.* Journal of food science, 2011. **76**(3): p. M225-M232.
124. Rudel, L.L. and M. Morris, *Determination of cholesterol using o-phthalaldehyde.* Journal of Lipid Research, 1973. **14**(3): p. 364-366.
125. Amer, M.N., et al., *Isolation of probiotic lactobacilli strains harboring l-asparaginase and arginine deiminase genes from human infant feces for their potential application in cancer prevention.* Annals of Microbiology, 2013. **63**(3): p. 1121-1129.

126. Tamura, K., et al., *MEGA6: molecular evolutionary genetics analysis version 6.0.* Molecular biology and evolution, 2013. **30**(12): p. 2725-2729.
127. Lin, S.-X., et al., *Subunit identity of the dimeric 17 beta-hydroxysteroid dehydrogenase from human placenta.* Journal of Biological Chemistry, 1992. **267**(23): p. 16182-16187.
128. Chen, C.-C., et al., *A Pichia pastoris fermentation strategy for enhancing the heterologous expression of an Escherichia coli phytase.* Enzyme and Microbial Technology, 2004. **35**(4): p. 315-320.
129. Lehrfeld, J., *HPLC separation and quantitation of phytic acid and some inositol phosphates in foods: problems and solutions.* Journal of Agricultural and Food Chemistry, 1994. **42**(12): p. 2726-2731.
130. Osmanagaoglu, O., F. Kiran, and I.F. Nes, *A probiotic bacterium, Pediococcus pentosaceus OZF, isolated from human breast milk produces pediocin AcH/PA-1*. African Journal of Biotechnology, 2013. **10**(11): p. 2070-2079.
131. Sergeev, B., et al., *Synthesis of protein A conjugates with silver nanoparticles.* Colloid Journal, 2003. **65**(5): p. 636-638.
132. Munro, C., et al., *Characterization of the surface of a citrate-reduced colloid optimized for use as a substrate for surface-enhanced resonance Raman scattering.* Langmuir, 1995. **11**(10): p. 3712-3720.
133. Berenson, C.S., et al., *Outer membrane protein P6 of nontypeable Haemophilus influenzae is a potent and selective inducer of human macrophage proinflammatory cytokines.* Infection and immunity, 2005. **73**(5): p. 2728-2735.
134. Agarwal, R., et al., *Effects of oral Lactobacillus GG on enteric microflora in low-birth-weight neonates.* Journal of pediatric gastroenterology and nutrition, 2003. **36**(3): p. 397-402.
135. Singh, B. and T. Satyanarayana, *Characterization of a HAP–phytase from a thermophilic mould Sporotrichum thermophile.* Bioresource technology, 2009. **100**(6): p. 2046-2051.
136. Noh, D., S. Kim, and S. Gilliland, *Incorporation of cholesterol into the cellular membrane of Lactobacillus acidophilus ATCC 43121*. Journal of dairy science, 1997. **80**(12): p. 3107-3113.
137. Lambert, J.M., et al., *Improved annotation of conjugated bile acid hydrolase superfamily members in Gram-positive bacteria.* Microbiology, 2008. **154**(8): p. 2492-2500.

138. Begley, M., C. Hill, and C.G. Gahan, *Bile salt hydrolase activity in probiotics.* Applied and environmental microbiology, 2006. **72**(3): p. 1729-1738.
139. Wong, D., J.D. Chao, and Y. Av-Gay, *Mycobacterium tuberculosis-secreted phosphatases: from pathogenesis to targets for TB drug development.* Trends in microbiology, 2013. **21**(2): p. 100-109.
140. Nir-Paz, R., et al., *Listeria monocytogenes tyrosine phosphatases affect wall teichoic acid composition and phage resistance.* FEMS microbiology letters, 2012. **326**(2): p. 151-160.
141. Alam, A., et al., *Redox signaling regulates commensal-mediated mucosal homeostasis and restitution and requires formyl peptide receptor 1.* Mucosal immunology, 2014. **7**(3): p. 645-655.
142. Buysschaert, G., et al., *Structural and biochemical characterization of an atypical short-chain dehydrogenase/reductase reveals an unusual cofactor preference.* FEBS Journal, 2013. **280**(5): p. 1358-1370.
143. Socrates, G., *Infrared and Raman characteristic group frequencies: tables and charts.* 2004: John Wiley & Sons.
144. Formaggio, F., et al., *The First Water-Soluble 310-Helical Peptides.* Chemistry-A European Journal, 2000. **6**(24): p. 4498-4504.
145. Gupta, H., et al., *Purification and characterization of enterocin FH 99 produced by a faecal isolate Enterococcus faecium FH 99.* Indian journal of microbiology, 2010. **50**(2): p. 145-155.
146. Mariam, J., P. Dongre, and D. Kothari, *Study of interaction of silver nanoparticles with bovine serum albumin using fluorescence spectroscopy.* Journal of fluorescence, 2011. **21**(6): p. 2193-2199.
147. Ruden, S., et al., *Synergistic interaction between silver nanoparticles and membrane-permeabilizing antimicrobial peptides.* Antimicrobial agents and chemotherapy, 2009. **53**(8): p. 3538-3540.
148. Park, S., et al., *Antimicrobial activity and cellular toxicity of nanoparticle–polymyxin B conjugates.* Nanotechnology, 2011. **22**(18): p. 185101.
149. Gaussier, H., T. Lefèvre, and M. Subirade, *Binding of pediocin PA-1 with anionic lipid induces model membrane destabilization.* Applied and environmental microbiology, 2003. **69**(11): p. 6777-6784.